MODELING OF SURFICIAL AND GROUNDWATER HYDROLOGY IN SOUTHEASTERN GEORGIA INCLUDING THE OKEFENOKEE SWAMP

by

Lauryn G. Falkenstein
(Under the Direction of C. Brock Woodson)

ABSTRACT

In recent years, interest in Georgia's groundwater resources has risen due to their importance for agriculture and coastal communities. In this study, regional and local groundwater models were developed using Visual MODFLOW Flex to examine the interactions between heavy mineral mining at two mining sites and the surrounding hydrology with a focus on the Okefenokee National Wildlife Refuge (ONWR). The regional groundwater model includes the surficial, Brunswick, and Upper Floridan aquifer systems as well as the intervening upper and middle confining units. The local model highlights the watershed around the primary mining site with both steady-state and transient conditions. The local models show that flows in the surficial aquifer beneath the main site flow outwards from the site. Meanwhile, the regional model shows that groundwater flows in the region generally move towards the coastline and that pumping wells across the state are likely an important factor contributing to groundwater levels.

INDEX WORDS: Southeast Georgia; Okefenokee National Wildlife Refuge; Okefenokee Swamp; Trail Ridge; Hydrology; Groundwater; Hydrological modeling; Groundwater modeling; MODFLOW; Floridan aquifer system; Surficial aquifer; Finite difference; Hydraulic conductivity; Boundary conditions

MODELING OF SURFICIAL AND GROUNDWATER HYDROLOGY IN SOUTHEASTERN GEORGIA INCLUDING THE OKEFENOKEE SWAMP

by

LAURYN G. FALKENSTEIN

B.S., The University of Georgia, 2020

A Thesis Submitted to the Graduate Faculty of The University of Georgia in Partial Fulfillment of the Requirements for the Degree

MASTER OF SCIENCE

ATHENS, GEORGIA

2023

MODELING OF SURFICIAL AND GROUNDWATER HYDROLOGY IN SOUTHEASTERN GEORGIA INCLUDING THE OKEFENOKEE SWAMP

by

LAURYN G. FALKENSTEIN

Major Professor:	C. Brock Woodson
Committee:	Todd C. Rasmussen
	Matthew V. Bilskie

Electronic Version Approved:

Ron Walcott
Vice Provost for Graduate Education and Dean of the Graduate School
The University of Georgia
August 2023

ACKNOWLEDGEMENTS

This research was made possible through the support of the University of Georgia College of Engineering and the Chemours Company. I am profoundly grateful to these organizations for the opportunity to expand my knowledge and skills through this research. I would like to add special thanks to the many professors and staff that supported and encouraged me throughout this process. I would specifically like to thank my major professor, Dr. C. Brock Woodson, for his guidance and Chemours representative James Renner for his assistance and support as this project developed. Additionally, I would like to thank the members of my advisory committee, Dr. Matthew Bilskie and Dr. Todd Rasmussen, for their guidance as I explored working with groundwater hydrology and numerical modeling. Finally, I would like to thank the Director of Graduate Affairs, Margaret Sapp, who was always helpful throughout my graduate education.

Of course, I must add to this acknowledgement my greatest heroes and motivators: my parents. I credit my passion and drive to understand and improve the world around me to their influence and guidance. This research was made possible by their unwavering love and support.

TABLE OF CONTENTS

Page

LIST OF TABLES

Page

LIST OF FIGURES

Page

ABBREVIATIONS

BAS	Brunswick Aquifer System
CDO	Climate Data Online
DEM	Digital Elevation Model
FAS	Floridan Aquifer System
GDG	Geospatial Data Gateway
HUC	Hydrologic Unit Code
MCU	Middle Confining Unit
NAVD88	North American Vertical Datum of 1988
NCDC	National Climatic Data Center
ONWR	Okefenokee National Wildlife Refuge
SAS	Surficial Aquifer System
SJWMD	St. Johns River Water Management District
UCU	Upper Confining Unit
UFA	Upper Floridan Aquifer
USDA	United States Department of Agriculture
VMF	Visual MODLFOW Flex

CHAPTER 1

INTRODUCTION

The region of study centers around two Chemours heavy mineral mining sites within southeastern Georgia and the Okefenokee Swamp within the Okefenokee National Wildlife Refuge (ONWR). The first mine site, Mission Mine, is located along Trail Ridge near Folkston, Georgia, and the second, Amelia Mine, is located near Jesup, Georgia. This study aims to accomplish three main goals. First, to analyze the hydrology of the study region and the interactions between surficial hydrology with groundwater conditions. Second, to examine and predict groundwater flows in the surficial, Brunswick, and Upper Floridan aquifers beneath the study region. And third, to investigate aquifer and confining unit properties by attempting to reasonably replicate real-world groundwater conditions using observational data from public and private monitoring wells.

In accomplishing these goals, regional and local groundwater models were developed using version 8 of Visual MODFLOW Flex. The models produced in this study were used to estimate the impacts of the groundwater withdrawal during heavy mineral mining operations at the Mission Mine and Amelia Mine sites on local and regional groundwater flows and groundwater levels. The developed models are a useful tool for public and private partners to better manage and protect regional water resources by allowing them to make informed decisions on the utilization of the groundwater resources within Southeast Georgia.

1.1 Purpose of Study

Groundwater is an increasingly important resource for communities across the county, particularly near coastlines. The aquifer systems below the Coastal Plains supply 8.1 billion liters of groundwater daily, representing 13% of the nation's public water usage (Maupin & Barber, 2005). Due to the importance of these systems for our nation's freshwater resources, there has been growing concern about aquifer management regarding groundwater contamination and groundwater withdrawal rates. For example, increasing withdrawal rates in the Maryland Coastal Plain have resulted in a decline in the water table by up to 30 meters from its levels prior to 1960. This drop in the water table has altered the direction of groundwater flows in many areas of the northern Coastal Plan aquifer systems (Drummond, 2007). This process also occurs at a localized level at most pumping well locations, where the uptake of water from an aquifer causes a cone of depression where the water table drops around the location of the pump. These cones of depression along with long-term trends in water table elevation can have lasting consequences on groundwater flows, depth of aquifers, and rates of aquifer recharge. Additionally, the method and rate of natural recharge of aquifers is substantially affected by their depth and the presence of confining units and ground outcrops.

Being the largest swamp in North America, the Okefenokee Swamp is one of the most important ecological features in Georgia. The Okefenokee Swamp has a diverse range of habitats due to its natural cycles of disturbances from flooding and fires. The swamp hosts a wide variety of wildlife including over 400 species of vertebrates, over 200 species of birds, and over 60 species of reptiles (Gibbons, 2002). The swamp is also home to multiple endangered or threatened species including the Eastern indigo snake (*Drymarchon couperi*), Wood stork (*Mycteria americana*), and Red-cockaded woodpecker (*Leuconotopicus borealis*) (Okefenokee

National Wildlife Refuge, n.d). Because the swamp receives very little overland surface runoff, there is minimal nutrient inflows from the surrounding areas, so nutrient cycling is mostly contained within the swamp (Schlesinger, 1978). Due to the linkage between hydrology and ecology, concerns for the hydrological conditions of the swamp also suggest concerns for the swamp's ecology.

1.2 Preliminary Model Study

An initial steady-state regional model (**Figure 1.1**) focusing on Mission Mine and the ONWR was developed by Landers (2022) using version 7 of Visual MODFLOW Flex. The Landers model was used as a foundation for this study and the insight it provided on the hydrology of this region was considered during model development. There were a few specific changes made in the development of the new regional model for this study that aimed to improve the ability to better examine the interactions between the surficial and groundwater hydrology of the region and resolve issues that were noted in the Landers study.

First, the model domain was expanded to include a secondary Chemours heavy mineral mining site and extended to the Georgia coastline. The addition of the second mining allowed for the inclusion of another groundwater pumping well. Additionally, extending the model boundary to the coastline was helpful in establishing a constant head boundary for the regional model and includes coastal areas that heavily rely on groundwater resources within the model domain. Second, the regional and local model boundaries were drawn around watersheds, rather than groundwater equipotential lines, to guarantee that most of the rivers are fully contained within the model domain and enter or exit the model domain only once. Third, pumping well conditions

were included in this model study to examine the effects these pumping wells have on the surrounding groundwater flows.

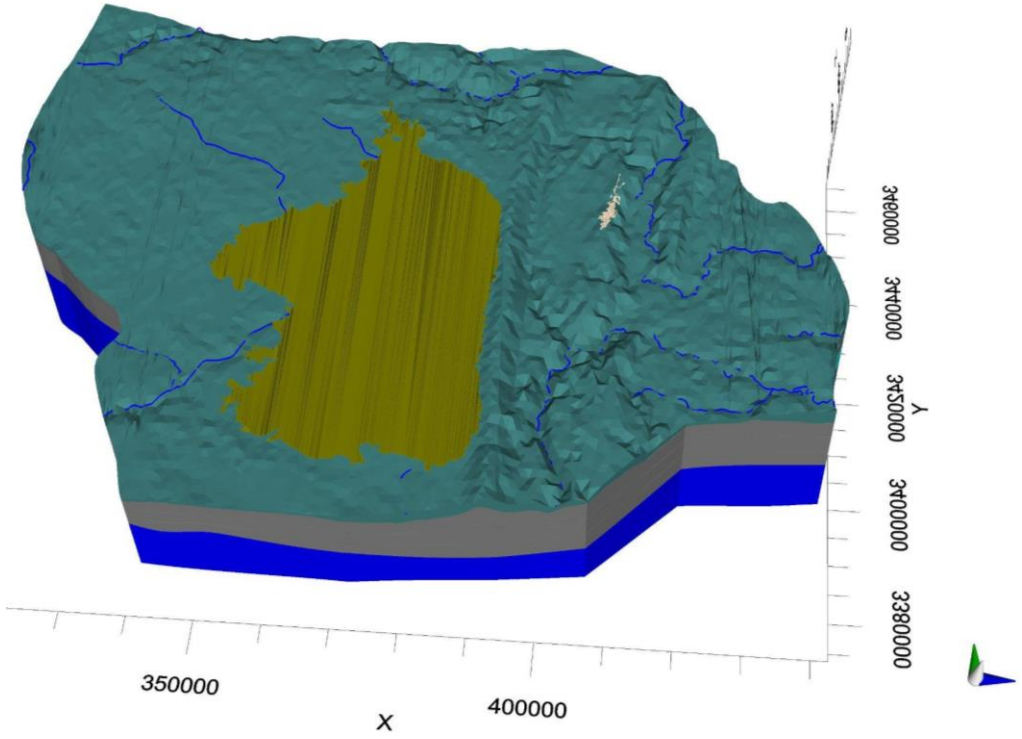

Figure 1.1: Conceptual regional model from preliminary study (Landers, 2022).

CHAPTER 2

LITERATURE REVIEW

This literature review discusses the hydrology of the southeastern United States, the Okefenokee Swamp, heavy mineral mining in this region, and the principles of groundwater modeling. The area of study for this project is mainly within South Georgia and extends into northern Florida. This region falls above some of the most productive aquifers in the country.

2.1 Atlantic and Gulf Coastal Plains

Georgia and Florida sit within a geological region known as the Atlantic Coastal Plain that expands from Florida along the Atlantic coast to Virginia. Connected to this is the Gulf Coastal Plain, which extends from eastern Texas along the Gulf of Mexico into Alabama. Ocean levels receded during the early Cretaceous period leaving behind deposits of sandy sediments which now make up the Coastal Plains (Shah et.al 2017). The recession of these oceans left-behind silts, sands, and clays that are distinct from the crystalline sediments deposited from erosion of the Appalachian Mountains that are found north of the Fall line (Phillips, 1987).

The Atlantic and Gulf Coastal Plain system has three primary aquifer systems: The Coastal Lowlands aquifer system, the Northern Atlantic Coastal Plain aquifer system, and the Southeastern Coastal Plain aquifer system. The Coastal Plain aquifers all vary in hydrology and structure, but most of the groundwater flow is directed towards the coast following a slight downward slope caused by the regression of the Atlantic Ocean over millions of years. This process also created a mix of seaward dipping layers of confining units, boundary layers

preventing flow and aquifer recharge, between aquifer layers and resulted in high water tables. As a result of these effects, rivers provide heightened recharge into the local aquifer systems. Some of the water in these aquifer systems is more than 190,000 years old (Degan et.al., 2020).

Deeper and older aquifers that are almost entirely confined contain older groundwater that is higher in pH and lower in oxygen content. These primarily confined aquifers receive little recharge through infiltration through the intervening confining units. Instead, they are mainly recharged through upgradient outcrops where the aquifers are free from the confining units. Because older groundwater has more time to flow across rocks and mineral deposits, they also tend to have higher concentrations of dissolved minerals. Aquifers that are less confined and/or have multiple points of recharge typically contain groundwater with a lower pH and higher oxygen contents (Degan et.al., 2020).

Beyond the effects of increasing groundwater withdrawal rates, another concern for the quality of these aquifer systems is the threat of saltwater intrusion due to the combined effect of global sea level rise and a trend of lowering water tables. Short-term increases in saltwater intrusion can also be caused by storm surges. For the past few decades, higher levels of chlorine have been recorded in both coastal groundwater aquifer systems and rivers that spill into the ocean along the Eastern coast. In-land travel of seawater into coastal rivers creates extreme conditions in coastal estuaries and wetlands that can result in the collapse of critical ecological systems. Infiltration of saline water into coastal rivers is the highest during combined high ocean tides and low flow in rivers (Brooks, 1983). Additionally, saltwater intrusion is the primary contaminant in coastal aquifer systems contributing to reduced water-quality in freshwater stores that are the main sources of drinking water for many coastal communities (Allen & Klassen, 2017). Since roughly 70 percent of the global population lives in coastal regions and the average

population density along coasts is roughly 3 times higher than the global average, contamination of groundwater resources is a significant concern for the security of freshwater resources globally (Webb & Howard, 2011; Small & Nicholls, 2003).

2.2 The Okefenokee Swamp and National Refuge

2.2.1 History of the Okefenokee Swamp

The Okefenokee Swamp is a major region of federally protected freshwater wetlands in the southern half of Georgia and northernmost part of Florida (**Figure 2.1**). In the 20th century, this 200,000-hectare region of wetlands was subject to draining for timber harvesting and peat mining (Loftin et.al., 2001). Most of the swamp is contained within the Okefenokee National Wildlife Refuge (ONWR). The ONWR is bounded on the eastern side by a geological feature known as Trail Ridge (**Figure 2.2**) that extends from the Altamaha River down into Northern Florida. The swamp is the headwaters for multiple streams including the Suwanee River, St. Mary's River, and Cypress Creek. The wetlands within the ONWR were created through peak accumulation some 6,500 years ago when a combination of sufficiently acidic conditions and frequent flooding slowed the rate of decay of vegetation (Cohen, 1973). In 1960, a low-earthen dam was built on the main channel of the Suwanee River at its outlet from the swamp in response to multiple forest fires that occurred within the ONWR in 1954 and 1955. The Suwanee River Sill is a five-mile-long dam (**Figure 2.3**) designed to increase the water levels in the swamp to reduce the risk of future fires, however, some have argued that the effects of the construction of the sill may have had little effect on the frequency of fires within the ONWR (Loftin et.al., 2000). Additionally, since natural fires can be an essential process for the natural cycling and functions of wetlands, there is some debate that the construction of the dam may

have had negative effects on the distribution of vegetation and the ability for the landscape to adapt to wildfires (Loftin & Wetzel, 2018).

Figure 2.1: Location of the ONWR within Georgia (Loftin et.al, 2001).

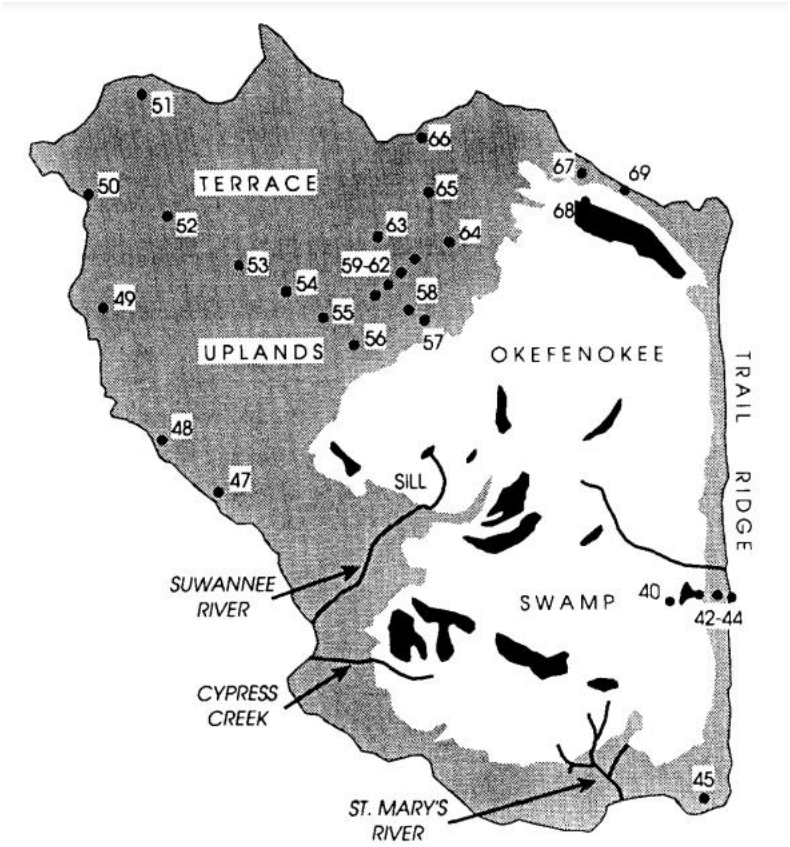

Figure 2.2: Locations of groundwater wells within the Okefenokee Swamp installed in 1981 and key features (Hyatt, 1984).

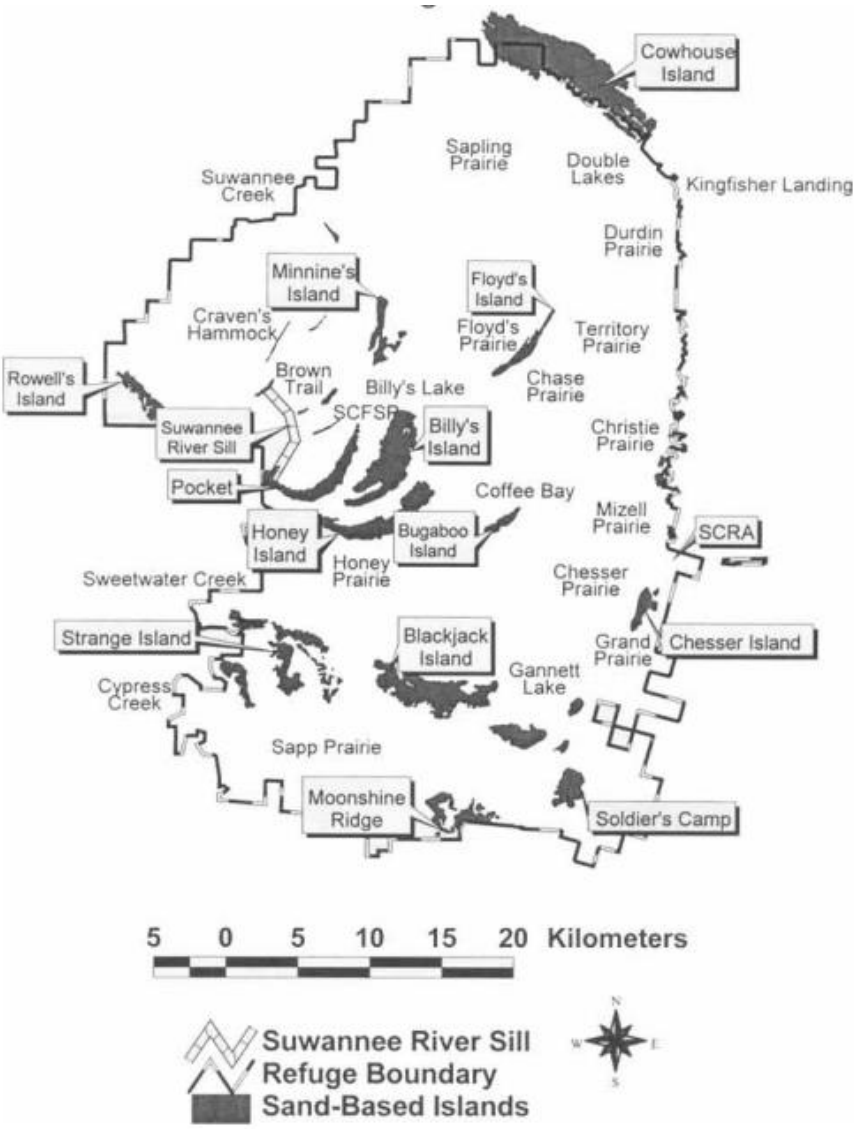

Figure 2.3: Location of the Suwanee River Sill and areas within the ONWR (Loftin et.al., 2001).

2.2.2 Swamp Hydrology

The hydrology of the Okefenokee swamp is complex and most of the water exchanges throughout the system occur through precipitation and evapotranspiration. More specifically, roughly 72-78% of the water input into the swamp comes from precipitation with the rest coming from surface runoff originating from the terrace uplands region of the swamp (Brook & Sun, 1987). The evapotranspiration rates across the Okefenokee Swamp are relatively high due to the

wide coverage of shallow ponds and water-filled depressions through the wetland (Yin & Brook, 1992). The portion of the outflow that is not due to evapotranspiration or vertical leakage exits the swamp through the Suwanee River and St. Mary's River (Parrish & Rykiel, 1979). Annual precipitation and evapotranspiration within the swamp average around 1298 mm and 1032 mm, respectively (Yin & Brook, 1992). However, precipitation and evapotranspiration rates are affected by climate conditions such as solar radiation and humidity levels, so there can be substantial variation in these rates throughout the year. Annual evapotranspiration within the Okefenokee watershed has been estimated to range from 1000 mm to around 1460 mm based on estimation method and location within the swamp (Yin & Brook, 1992).

Hydrological models of the Okefenokee Swamp and the surrounding area have been developed within the past few decades to examine the hydrological conditions of different regions in the swamp and the effects of the Suwanee River Sill on the water levels (Brook & Sun, 1987; Kitchens & Rasmussen, 1995; Loftin et.al., 2001). Water levels throughout the swamp vary regionally and seasonally from a few centimeters to a several meters, with the highest water levels typically occurring at the end of winter seasons (Loftin, 1998; Loftin et.al., 2001). The mean water levels through the different regions of the swamp range (**Figure 2.4**) from dry to about 1 m in depth (Loftin et.al., 2001). Another key factor that effects the water levels within the swamp is the water levels within the Suwanee and St. Mary's Rivers. The Suwannee and St. Mary's Rivers account for an estimated 85% and 11%, respectively, of the outflow from the western side of the swamp (Loftin et.al., 2001).

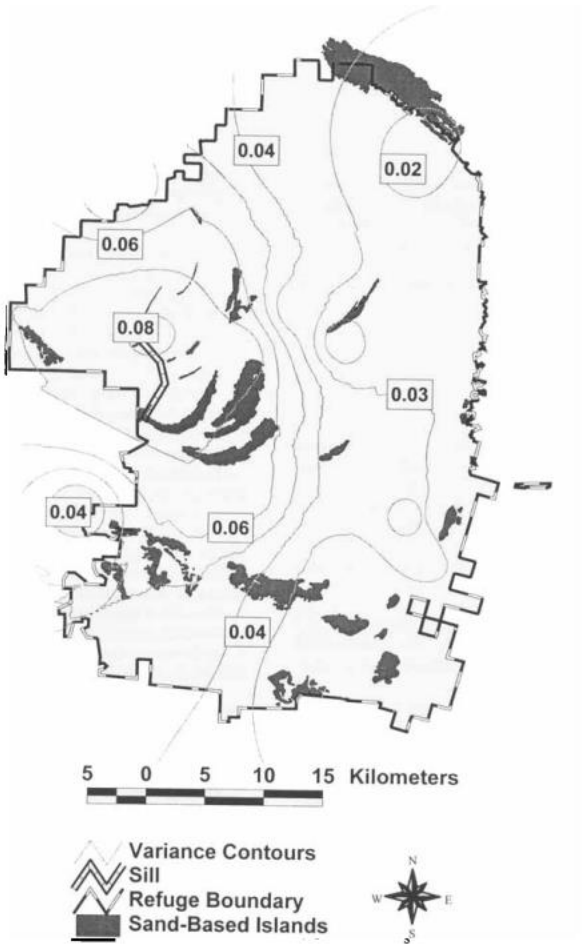

Figure 2.4: Water depth variance contours throughout the ONWR after the Suwannee River Sill was constructed (Loftin et.al., 2001).

2.2.3 Groundwater Contribution

There is some uncertainty about the Okefenokee Swamp's contribution to the Floridan aquifer system. It is generally considered that the contribution of the Okefenokee Swamp to groundwater aquifers is minimal such that many hydrological budgets of the swamp do not consider any groundwater outflow (Brook & Hyatt, 1984; Hyatt, 1984; Loftin et.al., 2001). Estimates from these earlier hydrological budgets of the swamp suggest that groundwater flow is only about 1 to 8% of total swamp inputs (Brook & Hyatt, 1984; Brook & Sun, 1987; Yin & Brook, 1992). However, more recent estimates suggest that surface flows and vertical leakance

from the swamp may be a more significant factor in groundwater flows than previously reported (Kitchens & Rasmussen, 1995; Mao & Wang, 2013). More specifically, observed water level fluxes within the swamp produced similar fluxes by a lag of about one month within the Floridan aquifer beneath it, suggesting that vertical leakance from the swamp has a more substantial role in the hydrological budget of the swamp than was previously assumed. However, quantifying the volume or rate of vertical leakance from the swamp requires further investigation into the storage coefficients and hydrological conductivity of the soils beneath the swamp (Kitchens & Rasmussen, 1995). Further examination of the current conditions of the swamp and the underlying aquifer units is necessary to accurately determine the significance of the swamp's contribution to groundwater because most studies on the hydrology of the Okefenokee Swamp only examined surface-level conditions and used observational data from before the 1990s.

2.3 Mining of Heavy Minerals in Georgia

The mining of heavy minerals in the Atlantic Coastal Plains goes back over a century. During this time, the most economically impactful heavy minerals were ilmenite ($FeTiO_3$), rutile (TiO_2), and zircon ($ZrSiO_4$). These titanium minerals have mostly been used for the development of titanium-based pigments while zircon has been used in ceramics and chemicals. Most heavy mineral deposits within the Atlantic Coastal Plains are found within areas of large sand deposition that developed within Georgia as a part of beach ridge formations from sand deposition as the succession of ocean levels created multiple ancient shorelines (Pirkle et.al., 2013). **Figure 2.5** shows the locations of major heavy mineral deposits within southeastern Georgia and northeastern Florida.

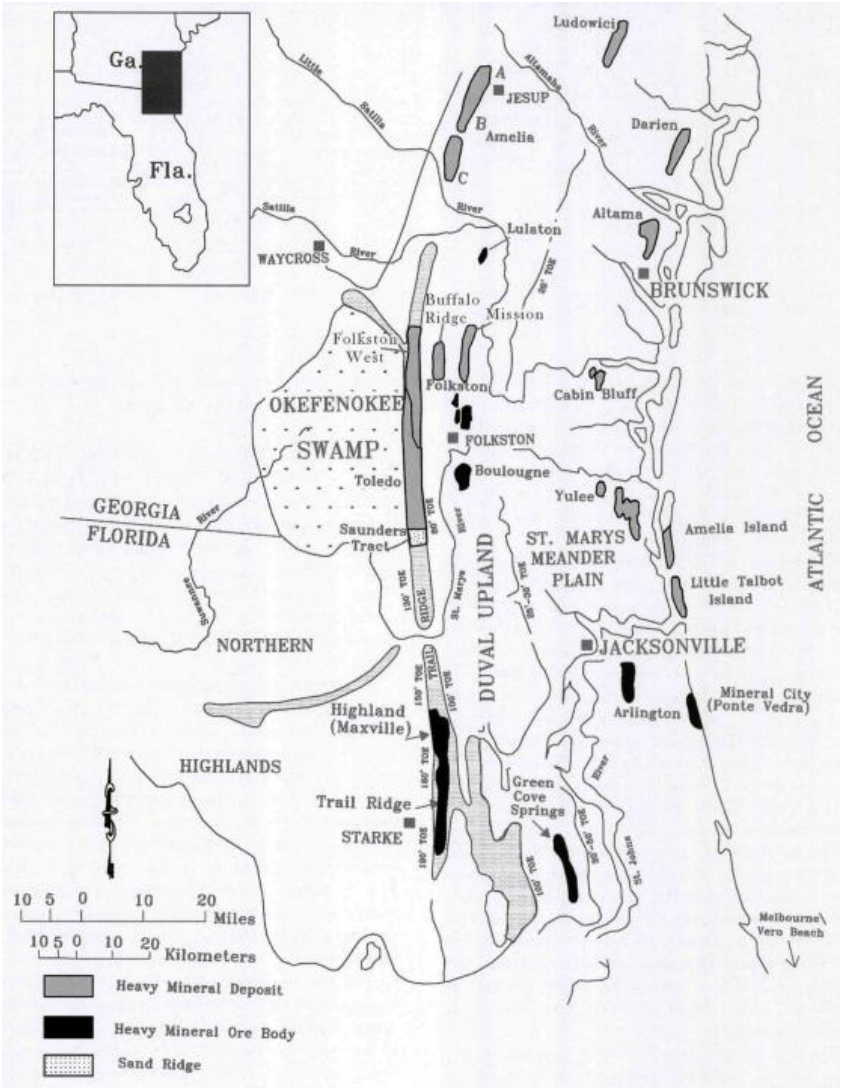

Figure 2.5: Locations of major heavy mineral deposits and ores along sand ridges in southeastern Georgia and northeastern Florida (Pirkle et.al., 2013).

2.4 Surficial and Regional Aquifers in Southeast Georgia

An aquifer system in a series of alternating layers of permeable and poorly permeable soils that act as water-yielding hydrological units (Clarke, 2003). Typically, aquifer systems are identified based on their regional extent or geohydrological characteristics.

The surficial aquifer system (SAS) is the topmost layer of unconfined groundwater resources that interacts with surface water systems. The SAS consists of layers of sand, clay, and limestone from the Miocene era or younger. Within Georgia, the SAS is thickest at the southeastern coast and becomes progressively thinner towards the northwest. (Clarke, 2003). In some locations, the SAS has thick layers of clay that act as confining units to produce two to three water-bearing zones (Clarke et.al., 1990). In southeastern Georgia, the SAS has three water-bearing zones, while northeastern Florida has two water-bearing zones with a total thickness ranging from 10 to 100 feet (about 3 to 30 meters; Williams & Kuniansky, 2016). The SAS is almost entirely recharged through rainfall and most of its discharge is through streams. Withdrawals from the SAS in coastal areas are mainly for domestic lawn irrigation but it can be the main source of drinking-water for some rural areas (Clarke et.al., 1990). The transmissivity of the water-bearing zones is estimated to be around 14 to 6,700 feet squared per day (ft^2/day) and the transmissivity of the confining zones is estimated to be around 150 to 6,000 ft^2/day (Clarke, 2003).

Georgia is a crossroads for several regional aquifer systems (**Figure 2.6**). One such regional system is referred to as the Brunswick aquifer system (BAS) which is centered around the city of Brunswick, Georgia and extends inland and upwards into South Carolina. The BAS consists of

fine to coarse grain, slightly phosphatic and calcareous or dolomitic quartz sand from the Miocene era and has two principal aquifers, an upper and lower aquifer, separated by a confining unit (Clarke, 2003). The top of the upper Brunswick aquifer is estimated to be around 88 to 340 feet below the land surface and ranges in thickness from around 20 to 150 feet. The lower Brunswick aquifer is around 400 to 460 feet below land surface and has a thickness of around 36 to 70 feet (Clarke et.al., 1990). However, groundwater levels within the BAS fluctuate with tidal conditions particularly near the coast (Cherry, 2015). The BAS has a relatively high transmissivity, with the upper aquifer having a transmissivity around 20 to 3,500 ft^2/day and the lower aquifer having a transmissivity around 2,000 to 4,700 ft^2/day (Clarke et.al., 1990; Clarke 2003).

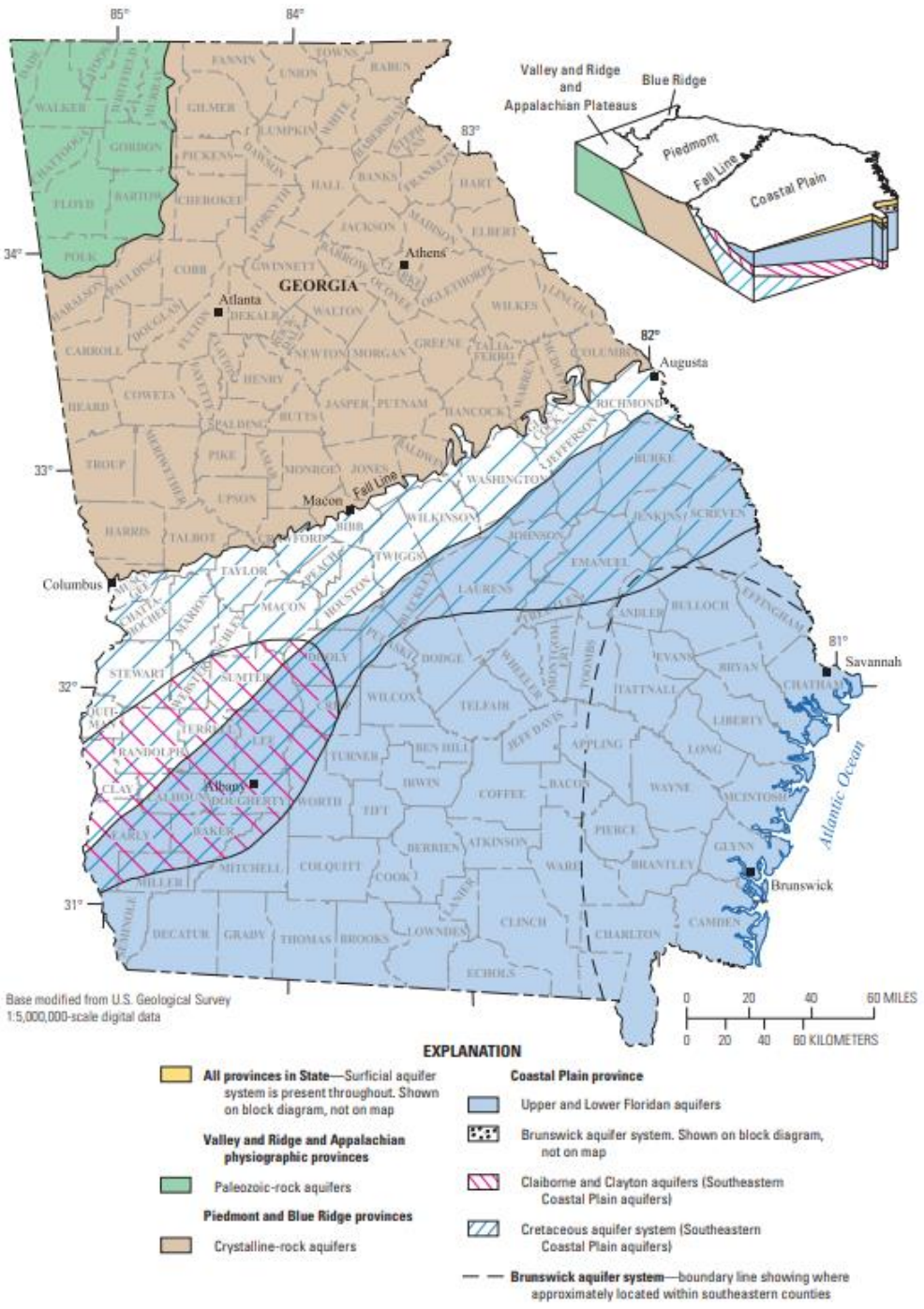

Figure 2.6: Providences and extent of principal aquifers in Georgia (Painter, 2019).

2.5 Floridan Aquifer System

The Floridan aquifer system (FAS) is a major aquifer extending from South Florida into the coastal plains of Alabama and Georgia and partially into southeastern South Carolina. It consists of a vertical series of carbonate rocks of the late Paleocene to early Miocene age (Ryder, 1985). The FAS has two main, permeable water bearing layers separated by a confining unit and semi-confining units in a few areas, which are referred to as the Upper Floridan aquifer (UFA) and the Lower Floridan aquifer (LFA) (**Figure 2.7**). The primary confining unit separating the UFA and LFA is referred to as the middle confining unit (MCU) (Reese, 2000). The FAS is separated from surficial aquifer systems by another confining unit called the upper confining unit (UCU) or intermediate confining unit. This confining unit is also sometimes referred to as the Hawthorn Formation as it resides within a geological formation known as the Hawthorn Group. In some areas, the UCU is thin or nearly absent, meaning the UFA is relatively unconfined in these areas (Wicks & Herman, 1994). In southwestern Florida, the thickness of the UCU is estimated to range from 120 to 460 ft (about 37 to 140 m; Ryder, 1985). Similar, in southeastern Georgia and northeastern, the thickness of the UCU is estimated to be around 400 ft (122 m) in Florida. However, in southern Florida and Alabama the thickness of the UCU can exceed 1,000 (305 m) and even 1,800 ft (549 m; Williams & Kuniansky, 2016).

The FAS is the primary source of groundwater in coastal Georgia and its upper aquifer unit is considered one of the most productive aquifers in the United States (Clarke et.al., 1990). The UFA ranges in thickness from 500 to more than 1,800 feet (152.4 to 548.64 meters) (Ryder, 1985). Although the transmissivity of the LFA has not been well-documented, the UFA is estimated to have a transmissivity as high as 500,000 to 1,000,000 ft^2/day (about 46,500 to 92,900 m^2/day) depending on sources (Clarke, 2003; Ryder, 1985). The UFA is recharged by

leakage from the surficial aquifer through the UCU in locations where it is present. Annual recharge for the UFA are also estimated to be as high as 20 inches (50 centimeters) in some locations. Previous steady-state models of the UFA in western Florida estimated that outflow from the UFA occurs as about 64% discharge from springs, 30% as well withdrawals, and 6% as upward leakage (Ryder, 1985).

The LFA typically has a higher level of chloride than the UFA. Chloride concentrations within the LFA can even reach a salinity similar to saltwater in some regions (Ryder, 1985; Reese, 2000). Although throughout most of the FAS the UFA and LFA are separated by a discontinuous series of confining units, in some parts of northeast Georgia and South Carolina the MCU becomes more permeable, allowing for limited to no separation between the two aquifers (Williams & Kuniansky, 2016).

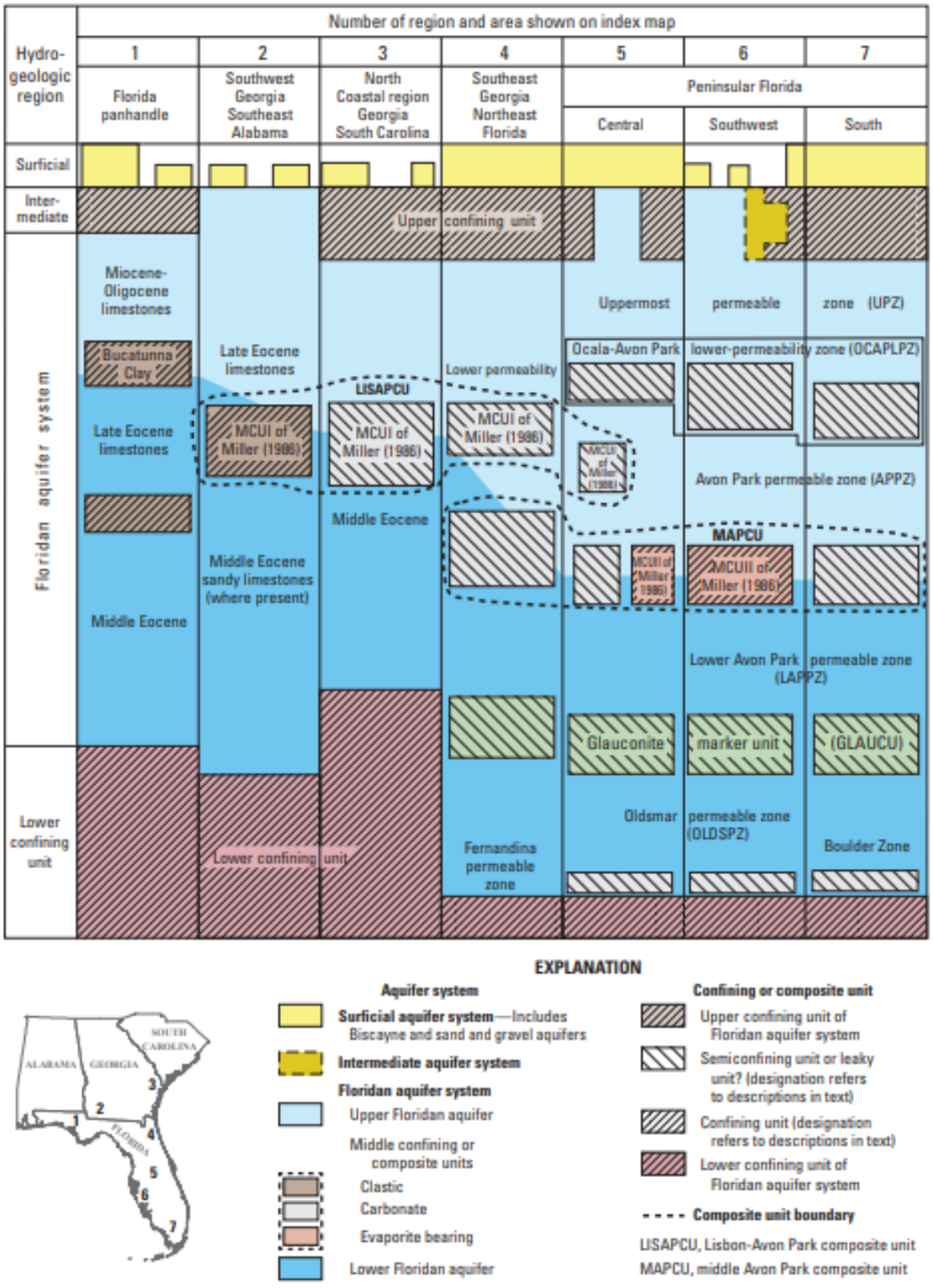

Figure 2.7: Composite regional hydrostratigraphic variation of the Floridan aquifer system (Williams & Kuniansky, 2016).

2.6 Groundwater Modeling

2.6.1 Introduction

Groundwater modeling has increased in its usage and applications in recent decades. The early uses for groundwater modeling were to determine the location and quantity of freshwater resources below the ground surface. More recently, the study of groundwater includes investigating groundwater quality and how water moves through the natural environment into and out of aquifers. (Pinder, 2002). In the past few decades, groundwater models have transitioned from physical or analog models to one-dimensional and later three-dimensional models. As computers have become more advance, the complexity of groundwater models has also increased, leading to the current state where some regional groundwater models could have millions of grid nodes (Baalousha & Lowry, 2022). These sophisticated groundwater models can be developed to provide a wide variety of information about a region's hydrology and the effects of human actions on the quality and/or quantity of groundwater resources. Both physical and mathematical groundwater models can be used to examine a variety of issues related to the management of groundwater resources such as how varying pumping well rates will affect groundwater levels around a well, the locations where a confining unit is likely leaking or absent, or the length of time for a contaminant to move from its source to another location.

Groundwater is a major source of both drinking and agricultural water usage throughout the United States. Unfortunately, the rate at which water is pumped out of some groundwater sources exceeds the rate at which these aquifers replenish their water supply. Due to this, groundwater resources are becoming scarcer, and the patterns of surface water movement into and out of these aquifers may be shifting. The process of pumping water out of a groundwater source creates a cone of depression around the well shaft, resulting in a drop in the water table at

the well point, which can affect the direction and speed of groundwater flow in that region (Pinder, 2002). Additionally, groundwater modeling is now also being incorporated into water contamination studies, where modeling of groundwater reservoirs and flows can be used to determine the magnitude and spread of contamination of groundwater resources from inflow of contaminated surface water or directly from contamination sources. Unfortunately, developing an accurate model of groundwater flow becomes difficult due to lack of available data on the exact location of groundwater features and the wide variability of soil permeabilities. Because groundwater moves vertically and horizontally at different rates, knowing soil types and average hydraulic conductivities becomes important.

The modeling groundwater flow is based on Darcy's law and uses parameters such as hydraulic conductivity and specific storage to determine hydraulic head. The general governing equation for flow in a 3-dimensional groundwater model is:

$$\frac{\partial}{\partial x}\left(K_x \frac{\partial h}{\partial x}\right) + \frac{\partial}{\partial y}\left(K_y \frac{\partial h}{\partial y}\right) + \frac{\partial}{\partial z}\left(K_z \frac{\partial h}{\partial z}\right) = S_s \frac{\partial h}{\partial t} - R^*$$

where (K_x, K_y, and K_z) are hydraulic conductivities in each direction, (S_s) is specific storage, (h) is hydraulic head, and (R^*) is a source or sink term representing the volume of inflow or outflow per unit volume of aquifer per unit time (Anderson & Woessner, 1992).

A common workflow for constructing a groundwater model includes: 1) determining an area of interest for the model and related features, 2) defining the model boundary and compiling hydrogeological information pertaining to the site for boundary conditions, 3) defining hydraulic properties of the model, 4) defining model parameters, 5) defining model stresses, 6) defining numerical approach, 7) execute and initial run of the model, 8) calibrate the model using observational data, 9) execute the model again for calibrated results, and 10) evaluate model accuracy results (Pinder, 2002).

2.6.2 Model Boundary

Defining the model boundary is the first step in developing a groundwater model. The area of the model should cover key hydrological and geological features as well as the area of interest. It is important to understand the environmental conditions of the region in which the model will be focused so that any responses from simulated changes are visible and accounted for by the model. This includes any cones of depression from pumping wells, runoff effects, storage features, and any water-level changes. On the other hand, the extent of the model will be limited by the computational capabilities available based on the acceptable waiting period for results. Typically, it is recommended that the model boundary be defined by distinct and identifiable hydrological boundary features or conditions. For example, a model boundary may be defined around watersheds, natural and man-made lakes, rivers or channels, estuaries, coastlines, or other hydrological features (Pinder, 2002).

2.6.3 Boundary Conditions

An important element in groundwater modeling is the establishment of boundary conditions. Boundary conditions specify the unique hydrological conditions of features and how they interact with their surroundings within the model domain. Typically, boundary conditions are applied to the top or bottom layers of polygon features within the model domain or to the whole model domain, however, they can also be set to the sides of the model. Important boundary conditions include constant head, general head, drain, recharge, evapotranspiration, specified flux, river, lake, and constant concentration. Some of these boundary conditions, such as the river and lake conditions, allow for the input of time variabilities to allow for the development of transient models.

Constant head and general head conditions can be applied to the top, bottom, or side of the model or at some intermediate point within the model. The constant head option assigns a particular head value to a cell so that the head value within that cell remains constant regardless of the effects of interactions in the surrounding cells. The general head condition tells the model to solve for a head value within a cell based on given stage and conductance values, and it typically used if there is a large element, such as a body of water, outside of the model domain that is still affecting the head values within the model domain and needs to be accounted for (Waterloo Hydrogeologic, 2022). The recharge and evapotranspiration conditions set the parameters for the volume of water entering and exiting the model. Similarly, the specified flux condition sets a known value for inflow or outflow per unit length (for polylines) or per unit area (for polygons). The drain condition calculates the volume of water leaving an aquifer based on a given elevation and leakance (Waterloo Hydrogeologic, 2022). The lake and river boundary conditions use shapefiles or polylines as well as input information such as bed thickness and bed conductivity to estimated leakage from these features into aquifers.

2.6.4 Numerical Grids

Two of the main approximation methods for developing steady-state models using finite series are finite-difference and finite-element approximations (Pinder, 2002). With both approximation methods, hydraulic heads and flows are calculated within each cell of a numerical grid based on the boundary conditions and parameters input into the model. A finite-difference approach uses a regularly spaced rectangular grid while finite-element approaches use a triangular mesh. Finite-difference grid nodes are based on the separation between grid lines, which are adjusted to add details around features within the model by decreasing cell size and

increasing the number of nodes in a region of the model. Similarly, the angle and number of triangle nodes can be adjusted within finite-element grids to add detail and represent irregular or curved boundaries. The important difference between these two approaches is the location of nodes within the grid, specifically because the derivative approximation is conducted at the nodes for both approaches. The finite-element approach allows for more flexibility due to the higher number of intersections between nodes but has limitations due to the increased computational power required. Because of computational power limitations and calculation time, the use of a finite-difference approach is typically more common.

The volume rate of outflow in a cell using a 2-dimensional finite-difference grid can be written using Poisson's equation for steady-state conditions:

$$\frac{\partial^2 h}{\partial x^2} + \frac{\partial^2 h}{\partial y^2} = -\frac{R(x,y)}{T}$$

where (T) is the transmissivity, R(x,y) is the volume of water added per unit time per unit aquifer area in cell (x,y). Transmissivity in this equation represents the product of the hydraulic conductivity and aquifer thickness (Wang & Anderson, 1982).

2.6.5 Calibration of Groundwater Models

Model calibration refers to the process of adjusting the model components, so the model produces results that are closer to observational data. Calibrating a groundwater model involves adjusting the parameters, boundary conditions, or forcing functions to reproduce observed head values (Pinder, 2002). Because model calibration is often ambiguous, there are a few guidelines that tend to be recommended for calibrating groundwater models. The first guideline is referred to as the principle of parsimony. This principle suggests that an initial model should be simplified and become more complex gradually through calibration. During the calibration

process, further details or sub-groups should only be added if model results cannot replicate observational data or if further information is obtained that disproves an assumption of good homogeneity. Additionally, because local changes in hydraulic conductivity typically do not have a substantial effect on surrounding local hydraulic heads, changes in hydraulic conductivity of larger zones tend to be more effective for the calibration process. Another guideline for effective calibration is to incorporate a variety of observational and geophysical data from multiple sources to have a clearer representation of the geohydrological system that is being modeled (Pinder, 2002).

2.6.6 MODFLOW and Visual MODFLOW Flex

MODFLOW, originally referred to as the USGS Modular Three-Dimensional Finite-Difference Ground-Water Flow Model, is a consolidated computer code developed by the USGS for computer simulation of groundwater flows in two or three-dimensional finite-difference models. MODFLOW was first developed in the early 1980s using Fortran 66 computer language. This early version of MODFLOW is referred to as MODFLOW-88. MODLFOW became the most popular code for the development of groundwater models by the 1990s (Harbough, 2005). The popularity of MODFLOW is credited to it being user-friendly and being a free public domain software (Harbough, 2005; Hariharan, 2017). In the past few decades, MODFLOW has gone through multiple updates that improved or expanded its capabilities. Some features included in the version of MODFLOW developed in 2000, referred to as MODFLOW-2000, include parameter estimation and sensitivity analysis. The 2005 version of MODFLOW, MODFLOW-2005, allows data to be shared without using subroutine arguments, but is otherwise a similar design to MODFLOW-2000 (Harbough, 2005).

Visual MODFLOW Flex (VMF) is a Graphical User Interface commercial software utilizing MODFLOW that was released by the Waterloo Hydrogeologic company in 1994. VMF improves the user experience of working with MODFLOW by allowing users to input data with a variety of file types from Microsoft Excel, Geographic Information Systems (GIS), and AutoCAD and powerful data visualization tools that create color maps/charts of the simulated model results (Hariharan, 2017). VMF allows for a simplified approach to groundwater modeling by allowing users to transition between conceptual and numerical models, each with a step-by-step workflow that guides users through the modeling process. Conceptual models can be developed using GIS surface and shapefiles to visualize a region's hydrology by defining boundary conditions, model layers, property zones, and observation data. Additionally, VMF allows users to select solver type and settings as well as select from a variety of grid types. Users can then adjust and refine model grids to their specific needs (Waterloo Hydrogeologic, 2022).

Like MODFLOW, VMF has undergone a series of updates and revisions that improved existing and added to its features. Version 8 of VMF added new observation point types , improvements to the model dashboard, improvements to the solver and model run packages, a surface water flow dashboard, and other improvements to the software. The new observation point types include well observations, stream and lake observations (stage, outflow, etc.), boundary condition flow, and zone budget flow (Waterloo Hydrogeologic, n.d).

2.6.7 MODPATH

Particle tracking refers to the process of following an infinitely small imaginary particle along its flow path as it moves through a flow field. Particle tracking is typically used to examine the direction and pattern of flows or to track contaminants in a flow field (Anderson &

Woessner, 1992). To trace a particle or a series of particles through its flow path requires that a transient flow model detailing the features of the flow field already exists. Particle tracking can also be used to locate recharge areas or to examine the effects of wells and pumps (Anderson & Woessner, 1992). Particles can be tracked either in the forwards or reverse direction depending on whether the goal of the tracking is to find the source of a particle in the flow field or to determine where the particle will go.

The USGS released a particle tracking package, referred to as MODPATH, in 2017 for use within either a structured or unstructured finite-difference grid in VMF version 7. MODPATH allows for both forward and reverse particle tracking and calculates the time of travel. In a 2-dimensional grid, the time it takes for a particle to travel from an initial point $(x,y)_{t1}$ at time (t_1) to another point (x_2,y_2) is calculated in MODPATH based on the velocities of the flow in each direction. Specifically, the time to travel (Δt) for a particle to move in the *x*-direction from the initial point to a point (x_2) is described by the equation:

$$\Delta t_x = \frac{1}{A_x} \ln \left[\frac{V_{x_2}}{(V_x)_{t_1}} \right]$$

A version of this equation modified for the *y*-direction is then used to calculate the total time to travel. The exit time (t_e) is found by adding longer time to travel (either Δt_x or Δt_y) to the initial time (t_1) (Pollock, 2016). This calculation is repeated for each cell in a grid until the particle reaches the endpoint or a specified location.

CHAPTER 3

METHODS

3.1 Model Boundary

The boundary for the regional model was expanded from the previous project (Landers, 2022) to include a second mining location, Amelia Mine, near Jesup, Georgia. The locations of both mine sites and the ONWR are shown in **Figure 3.1**. The model boundary was established by stitching together the HUC8 shapefiles from the United States Department of Agriculture (USDA) Geospatial Data Gateway (GDG) for the watershed boundaries of ten counties in Georgia and Florida (**Table 3.1**). These watershed shapefiles were input into ArcGIS Pro and merged into a single polygon feature that constituted the general shape of the model boundary. The outline of the model domain overlaying the Hydrologic Unit Code (HUC) 8 shapefiles for the counties listed in **Table 3.1** is shown in **Figure 3.2**. These shapefiles, however, extend outwards into the Atlantic Ocean, so the eastern border of the model was adjusted inwards to the topographic Georgia coastline as viewable in ArcGIS. The final extent of the regional model crosses over 31 counties in Georgia and Florida (**Figure 3.2**).

Table 3.1: List of counties used to establish regional model domain using HUC8 shapefiles.

State	**Counties**
FL	Nassua
GA	Appling, Atkinson, Brantley, Charlton, Clinch, Echols, Glynn, Pierce, Wayne

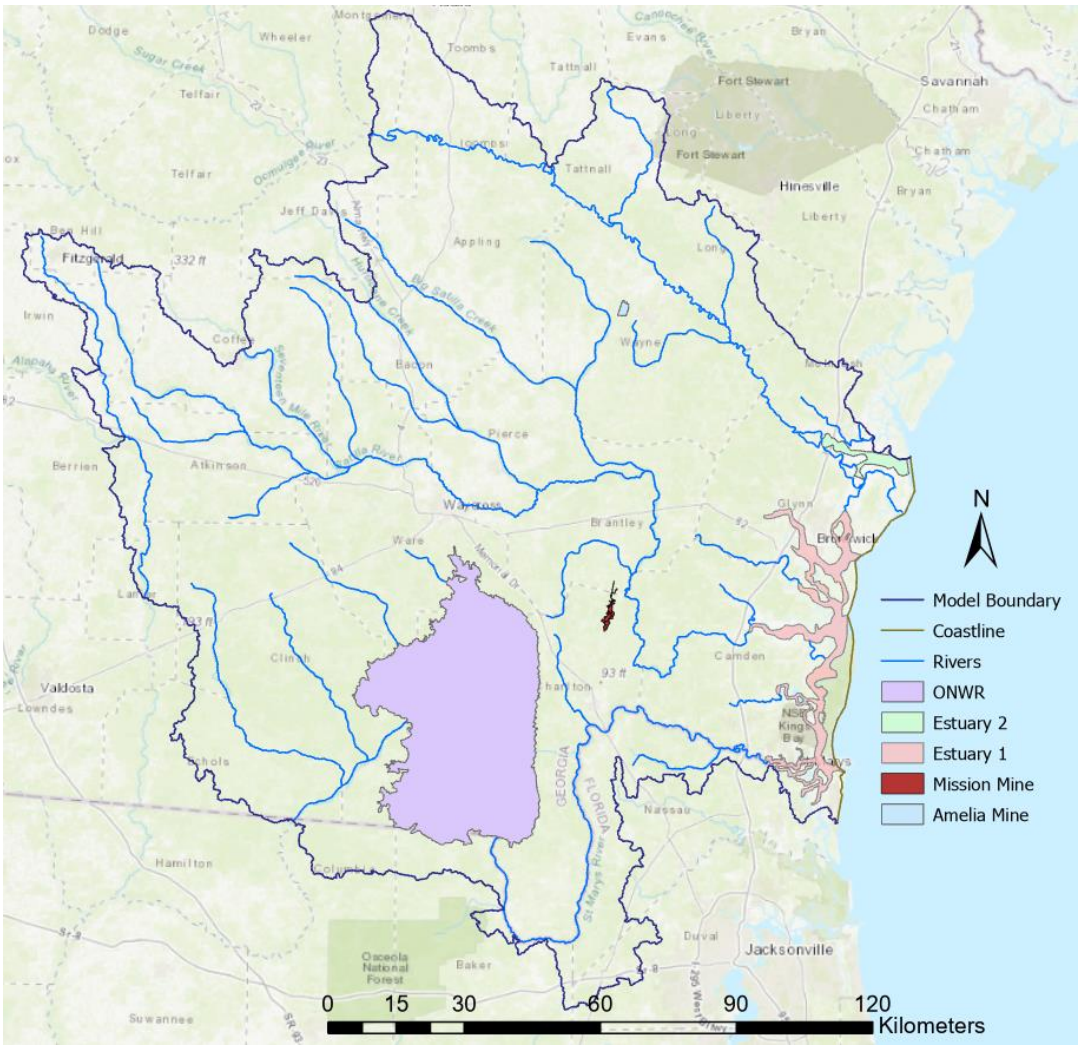

Figure 3.1: Regional model domain with Chemours Mission and Amelia mine sites and key hydrological features.

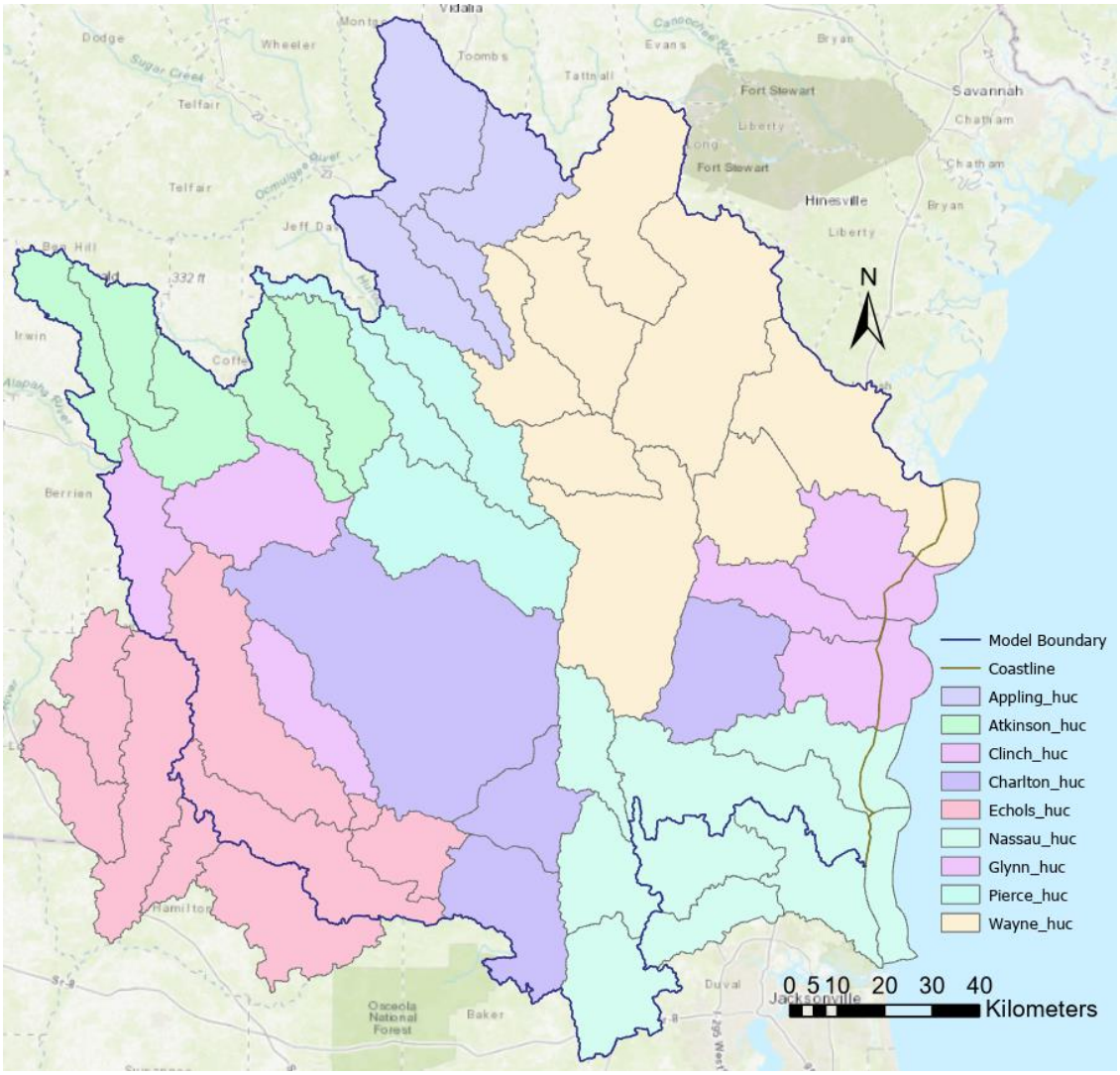

Figure 3.2: County watershed HUC8 files used for developing the regional model boundary.

A raster file detailing 2020 land cover was obtained from the North American Environmental Atlas through the Commission for Environmental Cooperation (Pasos, n.d.). This file detailing estimated physical landcover for North America with a 30 m spatial resolution was clipped in ArcGIS Pro to the model domain (**Figure 3.3**).

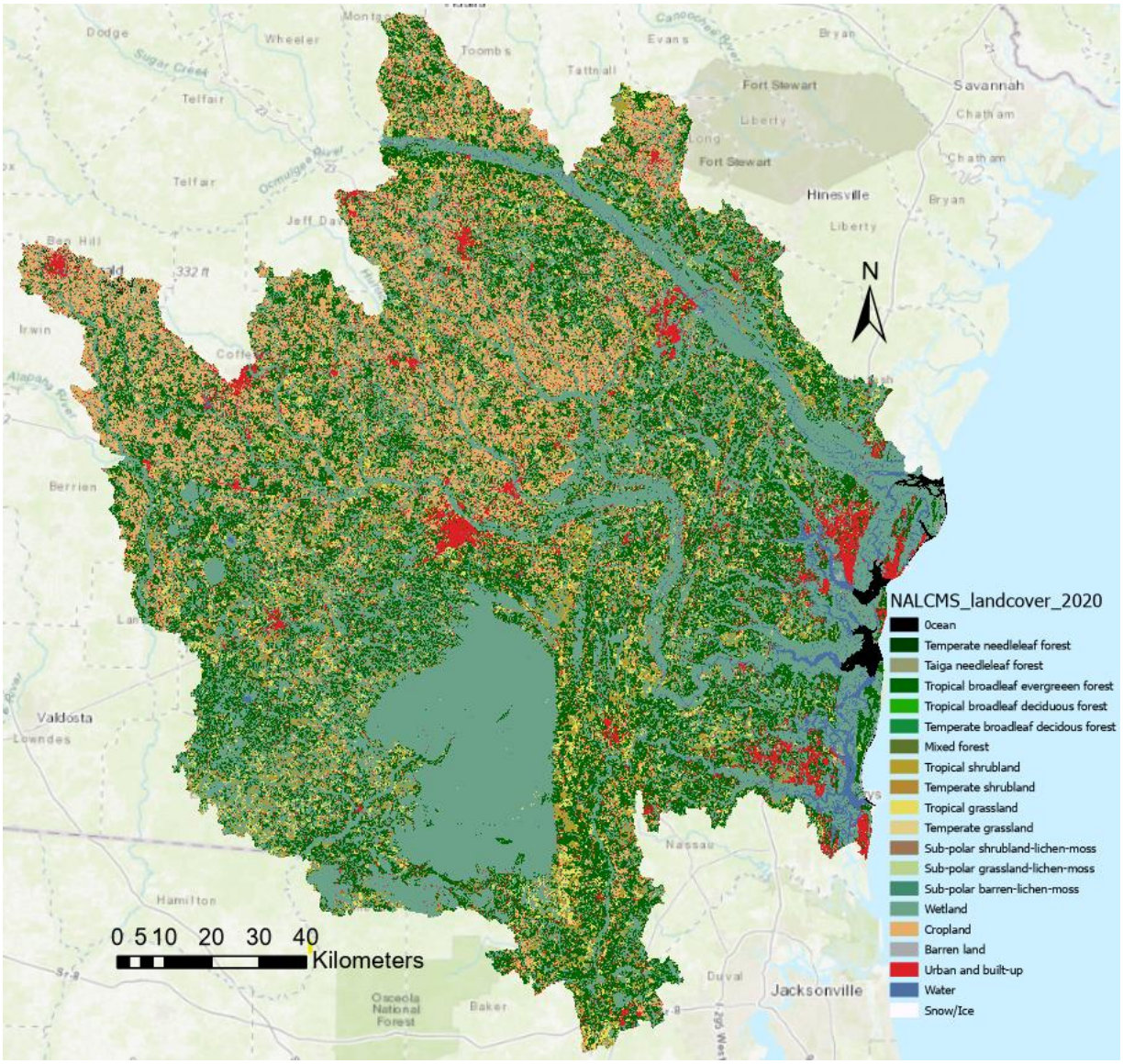

Figure 3.3: North American Environmental Atlas 2020 land cover (30m) over regional model domain.

3.2 Model Parameters

A start data of October 1, 2020, was established for all models to align with the USGS water year calendar schedule. The coordinate projection for all models was set to NAD 1983 UTM Zone 17N to align with the digital elevation (DEM) files used for the surface topography. These models were constructed using standard metric units. The models were set to assume a constant density for the groundwater.

3.3 Model Layers

3.3.1 Ground Elevation

The top layer of the regional model is the ground level topography. The ground layer was generated by stitching together a mosaic raster of 10 m resolution digital elevation model (DEM) files obtained for the thirty-one counties (**Table 3.2**) in the model domain again through the USDA Geospatial Data Gateway (GDG). The resolution of the digital elevation model (DEM) files on the accuracy of hydrologic models using them is an important factor that affects the model's estimations for peak discharge and water table depth such that a lower resolution file yielded high peak discharges and a lower water table depth (Zhang & Montgomery 1994). It was determined by this report that 10 m resolution provides the best compromise between the increased accuracy of higher resolutions and the limitations of program memory. The DEM files gathered from the GDG were imported to ArcGIS Pro to be merged and then clipped to the model boundary. Each county had multiple raster files covering different sections of the county which were merged using the "Mosaic to New Raster" function to create 31 DEM files, one for each county. Then, these county files were again merged using the mosaic raster functions to create a single mosaic raster file. This merged DEM mosaic raster file was then clipped to the

model boundary using the "clip" function within the raster functions section (**Figure 3.4**). Finally, to match the Data Series 936 surface files resolution, the DEM raster file was resampled from a 10 m resolution to a 1000 m resolution. This final file established the ground surface elevation and the projection for the model (**Figure 3.5**).

Table 3.2: List of counties within the regional model domain used for gathering DEM files.

State	Counties
FL	Baker, Columbia, Duval, Hamilton, Nassua
GA	Appling, Atkinson, Bacon, Ben Hill, Berrien, Brantley, Camden, Charlton, Clinch, Coffee, Echols, Evans, Glynn, Irwin, Jeff Davis, Lanier, Liberty, Long, McIntosh, Montgomery, Pierce, Tattnall, Toombs, Ware, Wayne, Wheeler

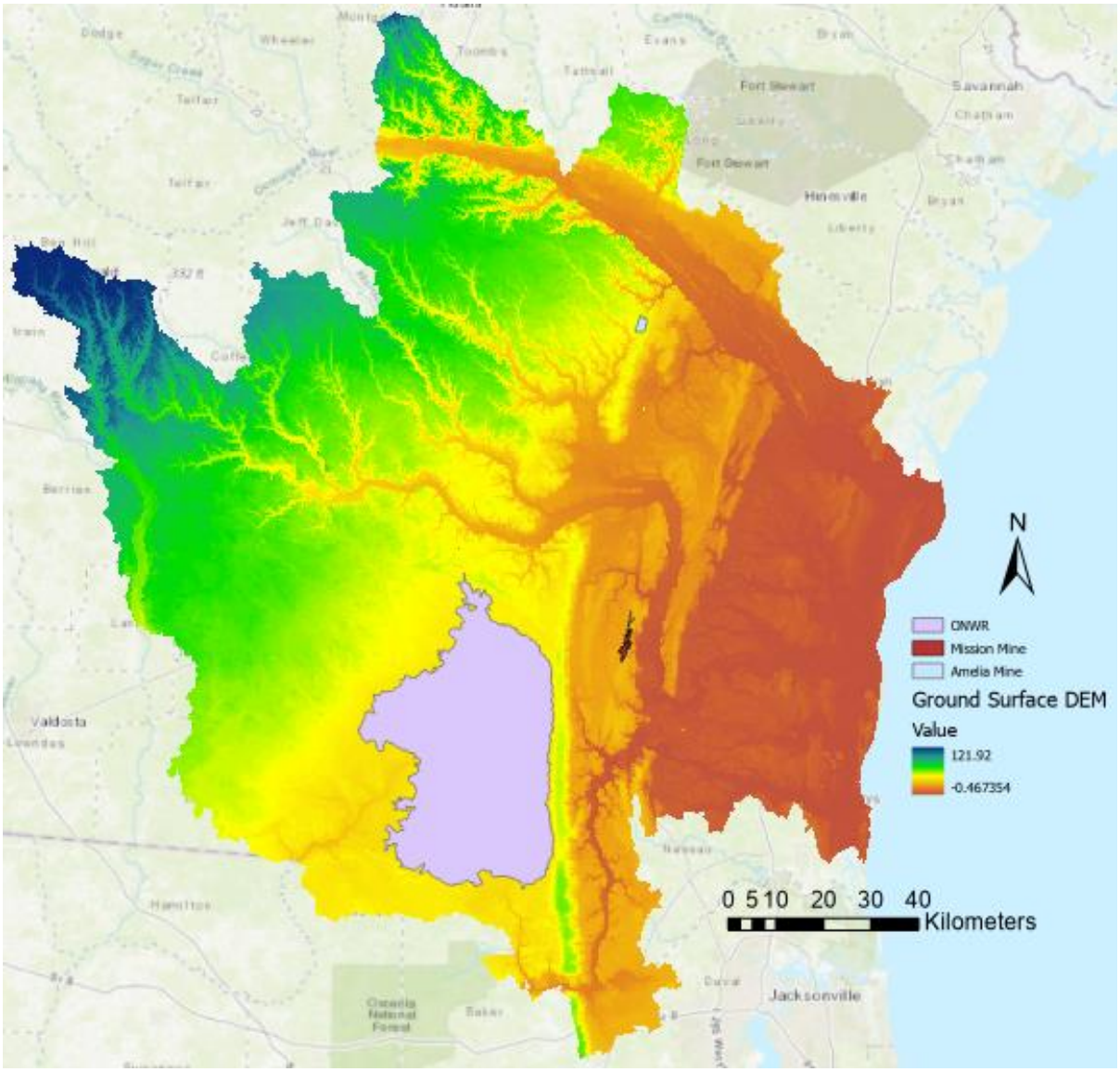

Figure 3.4: Regional model DEM (digital elevation model) in meters and the Amelia and Mission mine locations.

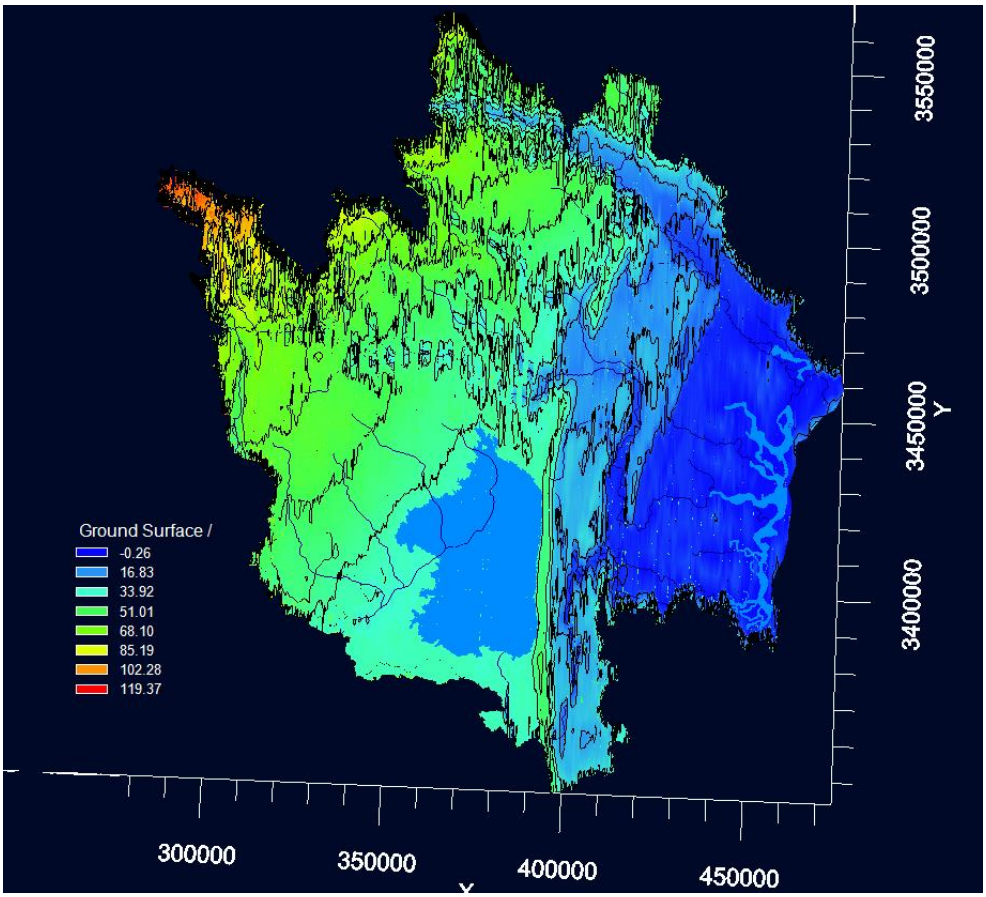

Figure 3.5: Top layer (ground surface) of regional model as shown in VMF.

3.3.2 Aquifers and Confining Units

The layers of the aquifers and confining units were developed using the relevant files from the USGS Data Series 926 report (**Table 3.3)**. and their purpose for this model gathered from the Series 926 dataset. The dataset downloads as text documents, so the files were imported into ArcGIS Pro using the "ASCII to Raster" function. These files from Series 926 were then reprojected in ArcGIS Pro to match the model projection (NAD83 and NAVD88). They were then converted from US Customary units to metric units and back into ASCII text files. Finally, these files were ready to be used to develop the layers of the models in VMF.

While further layers of aquifers exist within the area of the model boundary, this model only extends to the bottom of the Upper Floridan aquifer (equivalent to the top of the middle confining unit). This was due to lack of available data below this layer as well as the assumption that these lower layers would not be necessary for the objectives of this model. The conceptual model was built with five layers. The top layer consisted of the ground elevation developed using the DEM files. The next layer represents the bottom of the surficial aquifer, which was developed using raster subtraction in ArcGIS Pro where the surficial aquifer raster from the Series 926 (fig_20_thickness_surficial_raster) dataset was subtracted from the ground elevation raster file.

While the Brunswick aquifer system (BAS) naturally occurs as two layers with an intervening confining unit, it was treated as one layer in the middle of the upper confining unit for simplicity. Available data on the thickness and vertical location of the BAS is limited. Due to the limitations of consistent data, the vertical layers of the BAS were estimated using the thickness of the upper confining unit (UCU) obtained from Series 926 (plate3_thickness_UCU_raster). It is generally accepted that the BAS sits within the UCU above the UFA. For this model, the BAS layer was placed in the middle of the UCU. Using the raster calculator function, the thickness of the UCU raster was divided by three. The top of the BAS was then generated by subtracting the surficial aquifer layer by the one-third UCU thickness raster file. The extent of the BAS within the model (**Figure 3.6**) was assigned using a USGS shapefile (fig21_IAS_ICU_permeable_zone_extent) from Series 926. This shapefile was clipped to the model boundary in ArcGIS Pro to create a polygon used for establishing the Brunswick aquifer in Layer 3 of the model. The bottom of the surficial aquifer was then created by the same method using the top of BAS in place of the surficial aquifer layer. The bottom of the UCU is the

same as the top of the UFA, so the Series 926 file representing the top of the UFA (plate4__Top_FAS_raster) acted as the base of the UCU. Finally, the base of the entire model was established using the Series 926 file depicting the top of the middle confining unit (MCU) (mcu_regional_raster).

When inputting these layers into VMF, the topography layer was set as "erosional" to tell the system this is a surface layer. The bottom MCU layer was assigned as the "base" of the model. The other layers were all set as "conformable" so that each layer was established vertically in reference to the layer above it so that they "conform' to the shape of upper layer.

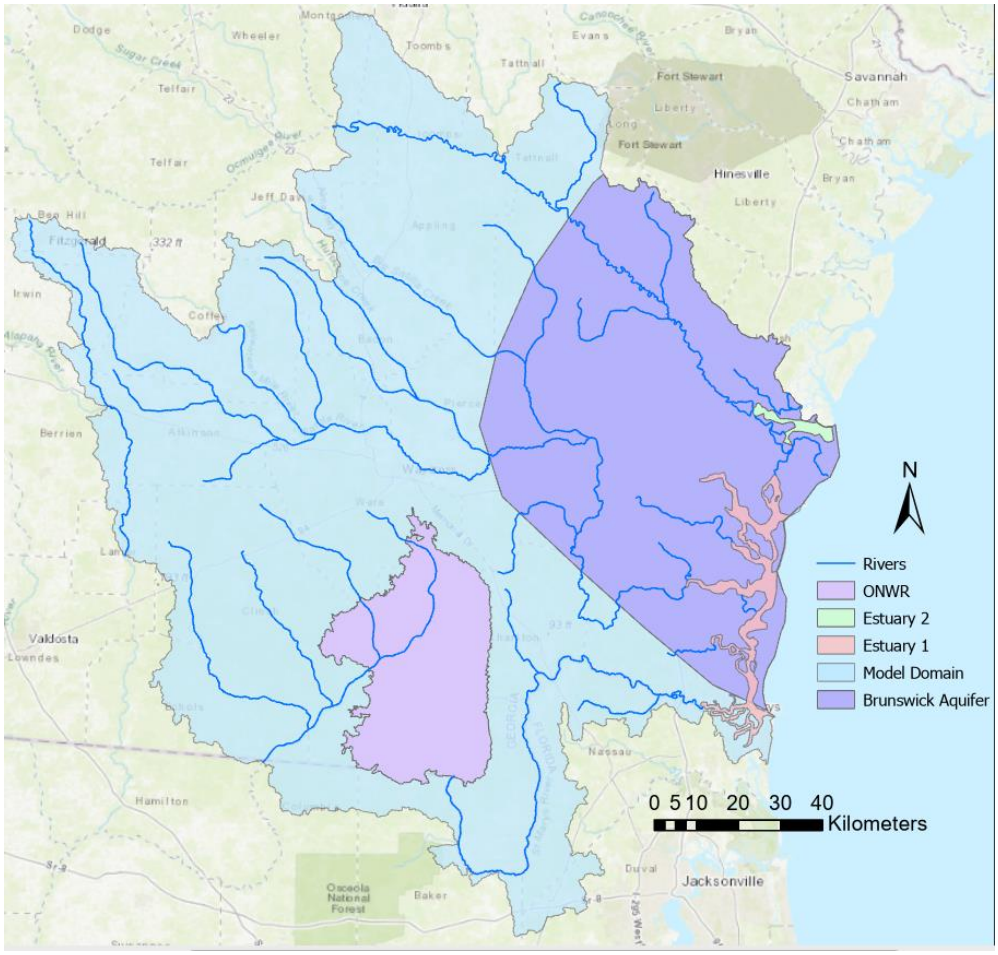

Figure 3.6: Regional model domain with estimated extent of Brunswick Aquifer.

Table 3.3: List of Series 926 files used for all models.

File Name	Series 926 Description	Usage
fig_20_thickness_surficial_raster	Thickness raster surface for surficial deposits	Used to estimate top layer of UCU
plate3_thickness_UCU_raster	Thickness of the UCU	Used to estimate placement of Brunswick aquifer
plate4__Top_FAS_raster	Raster surface depicting the top of the Floridan aquifer system	Used at top of UFA (bottom of UCU)
mcu_regional_raster	Raster surface depicting the top of the regional middle confining unit (base of Upper Floridan aquifer)	Used as base layer of model
fig21_IAS_ICU_permeable_zone_extent	Extent lines for permeable zones of the intermediate aquifer system and Brunswick aquifer system	Used to develop a polygon of the extent of the Brunswick aquifer

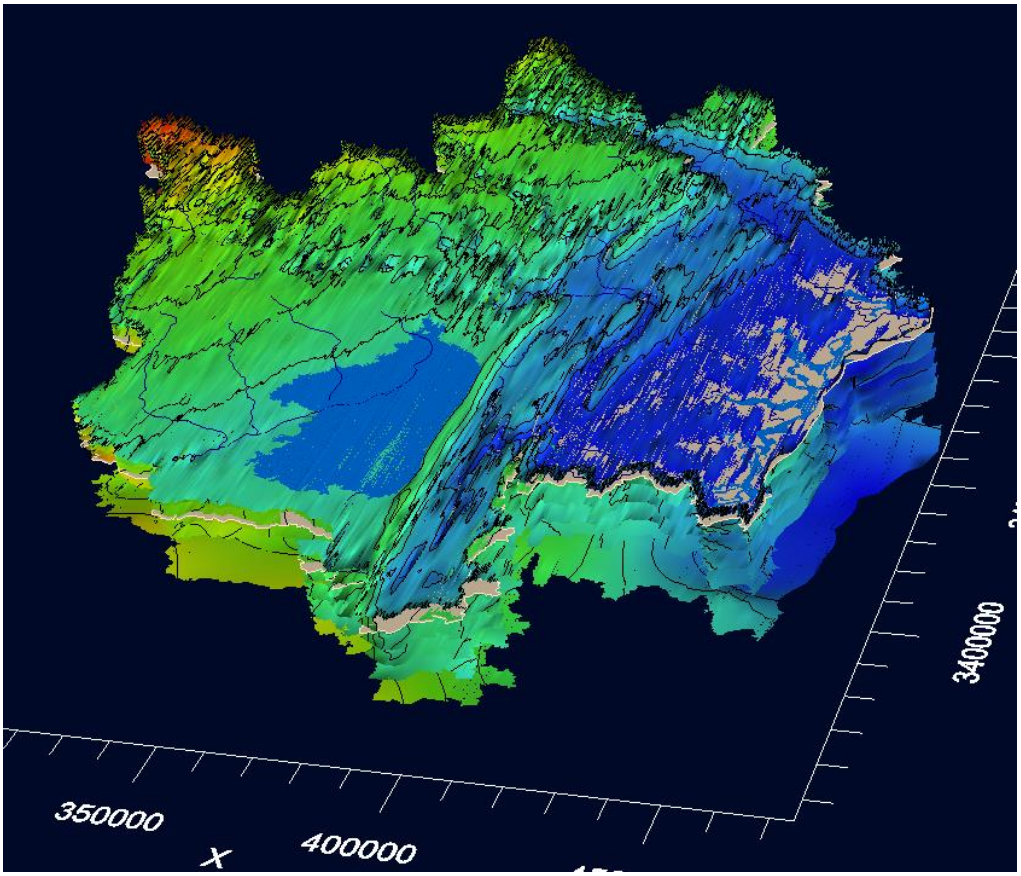

Figure 3.7: 3D perspective of the surface layers of regional model as shown in VMF.

3.4 Model Properties

3.4.1 Hydraulic Conductivities

The hydraulic conductivities for the model layers were established based on the previous study of this region (Landers, 2022). For the initial development of the regional model, vertical and horizontal conductivities were assigned the same value. **Table 3.4** shows the sources and estimated for hydraulic properties by layer from the previous study (Landers, 2022).

Table 3.4: Data sources for hydraulic conductivity by layer for regional model (Lander, 2022).

Layer	Source	Transmissivity (ft^2/day)	T (m^2/s)	Kh (ft/day)	Kh (m/s)	Kv (ft/day)	Kv (m/s)	Type
Layer 1- Surficial Aquifer	USGS Scientific Investigations Report 2019-5035	14 - 6,000	1.51E-05 - 6.45E-03	105	3.70E-04	105	3.70E-04	Model Input
	USGS Scientific Investigations Report 2005-5065	500	5.38E-04	6	2.12E-05	6	2.12E-05	Reported
	Ground-Water Conditions and Studies in Georgia, 2004-2005	6,000	6.45E-03	70	2.47E-04	70	2.47E-04	Reported
	USGS Scientific Investigations Report 2005-5089	14 - 6,700	1.51E-05 - 7.2E-03	70	2.47E-04	70	2.47E-04	Reported
	USGS Scientific Investigations Report 2010-5072	1,000 - 10,000	1.08E-03 - 1.08E-02					Reported
Layer 2-4 -Upper Confining Unit	USGS Professional Paper 1807			1.00E-03	3.53E-09	1.00E-03	3.53E-09	Reported
	USGS Scientific Investigations Report 2015-5061			5.30E-05 - 3	1.87E-10 - 1.06E-05	5.30E-05 - 3	1.87E-10 - 1.06E-05	Reported
	USGS Scientific Investigations Report 2005-5089			5.30E-05 - 3	1.87E-10 - 1.06E-05	5.30E-05 - 3	1.87E-10 - 1.06E-05	Reported
	USGS Scientific Investigations Report 2019-5035			1.70E-04 - 0.2	5.99E-10 - 7.06E-07	1.70E-04 - 0.2	5.99E-10 - 7.06E-07	Simulated
				1.00E-05	3.53E-11	1.00E-05	3.53E-11	Model Input
Layer 3- Brunswick Aquifer Zone	USGS Professional Paper 1807	15 - 4,700	1.61E-05 - 5.05E-03					Reported
	USGS Scientific Investigations Report 2015-5061	20 - 4,700	2.15E-05 - 5.05E-03	10 - 20	3.53E-05 - 7.06E-05	10 - 20	3.53E-05 - 7.06E-05	Model Input
	USGS Scientific Investigations Report 2005-5089	15 - 4,700	1.61E-05 - 5.05E-03	50	1.76E-04	50	1.76E-04	Model Input
	USGS Scientific Investigations Report 2019-5035			10 - 20	3.53E-05 - 7.06E-05	10 - 20	3.53E-05 - 7.06E-05	Model Input
	Ground-Water Conditions and Studies in Georgia, 2004-2005			20	7.06E-05	20	7.06E-05	Reported
	Ground-Water Conditions and Studies in Georgia, 2002-2003			2	7.06E-06	2	7.06E-06	Reported
Layer 5-Upper Floridan Aquifer	USGS Data Series 669	98,000 (AVG from Aquifer Pump Test)	1.05E-01					
	USGS Scientific Investigations Report 2019-5035	40,000 (AVG from Specific Capacity Data)	4.30E-02	750 - 3,415	2.65E-03 - 1.20E-02	750 - 3,415	2.65E-03 - 1.20E-02	Model Input
	USGS Scientific Investigations Report 2005-5089	530 - 600,000	5.70E-04 - 6.45E-01	150 - 2,819	5.29E-04 - 9.94E-03	150 - 2,819	5.29E-04 - 9.94E-03	Model Input
	USGS Scientific Investigations Report 2010-5072			0.7 - 58,000	2.47E-06 - 2.05E-01	0.7 - 58,000	2.47E-06 - 2.05E-01	Reported
	USGS Scientific Investigations Report 2004-5264	530 - 600,000	5.70E-04 - 6.45E-01	1.34E-03 - 160.4	4.73E-09 - 5.66E-04	1.34E-03 - 160.4	4.73E-09 - 5.66E-04	Reported

3.4.2 Initial Heads

For the conceptual model, an initial head of 20 meters was assigned to the entire model. This value is the same as was used in the previous study (Landers, 2022). However, the model initial heads were adjusted within the numerical model. The initial heads for the numerical model were estimated based on the available monitoring well data within the model domain. A total of four property zones were created to represent the initial heads throughout the model with the top layer (representing the surficial aquifer) having three property zones (**Figure 3.8**) and the layer 5 (representing the UFA) having its own property zone. Two of the top layer (Layer 1) property zones split the model mostly in half around the ONWR to match observed head elevations data and to follow the elevation changes throughout the model. The final property zone on the top layer of the model was applied to only the cells along the Georgia coastline and was assigned to every layer in the model. The western property zone of Layer 1 was assigned an initial head of 40 m, the middle zone an initial head of 20 m, and the coastline 0 m. Layers 2 through 3, representing the BAS and UCU, were assigned an initial head of 20 meters across the full model domain apart from the coastline. Finally, Layer 4 and 5 (representing the bottom of the UCU and the UFA) were assigned an initial head of 15 m.

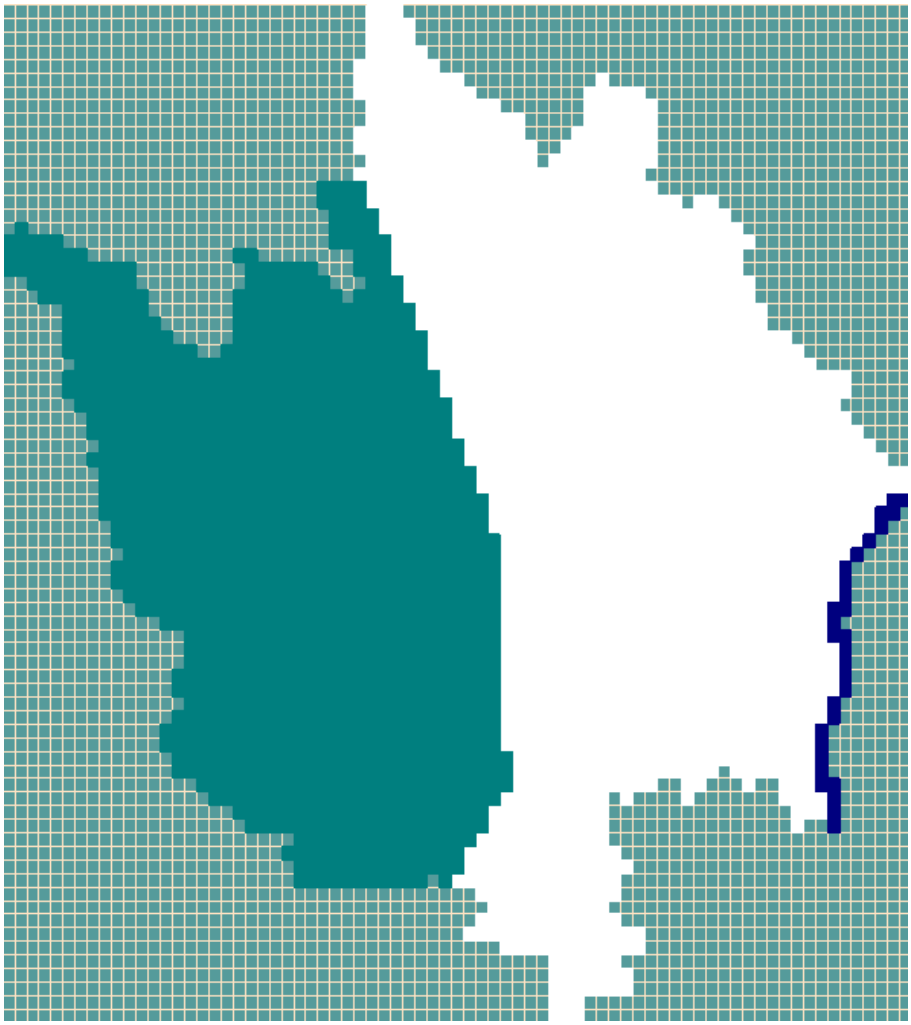

Figure 3.8: Initial heads applied to Layer 1 of the regional steady-state model.

3.5 Boundary Conditions

MODFLOW allows for a variety of different types of boundary condition packages to be used in the groundwater model. VMF's list of boundary condition options include lakes, rivers, constant head and general head boundaries, specified flux boundaries, pumping wells, recharge and drain conditions, evaporation conditions, and a few more options. This model will only use the river (RIV), lake (LAK), recharge (RCH), evaporation (EVT), and specified flux (FHB) boundary condition packages.

3.5.1 Recharge

The initial recharge value used for the conceptual model was established following the same manner as the previous model (Landers, 2022). A constant recharge value was set to the full extent of the top layer of the model to represent the hydrologic inputs from precipitation. The average annual precipitation for this region of Georgia above the FAS was estimated based on USGS Data Series 584 using the annual precipitation shapefile to be 1,397 mm/year (Bellino, 2011). This value also accounts for the effects of evapotranspiration generally across the model domain. Approximating that around 12 percent of precipitation in this region seeping into the surficial aquifer system (Joiner & Cressler, 1993), the final recharge constant used for the initial set up of the model was 167.6 mm/year.

3.5.2 Okefenokee Swamp

The Okefenokee Swamp is a complex and transient hydrological feature with great significance within Georgia. While the borders of the swamp fluctuate with water level changes, an estimate for the domain of the swamp was estimated using a shapefile of the ONWR wetlands area. This shapefile along with a few other GIS shapefiles were originally obtained from representatives of the USFWS and used in the previous version of this conceptual model (Landers, 2022). Once imported into VMF, this shapefile was used to establish the boundaries of a lake (LAK) boundary condition. This type of boundary condition was chosen to best represent the storage function of the swamp.

The lake (LAK) boundary condition allows for the calculation of lakebed conductance within a specific polygon area using inputs such as lakebed thickness and hydraulic conductivity.

Lakebed conductance (C) is calculated by the LAK package using the following equation (Waterloo Hydrogeologic, 2022):

$$C = \frac{L \times K_v \times W \times u}{B}$$

where (K_v) is the vertical hydraulic conductivity of the lakebed, (W) is the width of each grid cell, (L) is the length of each grid cell, (B) is the lakebed thickness, and (u) is a conversion factor for converting (K) to [L] and [T] units.

VMF also asks for users to input a few other parameters when setting up a lake boundary condition including stage, lake bottom, precipitation per unit area, evaporation per unit area, overland runoff, and artificial withdrawal rate. These values were the same as were used in the previous model study (Landers, 2022). An average stage of 1.0 m (Loftin & Kitchens, 2001) and an average peat layer thickness of 1.5 m (Bellino, 2011; Smedley, 1968) were used to establish a total lake depth of 2.5 m. The lake bottom was assigned using a surface file created by subtracting the ground surface DEM by 2.5 m using the Raster Calculator in ArcGIS Pro and the ground surface DEM was assigned as the lake stage. The lakebed thickness was assigned a constant value of 1.5 m (Smedley, 1968). The hydraulic conductivity of the wetland peat soils is estimated to have a range between 1.6E-01 m s^{-1} and 1.7E-03 m s^{-1} (Rizzuti et.al., 2004), so a bed conductivity of 1.6E-03 m s^{-1} was initially used for the previous model study (Landers, 2022). However, because hydraulic heads beneath the swamp in the previous model (Landers, 2022) initial results were too high to reasonably reflect real-world conditions, the bed conductivity was incrementally lowered during model calibration. The final value after calibration, a bed conductivity of 1.6E-07 m s^{-1}, was initially assumed for this model. Annual precipitation was assigned a value of 1298 mm yr^{-1} and evapotranspiration was assigned a value of 1032 mm yr^{-1} (Yin & Brook, 1992). Because around 72-78% of water input into the swamp is

from direct precipitation, overland flow contributions are assumed to be negligible. The artificial withdrawal rate from the swamp was also assumed to be absent.

3.5.3 Rivers and Streams

A wide variety of rivers and streams fall within the model boundary. Some of the major rivers within the model domain include the St. Mary's, the Satilla, and the Altamaha Rivers. The polylines for the rivers and streams were from the 2 m resolution GIS river shapefile from USGS Data Series 926. This file was imported into ArcGIS Pro and then clipped to the model boundary. There were five creeks that were added to the clipped shapefile using the freehand draw tool and the topography map layer provided in ArcGIS Pro. The five creeks added to the shapefile were Buffalo, Spanish, White Oak, Tatum, and Hog Creeks. The rivers as shown in the USGS file continue to widen and eventually split to represent the estuaries that form near the coast. Using these polylines, two polygons (**Figure 3.6**) were generated using the trace feature to represent two estuary features within the model domain. The polylines used to generate these features were then removed from the streams file. This final stream file was then imported into VMF and used for defining the extent of the river boundary condition.

River boundary conditions are used in VMF to model the riverbed conductance, or the flow of surface water within rivers into the aquifer features below. Riverbed conductance (C) is calculated by the river (RIV) package using the same equation as the lake (LAK) package such that (Waterloo Hydrogeologic, 2022):

$$C = \frac{L \times K_v \times W \times u}{B}$$

where (K_v) is the vertical hydraulic conductivity of the riverbed, (W) is the width of river in each grid cell, (L) is the length of river reach in each grid cell, (B) is the riverbed thickness, and (u) is

a conversion factor for converting (K) to [L] and [T] units. **Figure 3.9** shows a 3-dimensional representation of how river boundary conditions are viewed in a grid cell by the MODFLOW software.

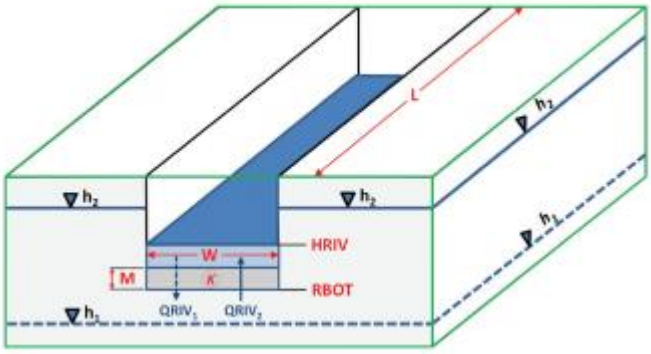

Figure 3.9: 3D representation of a cell with a river boundary condition in MODFLOW (Oliveira & Martins, 2019).

The software automatically sectioned the different rivers at intersections when the polyline file for the rivers/streams was imported into VMF. This generated sixty-two river sections for which riverbed conductance would be calculated using the equation specified above. Following the same principles are the previous model in terms of generating the necessary data for the steady-state model's river boundary condition parameters, the sixty-two river sections were organized into two groups based on river size. A distinction was made between "rivers" and "streams" based on estimates of river width using USGS stream gages and distance measuring tools in both Google Earth and ArcGIS Pro. Since river width is variable with discharge, an average river width across the river section length was assumed for each river section. Rivers with estimated average widths greater than 30 m were designated as a "river" and given a riverbed thickness of 0.5 m. Rivers with a river width equal to or less than 30 m were designated as a "stream" and given a riverbed thickness of 0.25 m. Similarly, a constant stage value was

assigned such that “rivers” were assumed to have an average stage of 2 m and “streams” have an average stage of 1 m. Two new surface files were created for the river sections in the same manner as was done for establishing the lake bottom for the swamp boundary condition. “Rivers” bottom and “streams” bottom surface files were generated in ArcGIS Pro using raster subtraction where the topography DEM file was subtracted by the assumed stage plus the riverbed thickness. In other words, the river bottom files were created by subtracting the topography DEM file by 2.5 m for “rivers” and 1.25 m for “streams”. In VMF, the DEM topography file was assigned for all river section stages and either the “streams” bottom or the “rivers” bottom surface was assigned as the river bottoms.

The Atlantic Coastal Plains region is characterized by its sandy clay soils, so the dominant streambed type is expected to be sand beds. Additionally, this region is also known for its significant recharge rates from rivers into the surficial aquifer systems (Degan et.al, 2020). Sand bed streams have a wide range of hydraulic conductivities, so a median value of 1.04E-06 m/s was chosen to be the best representation for the vertical hydraulic conductivity of all rivers and streams within this model (Wojnar et al., 2013).

3.5.4 Estuaries

As mentioned above, the original USGS river polyline shapefile represents river outlets to the Atlantic Ocean by outlining the edges of the rivers once they reach a certain width. Because this would appear to the VMF software as two separate rivers, two estuary polygon files were created to instead represent these sections of the rivers using the already established USGS polylines as the borders.

The vertical hydraulic conductivity (Kv) of the lakebed in both estuaries was estimated to be 0.015 m d^{-1} (1.736E-07 m s^{-1}) based on meteoric groundwater discharge calibration data from

another study using MODFLOW to model the estuary within the Indian River Lagoon in Florida (Pandit et.al 2011). Precipitation and evaporation rates for the estuary boundary conditions were set to match the values for the Okefenokee Swamp boundary condition based on the assumption that the swamp wetlands likely have similar climate conditions as these estuaries. Additionally, the lakebed thickness parameter was set to 1.5 meters, the same as the Okefenokee Swamp boundary condition. As a result, the same surface file was used for establishing the lake bottoms as was generated for use in the Okefenokee Swamp boundary condition and the topography DEM file was used for the lake stage parameters. Additionally, there was assumed to be negligible overland runoff and artificial withdrawal.

3.5.5 No Flow and Constant Head Boundaries

In instances where a groundwater model extends to coastline, the interface between saltwater and freshwater can be treated as a constant head boundary condition. Because the model boundary was established based on watershed boundaries, the top layer of the model also included a no-flow boundary along the model boundary. The cells outside of the model domain are automatically labeled as inactive cells, so no actions were necessary to establish the no-flow boundaries.

Only one constant head boundary condition was initially applied to the coastline of the model, but a second constant head boundary condition was necessary for model convergence (**Figure 3.10**). Cells along the coastline that do not have river or lake boundary conditions applied were assigned a constant head boundary condition such that the starting and ending heads are 0. The second constant head boundary was applied to the southwestern side of the model domain where the results initially produced large hydraulic heads. This constant head

boundary was adjusted throughout the calibration process but was initially assigned a value of 40.5 m for both starting and ending heads based on observational data and the necessary conditions for the model to converge.

Figure 3.10: Constant head boundary conditions (red) in layer 2 of the regional steady-state model.

3.5.6 Pumping Wells

The last boundary condition established for this model were the Chemours pumping wells for both the Mission Mine and Amelia Mine sites. Groundwater withdrawal logs were provided by Chemours for this project and used to establish groundwater withdrawals. Chemours withdraws groundwater from the Upper Floridan aquifer at both the Mission Mine and Amelia Mine sites.

At the Mission Mine site, Chemours withdraws their groundwater through two wells but, due to the closeness of the two pumping wells in comparison to the model size, the wells were simplified to one well using Chemours' total monthly withdrawal rates for their Mission Mine operations during the 2021 water year. The well selected to be represented in the model extends 700 ft below the ground surface with a well screen beginning at 510 ft below the ground surface. The well was placed at coordinates (406884 m E, 3435700 m N) within the model with a maximum well depth (Zmax) below the surface being 700 ft (213.36 m) and a minimum depth (Zmin) of 0. Similarly, the well screen was established using the "measured depths" option using a bottom depth of 700 ft (213.36 m) and a top depth of 510 ft (155.448 m). Since the regional model only runs for 1 day, and daily withdrawal data was not available, the monthly total water withdrawn during October (5,116,00 gallons) was divided by 31 days to achieve an estimated daily water withdrawal rate of 165,032 GPD (624.71 $m^3 d^{-1}$). The withdrawal total in October was the highest recorded for the 2021 water year, so this rate was nearly two times higher than the average (358.60 $m^3 d^{-1}$) for this site. Regardless, the October rate was used to that the model simulations could be calibrated using October 1st recorded water levels from the Chemours monitoring wells.

Only one pumping well was determined to be located at the Amelia Mine at the time of the study. The pumping well at this site has a well depth of 720 ft and is not screened. The Amelia Mine pumping well boundary condition was placed at coordinates (410371 m E, 3498423 m N) with a Zmax of 720 ft (219.46 m) and a Zmin of 0 m. A screen was assigned to the well using measured depths with a bottom depth of 219.46 m and a top depth of 174.121 m. The total withdrawal amount for the Amelia Mine site for October was 12,871,000 gal (1,571.68 $m^3\ d^{-1}$). The amount of groundwater withdrawn in October was slightly lower than the average (1,886 $m^3\ d^{-1}$) for this site during 2020.

3.6 Numerical Model and Grid

3.6.1 Grid Spacing

A finite-difference approach was chosen for developing the numerical model and finite-difference mesh was generated within MODFLOW using a 75x75 cell grid (**Figure 3.11**). With this grid spacing, each cell has a height of about 2.936 km and a width of 2.624 km.

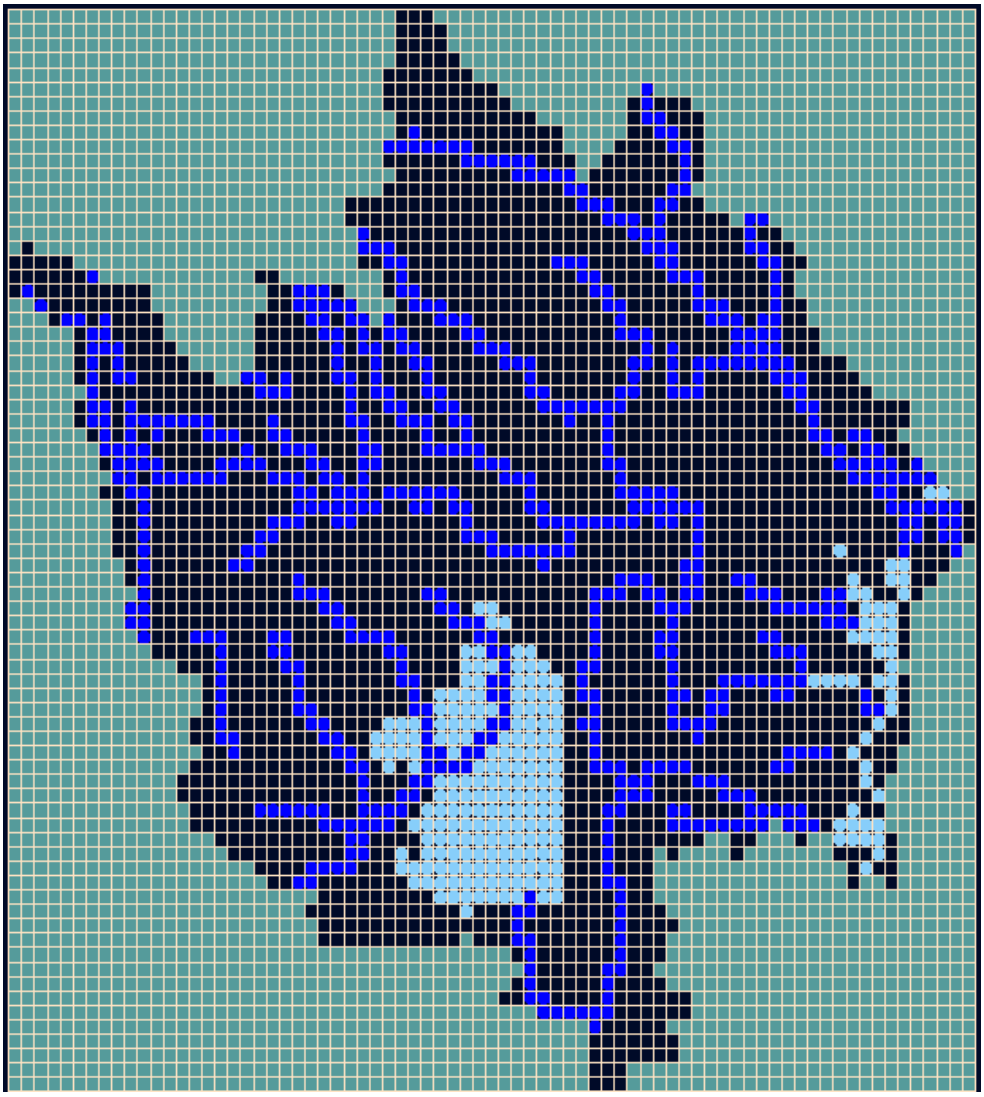

Figure 3.11: Numerical model with finite-difference grid and relevant boundary conditions.

3.6.2 Translation Settings

A single run was selected for the run-type and MODFLOW-2005 was selected for the flow engine. The default property package, Layer-Property Flow, and default solver option, Conjugate Gradient Solver (PCG), were also selected. Under the Conjugate Gradient Solver settings, only the maximum outer iteration (MXITER), maximum inner iteration (ITER1), and cell rewetting were modified from the default settings. For initial simulations, the maximum

outer iteration was set to 300 and the maximum inner iteration set to 150. Cell rewetting was enabled and the option to allow rewetting from the bottom and sides of cells was selected. Without cell rewetting, cells that become "dry" by reaching a head value of 0 remain dry for the rest of the simulation. Cell rewetting was enabled to prevent dry cells from acting as barriers to groundwater flow during the simulation. This setting likely had a greater effect on the transient local model than either of the steady-state models.

3.7 Local Model Development

In addition to the regional model, a secondary localized model was developed to test the process of developing a transient model due to its reduced data needs. This model is also useful to examine the movement of groundwater around the Mission Mine site in greater detail. The local model focuses on the interactions between the Mission Mine site and the surficial aquifer within the watershed surrounding the mine site.

The process for developing this local model was the same as for the regional model, except that many of the additional features that were added to the regional model were not necessary for the local model. More specifically, because the local model only considers the surficial aquifer, only the ground elevation DEM surface and the top of the UCU surface were used for constructing the model layers. Additionally, only a few of the boundary conditions that were developed in the regional model were used in this model.

The new model domain was established in ArcGIS Pro using the same watershed HUC8 files that were used for the regional model. However, only the polygon representing the watershed area in which the Mission Mine site resides was used for developing the new model domain shapefile (**Figure 3.12**). Then, the surface files for the ground topography and top of the

UCU were cropped down to the new model domain. Additionally, the surface files representing the bottom of both "rivers" and "streams" were cropped to the new model domain. Since neither the Okefenokee Swamp nor either of the estuary zones fall within this model's domain, their boundary conditions and surface files were not needed. However, the river bottom and stream bottom surface data were clipped to the model domain. Only a section of the Satilla River and Buffalo Creek are present within the local model domain. This section of the Satilla River has one USGS stream gage upstream of the point where Buffalo Creek flows into the Satilla.

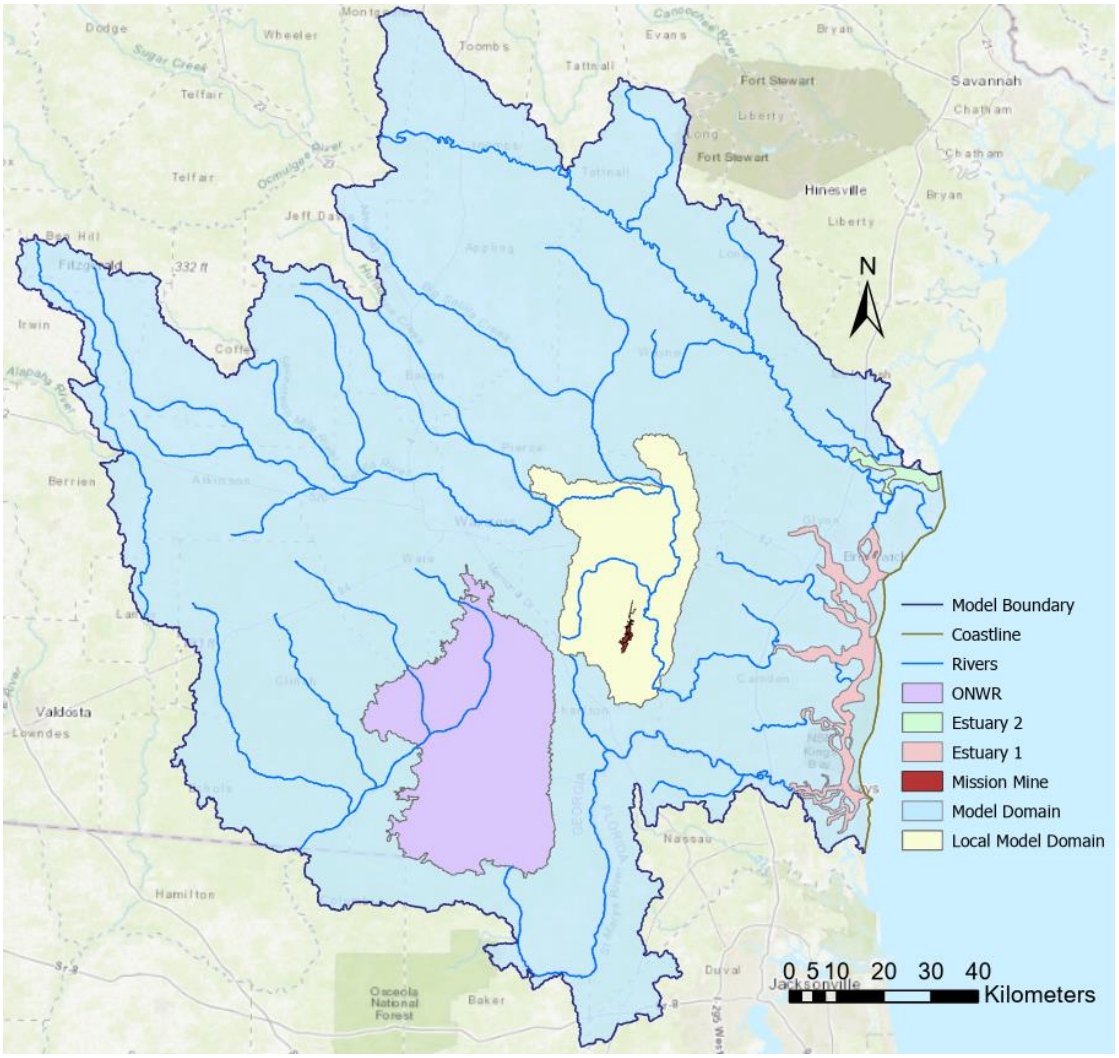

Figure 3.12: Overlay of local model domain compared to regional model domain with relevant hydrological features.

A uniform initial head value of 20 m was established for the entirety of the local model. This initial head value of 20 m was also used with the previous model and falls within the range of observed head values from the yearly monitoring well data provided by Chemours for their Mission Mine site (Landers, 2022).

Both Chemours pumping wells at the Mission Mine site draw water from the UFA, so this pumping well boundary condition was not included in the local model. **Figure 3.13** shows the well location within the local model domain for reference.

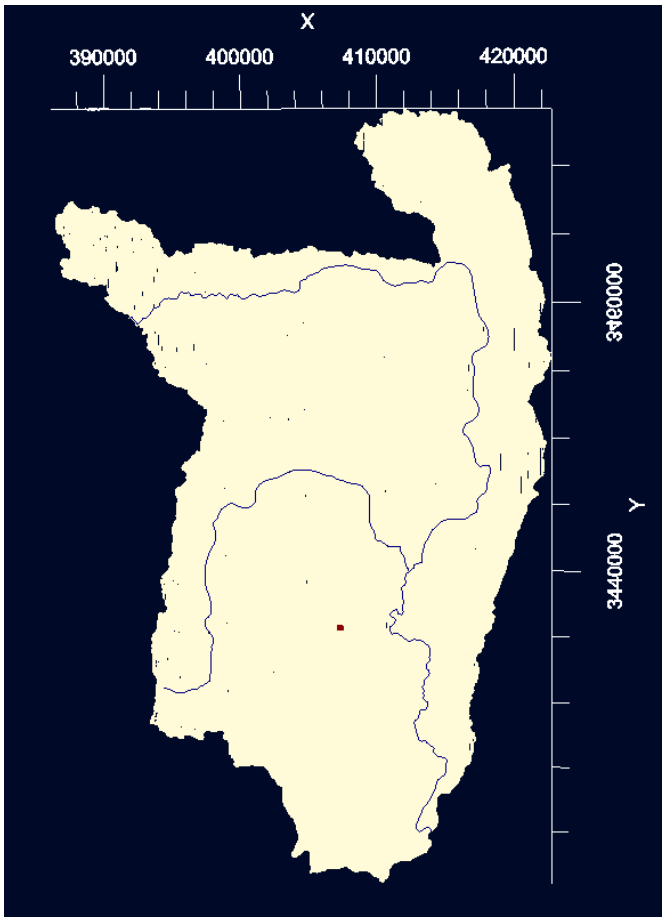

Figure 3.13: Chemours pumping well location within local transient model.

Like the regional model, a finite-difference grid was generated for the development of a numerical model, but this time using a 50 by 50 cell grid. This grid spacing yielded a cell height of 1162.787 m and a cell width of 732.835 m. The same translation settings and convergence criteria were selected for the steady-state local model as the regional model.

3.8 Local Transient Model

Generally, the effects of changes in the environment on groundwater flow manifest within a few hours to a few days, so the time interval of interest for the model aimed to look at changes at the daily level (Pinder 2002). Developing a transient model involves incorporating time-sensitive data into the boundary conditions of the model. Specifically, this is done in VMF using Excel sheet with observed or estimated data representing the changes in hydrological conditions that occur naturally over a specified period. Examples of how transient data can be included in MODFLOW models include adding a time series for pumping wells, river and lake stages, and specified fluxes. The initial time values for the transient version of the local model were at the daily scale from October 1, 2020, to September 30, 2021, to represent the 2021 water year.

3.9.1 Recharge

Precipitation values for the transient model were obtained through the National Climatic Data Center's (NCDC) online weather database called Climate Data Online (CDO). For the local model precipitation data for the 2021 water year were obtained using the NAHUNTA 6 S, GA US (US1GABY0001) station in Brantley County, GA. The 2021 water year represents a somewhat wetter than average year based on the precipitation records for this station going back

to 1902. However, the degree to which it seems to deviate from the average year does not suggest that the 2021 water year represents an extreme case in terms of precipitation. These daily precipitation rates were then multiplied by 0.12 to represent the estimated 12% of precipitation that is recharged into the surficial aquifers in this region (Joiner & Cressler, 1993). After converting these values to metric units, the result was a time series of daily recharge (mm/d) with a yearly recharge of 186.13 mm/yr. Because the recharge boundary condition in VMF requires units of mm/yr, VMF automatically converts the mm/d values to mm/y by multiplying each value by 365 after loading the Excel sheet into the program, so no further unit changes were necessary (**Table 3.7**).

Table 3.5: Monthly summation of daily precipitation and recharge for local transient model

MONTH	PRCP (in.)	PRCP (mm)	RCH (mm/m)
Oct-20	2.90	73.78	8.85
Nov-20	3.27	83.19	9.98
Dec-20	2.07	52.66	6.32
Jan-21	2.22	56.48	6.78
Feb-21	5.55	141.19	16.94
Mar-21	3.72	94.64	11.36
Apr-21	4.25	108.12	12.97
May-21	1.78	45.28	5.43
Jun-21	4.38	111.43	13.37
Jul-21	12.81	325.89	39.11
Aug-21	9.15	232.78	27.93
Sep-21	8.87	225.65	27.08
Total	**60.97**	**1551.08**	**186.13**

3.9.2 Rivers and Streams

Daily stage height records for the USGS Satilla River stream gage (02228000) within the model domain was obtained from the USGS online database for the 2021 water year. Since a

gage was not available for Buffalo Creek, the stage for this creek was assumed to be 1 m below the daily record for the Satilla River. These records were imported into Microsoft Excel and then organized to make a time series for each river. For each stream gage, the distance between the gage and the NAVD88 datum was added to the recorded river stage to match the model vertical elevation. For stream gages where the datums are NAVD29, the estimation that NAVD88 is NAVD29 – 1.15 feet (0.33 meters) based on the difference between the adjusted elevation height using the NAVD88 datum and the previous elevation records using NAVD29 from the National Geodetic Survey's vertical control point (X110) in Nahunta, GA. The records for this site's elevation adjustment were obtained through the National Geodetic Survey Data Explorer.

A new method for representing the river bottoms was necessary for the transient model because the observed stage heights from the gage data sometimes dropped below the assumed average stage used for developing the river bottoms layer. As a result, an error occurs where the river stage drops below the height of the river bottoms. Instead, the depths of the river bottoms were established by subtracting 0.01 m from the lowest corrected stage values for each river. This guaranteed that the river stage was always above the river bottoms by at least 1 cm.

3.9.3 Wetlands

The previous model study (Landers, 2022) included a series of freshwater wetlands around the Mission Mine site as another set of lake boundary conditions. These wetlands (**Figure 3.14**) were added to the transient version of the local model to examine the potential influence they may have on the local hydrology around the mine site. The same parameters and values used in the Landers model were again used in the transient local model. There was not any additional data on the wetlands available by the time of this study, so the parameters for the

wetlands were assumed based on reasonable estimation. The wetlands were assumed to have a stage of 1 m and a bed thickness of 0.25 meters. The lake stage was assigned using the DEM surface file and the lake bottom was defined using the stream bottom surface file since these two boundary conditions have the same assumed total depth. The remaining inputs for the wetlands were the same values as the Okefenokee Swamp boundary condition.

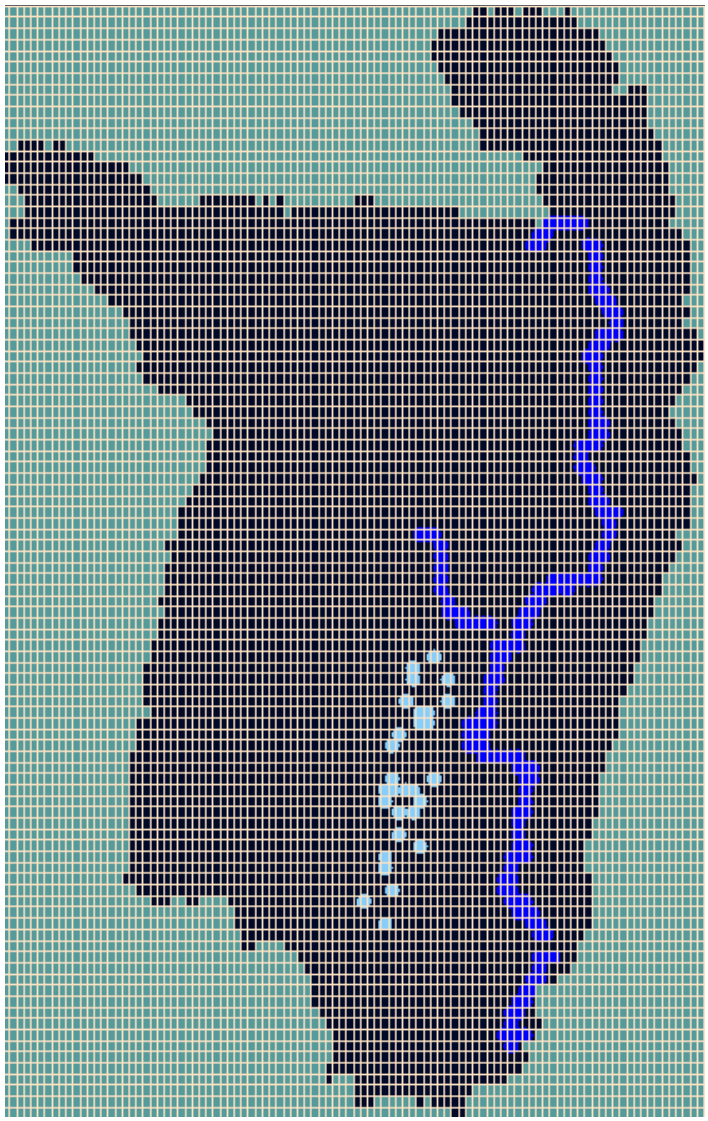

Figure 3.14: Wetlands boundary condition applied to transient local model (layer 1).

3.9.3 Transient Numerical Model

The numerical model for the transient local model was developed using a 100 by 100 cell finite-difference grid. This grid spacing yielded cells with a height of 581.393 m and a width of 366.418 m. This grid (**Figure 3.15**) was also separated into four vertical layers so that a more detailed analysis of the direction of groundwater flows within the SAS around the Mission Mine site could be done.

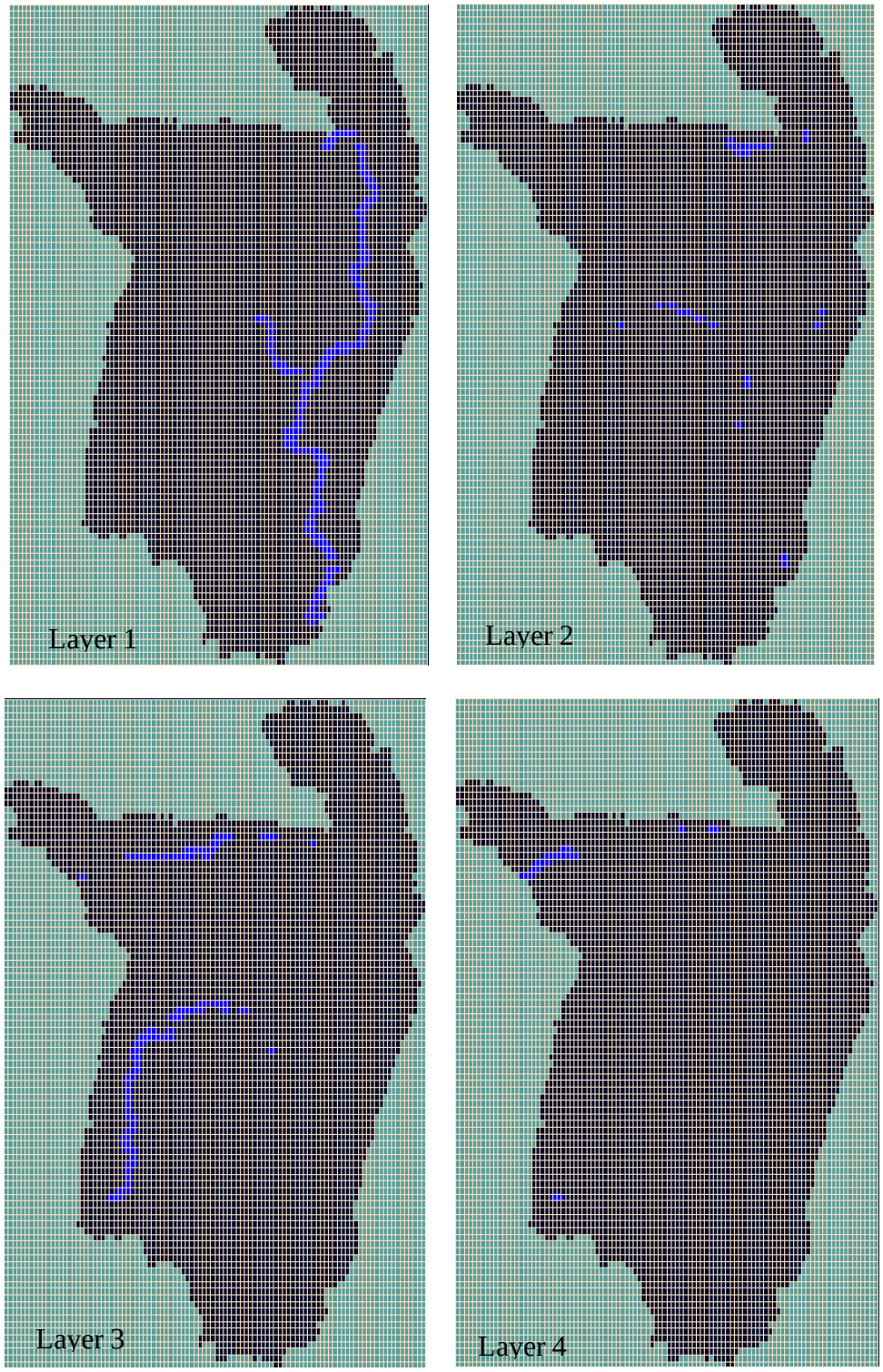

Figure 3.15: Finite-difference grid generated for the transient local model with river boundary conditions.

3.9 Model Calibration

3.9.1 Observation Data Sources

After all three of the models were fully developed and had completed an initial run successfully, it was necessary to examine the accuracy of the model to produce results that were reasonably within the range of expectations when compared to real-world observations and field data. The goal of model calibration is to a take a simplistic model and add details and heterogeneity to produce results that better replicate observed values. Local changes do not typically have substantial impacts on broader groundwater conditions, so the focus of calibration should be to add complexity gradually by altering larger-scale property zones rather than adding more zones to the model unless adding more zones becomes ultimately necessary. Equally important in calibration is incorporating a wide array of observational data because different model results, such as velocity and water table elevations, may be more sensitive to changes in different model attributes (Pinder, 2002).

Field monitoring data was provided by Chemours from their multiple groundwater monitoring wells located throughout their Mission Mine property (**Figure 3.16**). Because many of these wells would fall within the same cells in the numerical grid for both the local and regional models, eight wells were selected from the provided list and used for model calibration (CC1, CC2, DD1, WW1, IBM-W4, and Z). These wells were chosen based on their location before examining their comparison to any model results and were selected such that each cell involved would only be represented by one monitoring well. The well data provided represents water level compared to the ground surface in feet and was obtained using piezometers. The land surface elevation at each well was estimated using the DEM file for the ground surface. The well monitoring data was then converted into a daily average in meters. Their records for Mission

Mine did not cover the full 2020 water year and only data up to February 24th, 2021 was available.

In addition to the data provided by Chemours, observational well data for the 2021 water year was obtained through the USGS and St. Johns River Water Management District (SJWMD) online water databases. The locations of both surface stream gages and groundwater well gages operated by the United States Geological Survey (USGS) within Georgia were obtained from the USGS Water Database website. The point file was then used in ArcGIS Pro to determine the number and locations of USGS stream and groundwater gages throughout the model boundary. There are nine groundwater wells and sixteen stream gages through USGS within the model boundary (**Figures 3.17 and 3.18**). A list of the USGS groundwater wells within the model domain and their relevant information is provided in **Table 3.6**. Additional groundwater wells and their relevant data were also located through the St. Johns River Water Management District (SJRWMD) hydrologic data interactive map (SJWMD, n.d.). From the SJWMD source, another ten groundwater wells (five for the surficial aquifer and five for the Upper Floridan aquifer) were identified and their locations added as points in ArcGIS Pro (**Figure 3.19)**. A list of these wells and their associated aquifers is provided in **Table 3.7**. In places where well data was missing or there were outliers that were beyond a reasonable difference compared to previous years of data, data was interpolated between assumed correct estimate points. The decisions for what data were presumed unreasonable were also compared to any notes referencing the quality or accuracy of the recorded data by its authors.

Figure 3.20 shows the ground water level in meters above the North American Vertical Datum of 1988 (NAVD88) for the USGS and SJWMD wells within the model domain for October 1st, 2020. Data for October 1st, 2020 was not available for USGS well 33H325, so data

from the next nearest date, October 5th, 2020, was used for this figure instead. The data from this well was only used as a reference and not used for determining the model accuracy. The groundwater levels shown in this figure are representative of the surficial aquifer, UFA, and BAS. A closer image of the observed water levels near the city of Brunswick is shown in **Figure 3.21**.

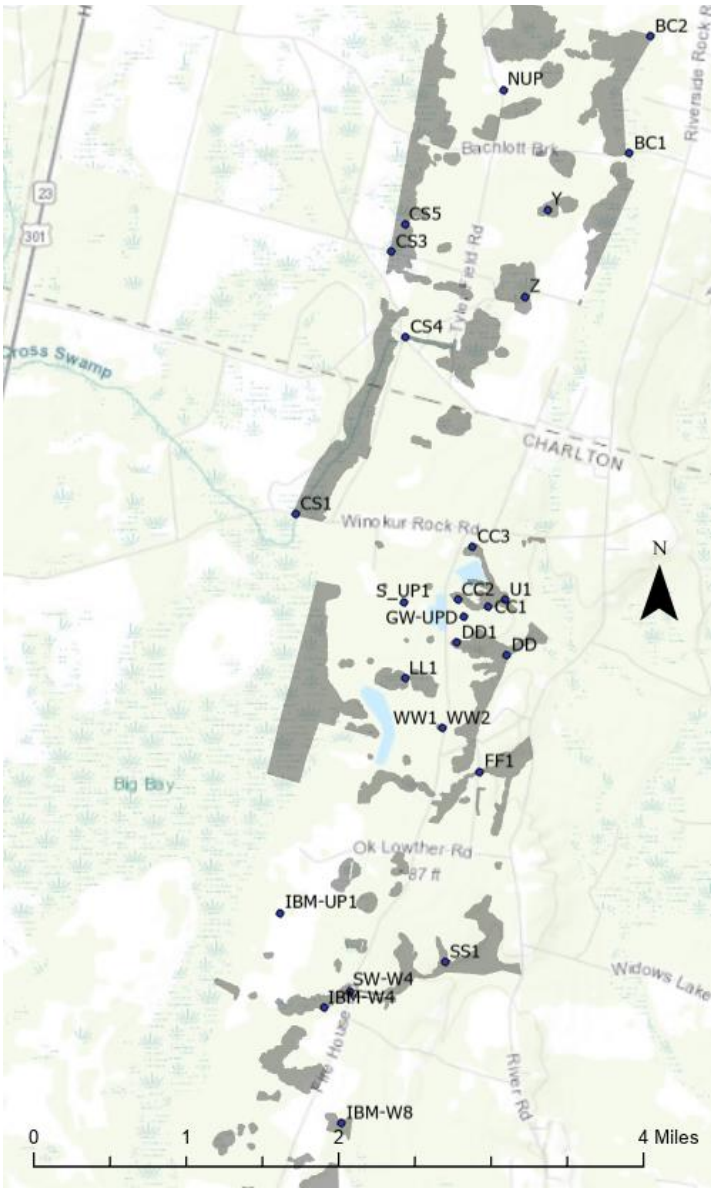

Figure 3.16: Locations of wetlands and Chemours groundwater monitoring wells at the Mission Mine site.

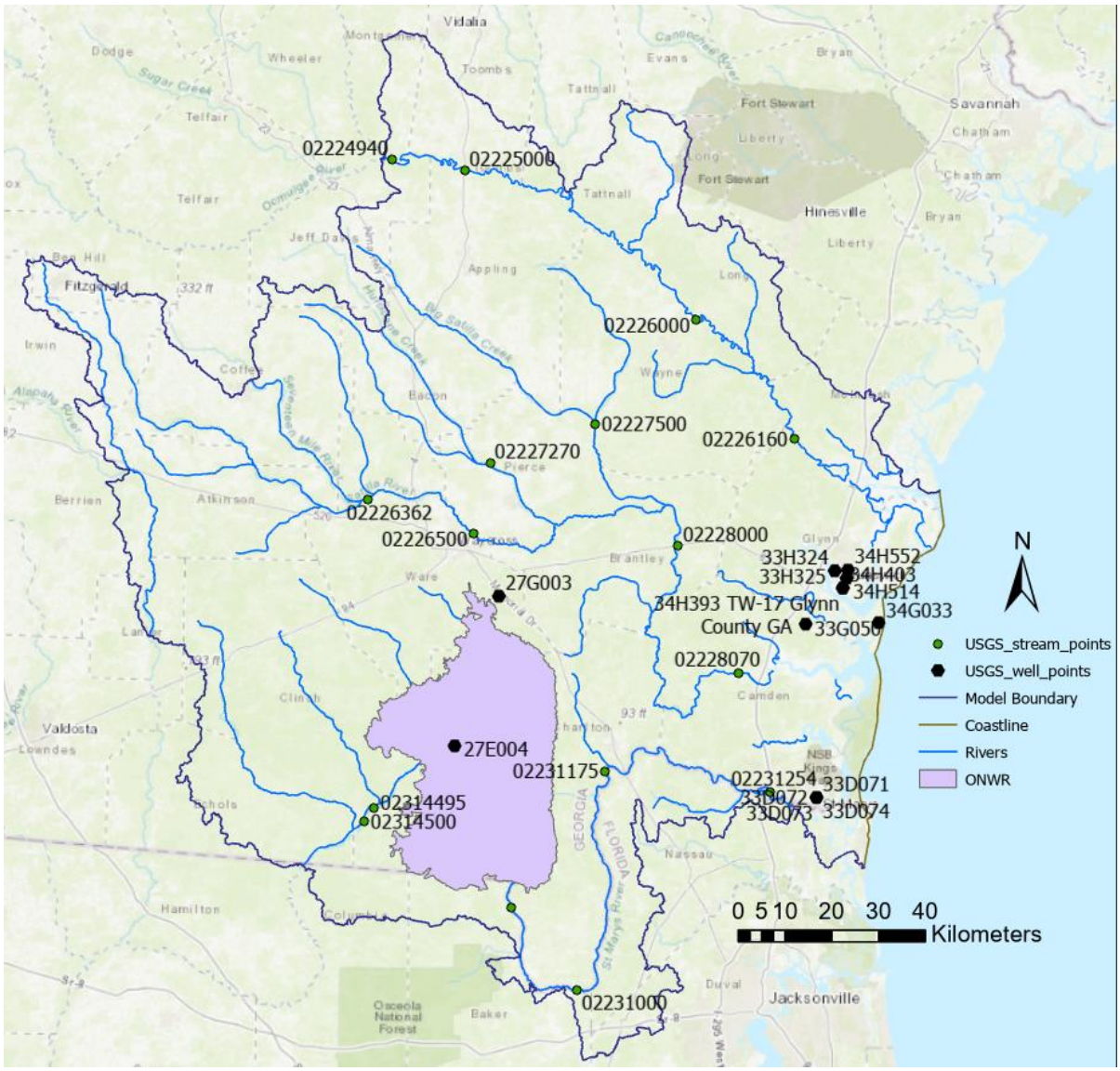

Figure 3.17: Locations of USGS stream and groundwater well monitoring locations within model domain.

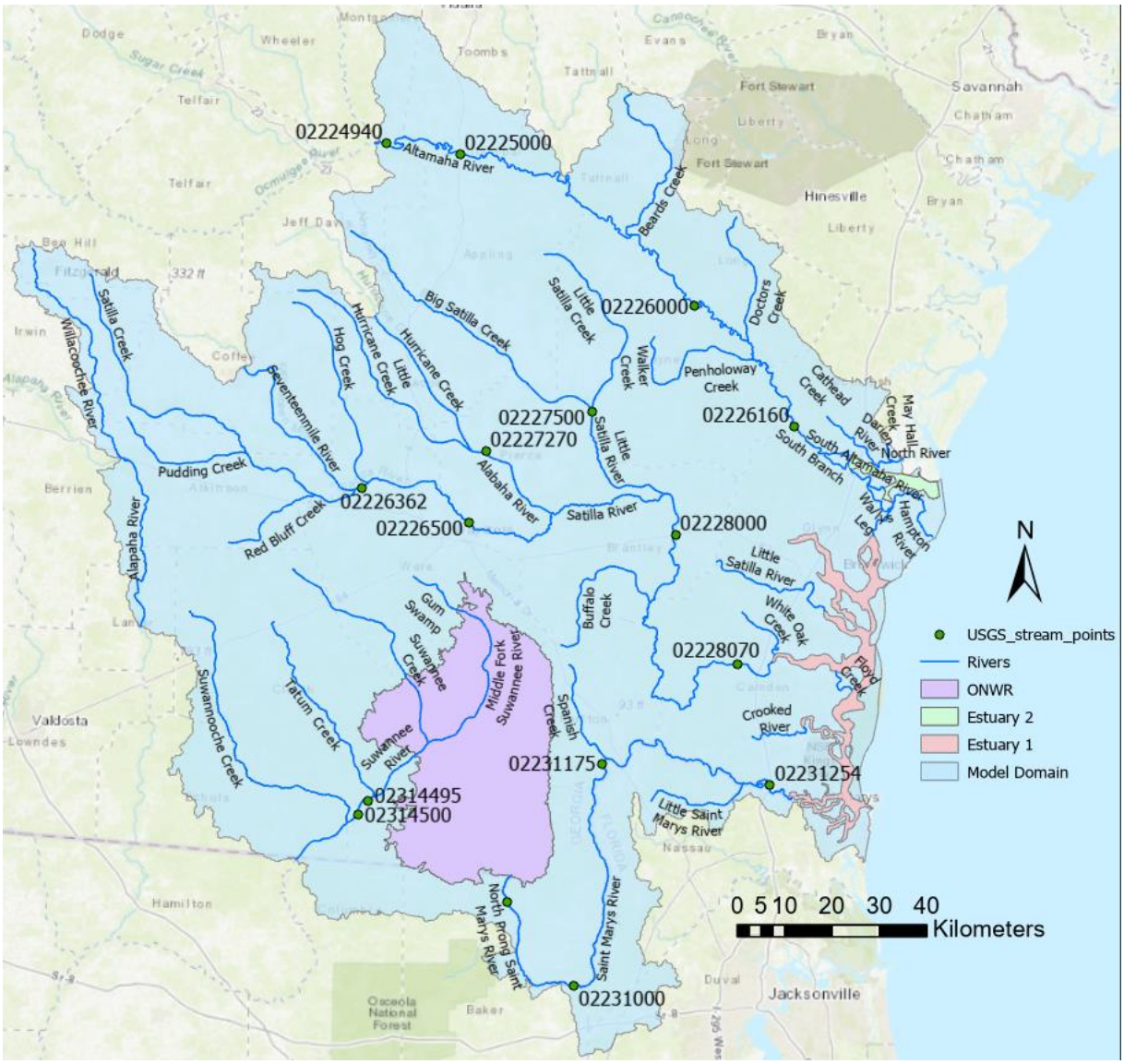

Figure 3.18: Modeled stream names and locations of USGS stream monitoring points within model domain.

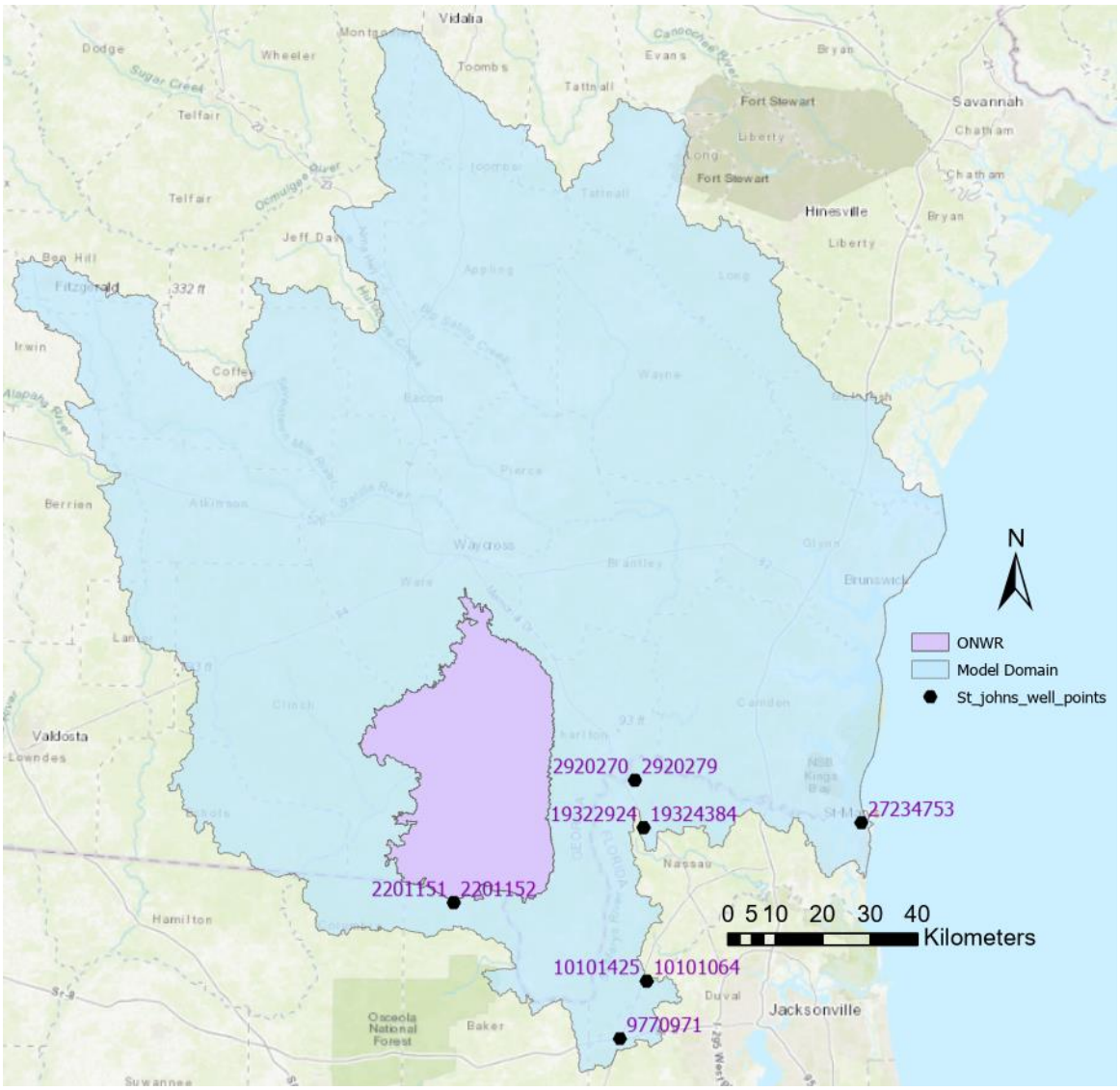

Figure 3.19: Locations and name of SJRWMD groundwater wells within model domain.

Table 3.6: USGS groundwater wells gages within model domain

County	USGS Code	Local Code	Latitude	Longitude	Projection	Aquifer	Well Depth (ft)	Surface Datum
Charlton	USGS 304942 082213 801	27E004	30°49'43	82°21'38	NAD27	UFA	700	NGVD29
Ware	USGS 310706 082155 101	27G003	31°07'06	31°07'06	NAD27	FAS	1856	NGVD29
Camden	USGS 304406 081330 505	33D074	30°44'06	81°33'05	NAD83	LFA	2004	NGVD29
Camden	USGS 310410 081343 801	33G050	31°04'10 .83	81°34'38.9	NAD83	UFA	650	NGVD29
Glynn	USGS 310418 081244 701	34G033	31°04'23 .2	81°24'51.1	NAD83	UFA	751	NGVD29
Glynn	USGS 310822 081294 201	34H403	31°08'18 .8	81°29'41.5	NAD27	FAS	982	NGVD29
Glynn	USGS 310931 081291 002	34H514	31°09'31	81°29'10	NAD83	UFA	685	NAD88
Glynn	USGS 311022 081304 602	33H325	31°10'22	81°30'46	NAD83	UFA	1000	NGVD29
Glynn	USGS 311028 081285 902	34H552	31°10'28 .3	81°28'59.8	NAD83	UFA	750	NAD88

Table 3.7: SJRWMD groundwater well gages within model domain

Station Code	Station Name	Aquifer	Datum
02201152	BA0057 Eddy Fire Tower	UFA	NAVD88
27234753	N-0302 Ft. Clinch State Park at Fernandina Beach	SF	NAVD88
19324384	N-0316 Hilliard Elementary School	SF	NAVD88
19322924	N-0334 Hilliard Elementary School	UFA	NAVD88
10101064	N-0229 Carey State Forest at Baldwin	SF	NAVD88
10101425	N-0237 Carey State Forest at Baldwin	UFA	NAVD88
02920279	N-0221 St. Marys WMA at Boulogne	UFA	NAVD88
02920270	N-0226 St. Marys WMA at Boulogne	SF	NAVD88
02201151	BA0059 Eddy Fire Tower	SF	NAVD88
09770971	D-0254 J-0321 Seaboard Railroad	UFA	NAVD88

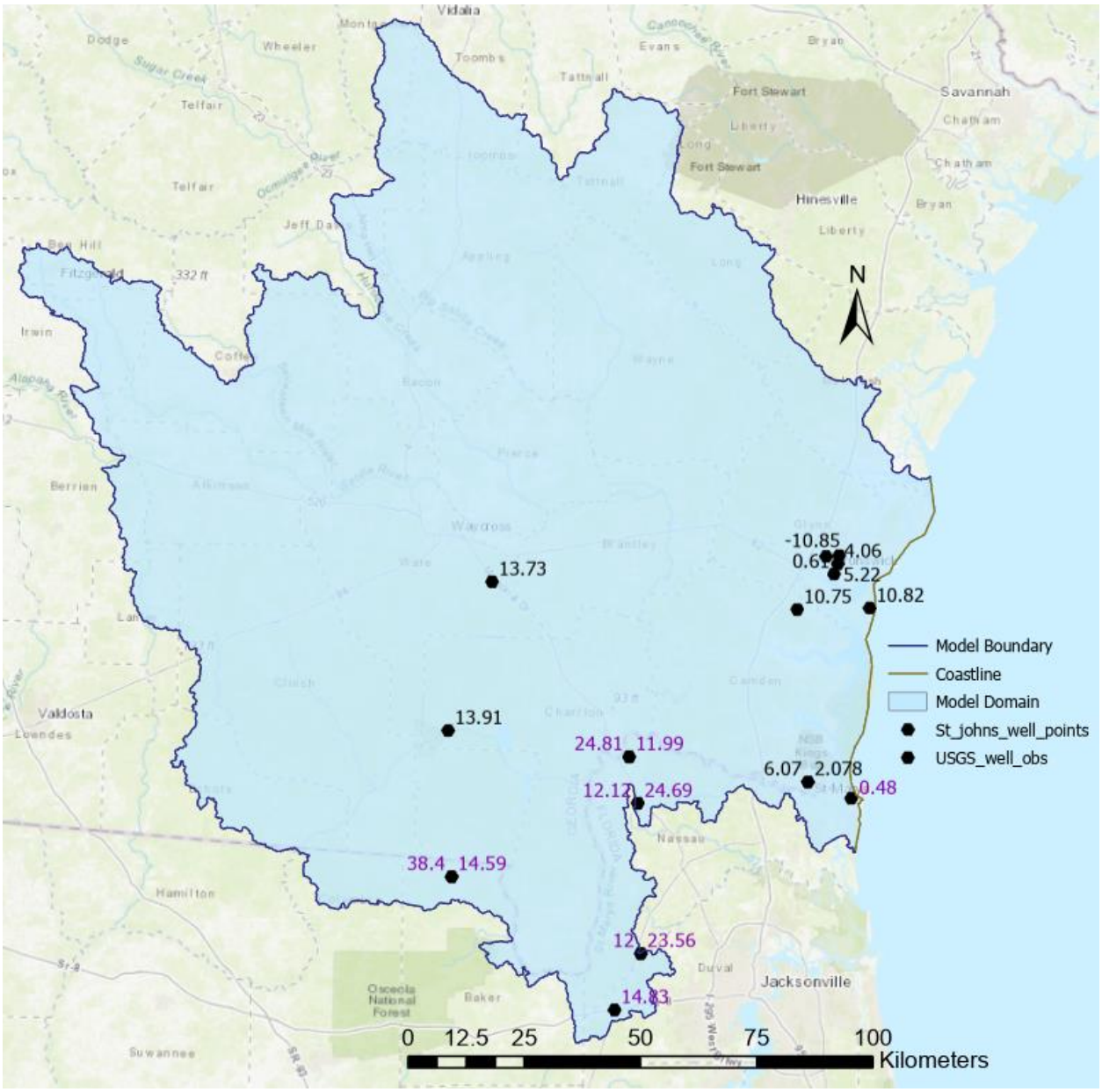

Figure 3.20: Groundwater levels in meters above NAVD88 for USGS (black) and SJWMD (purple) wells within model domain on October 1st, 2020.

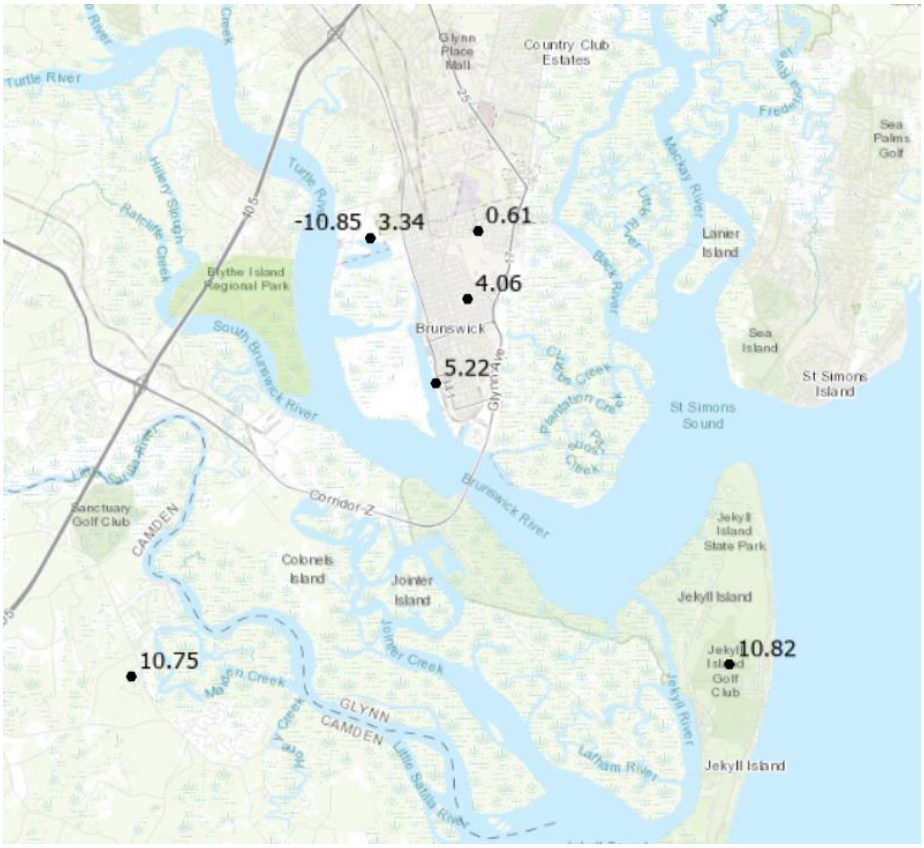

Figure 3.21: Observed water levels around Brunswick for October 1, 2020.

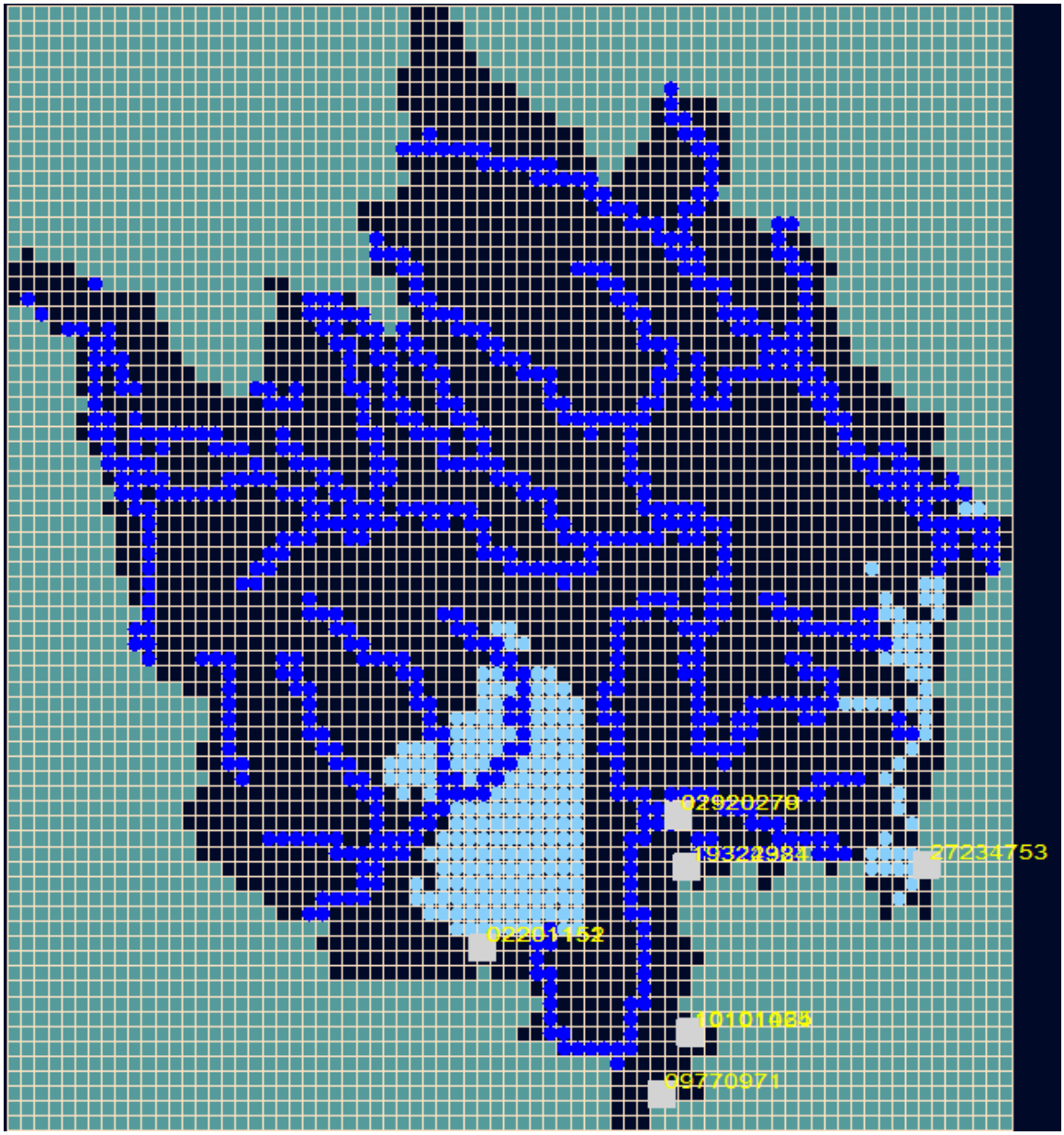

Figure 3.22: Locations of SJWMD monitoring wells in numerical grid.

3.9.2 Regional Model Calibration

The resulting hydraulic heads and water table elevation from the initial regional model run were around three magnitudes higher than expected at the Okefenokee Swamp and along the left side of the model. Ultimately, it was concluded that groundwater was pooling on the top

layer, particularly beneath the ONWR, and not passing into the lower aquifers effectively. The first effort to lower the hydraulic heads around the Okefenokee Swamp region was to increase the lakebed leakance by three orders of magnitude. However, this change only increased the heads within this region, so the original value was restored.

The next attempt to calibrate the model was to increase the hydraulic conductivity of the confining units within the model. After testing this method with Layer 2 and noticing a drop in hydraulic heads in Layer 1, the hydraulic conductivity of Layers 3 and 4 were lowered gradually as well. During this process, there became a point where the hydraulic conductivities of the confining units could not be lowered any further without the model failing to converge. Additionally, there was a trade-off between lowering the hydraulic heads in Layer 1 by increasing the conductivity of the UCU layers causing an increase in the heads in Layer 5 (UFA). For this study, the adjustments made during calibration prioritized the recreating the observational data in Layer 1 (particularly around Mission Mine) over the observational data for Layer 5. By the end of the calibration process, the hydraulic conductivity of the UCU in Layers 2 through 4 were increased by between 4 and 6 orders of magnitude (**Table 3.8**).

While adjusting the hydraulic conductivities of the confining unit layers, one area in the southwest corner of the model remained high (around 180 m) compared to the rest of the model. This region occurs along the border of the model domain, which may suggest that this is a result of water pooling at the edge of the model. Additionally, this region seemed to be affecting the ability for the model to converge. As discussed earlier in Section 3.5.5, a constant head boundary condition was added to the lower left-side of the model. Initially this constant head was assigned a starting and ending head of 40 m, but this was adjusted throughout the calibration process. The

final constant head was 40.5 m. The inclusion of this boundary condition lowered the hydraulic heads of the western region of the model and ultimately allowed the model to converge.

Table 3.8: Hydraulic conductivity (Kz and Kh) assigned to regional model layers before and after manual calibration.

Layer	Property Zone	K Before Manual Calibration (m/s)	K After Manual Calibration (m/s)
1	1	0.00037	0.00037
2	8	3.53E-11	3.53E-07
3 (Left)	3	3.53E-11	5E-05
3 (Middle)	9	3.53E-11	3.53E-07
3 (BAS)	4	5.3E-05	5.3E-05
4	5	3.53E-11	3.53E-04
5	6	0.0106	0.03

3.9.3 Local Steady-State Model Calibration

Initial results for the steady-state local model were mostly within a few meters difference from the observational data from the Chemours monitoring wells. However, a few locations within the model domain had zero or negative head values, which is not consistent of what would be expected for this region (**Figure 3.23**). These low point cells did not overlap with any boundary conditions. The results section has additional figures showing the contour lines for the hydraulic heads for this initial run as well as other results.

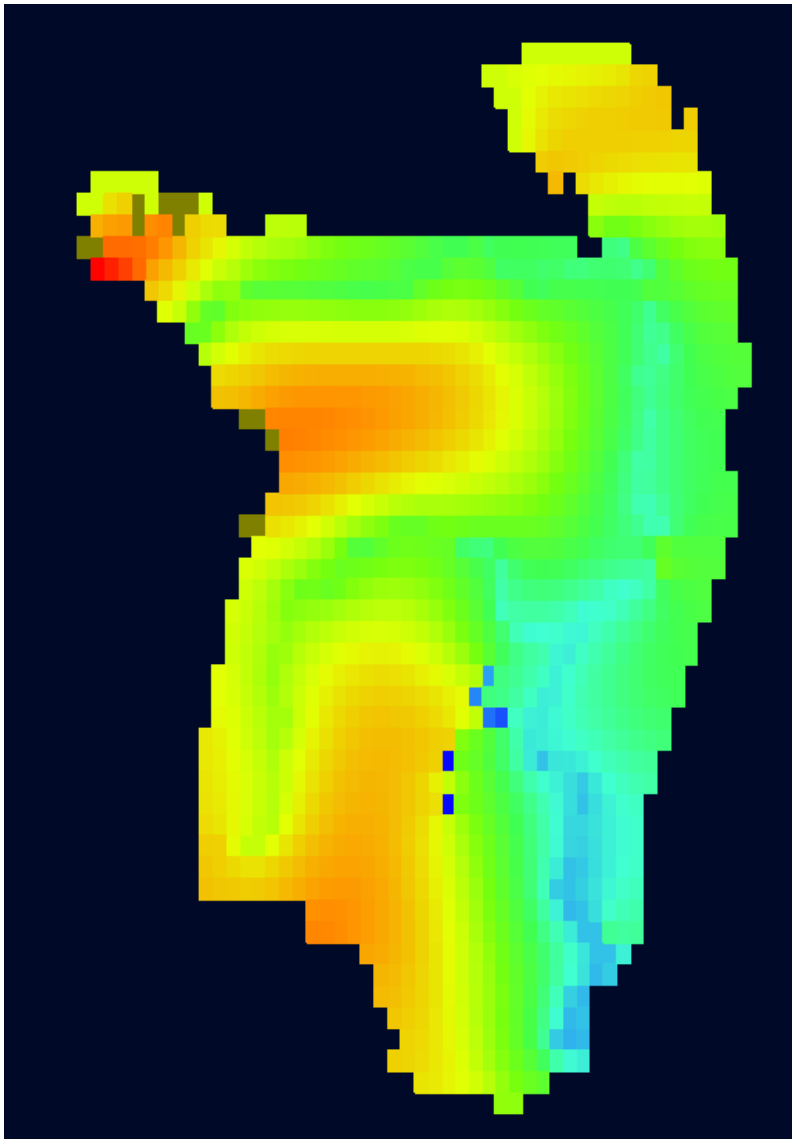

Figure 3.23: Hydraulic head (m) by cell for the initial run of the steady-state local model.

Version 8 of VMF includes an option for automatic parameter estimation to aid in the calibration process, referred to as the PEST program. Running the PEST program requires several inputs, mainly observations and pilot points. Pilot points refer to points in a 2D environment set by the modeler where parameter estimation will be calculated. After defining the observation and pilot points, the modeler sets a parameter, such as vertical or horizontal conductivity, and Kriging setting to be used for interpolating the pilot point data. Lastly, the

modeler selects a regularization setting and then the PEST program can be run (Waterloo Hydrogeologic, 2022). VMF also has a program for producing a sensitivity analysis for the model, which can provide insight into which parameters will have the greatest effect on the model results if adjusted during the calibration process.

Because initial results for the steady-state local model were relatively close to observed head values from the chosen Chemours monitoring wells, calibration of the local steady-state model was conducted using the Parameter Estimation (PEST) program within VMF.

A series of eleven points were assigned throughout the model domain for use as the pilot points (**Figure 3.24**). Vertical hydraulic conductivity (Kv) was selected as the parameter to be estimated using these pilot points. The default settings for using a Kriging setting of exponential variogram were used and the program was set to run without regularization. Once the PEST program had completed its run, a clone of the initial model run was created using the PEST generated vertical conductivity values.

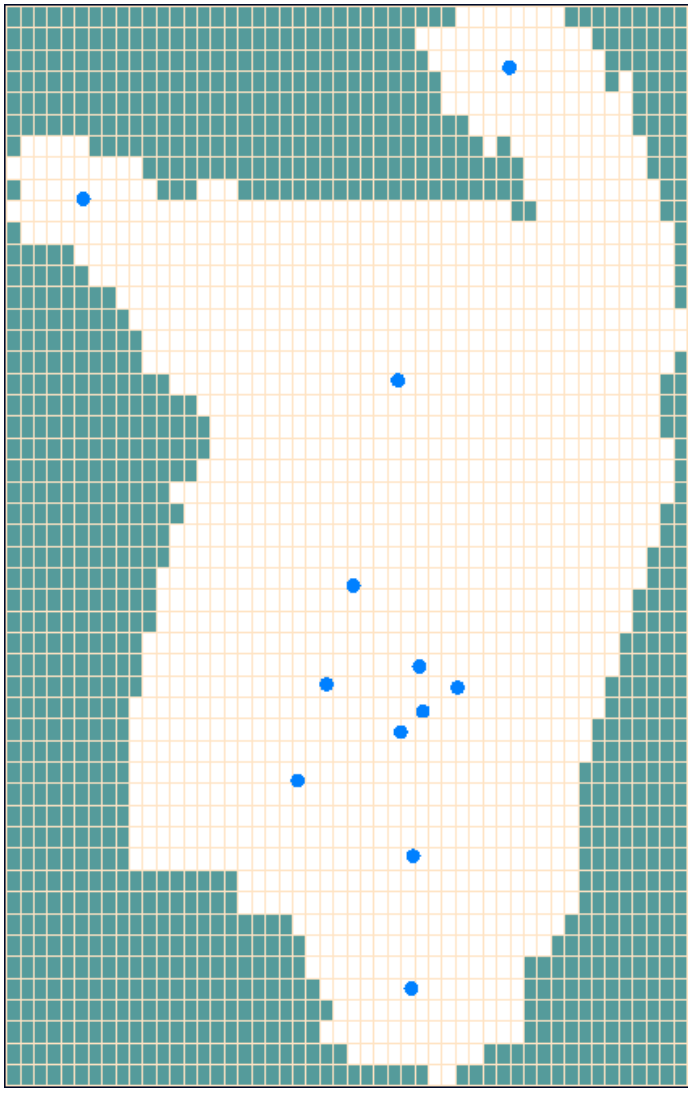

Figure 3.24: Locations of pilot points used for the PEST run of the steady-state local model.

CHAPTER 4

RESULTS

4.1 Steady State Regional Model

4.1.1 Regional Model Without Wells

```
 VOLUMETRIC BUDGET FOR ENTIRE MODEL AT END OF TIME STEP    1, STRESS PERIOD   1
 ------------------------------------------------------------------------------

    CUMULATIVE VOLUMES      L**3       RATES FOR THIS TIME STEP      L**3/T
    ------------------                 ------------------------

          IN:                                IN:
          ---                                ---
            STORAGE =           0.0000           STORAGE =           0.0000
      CONSTANT HEAD =     2158560.0000     CONSTANT HEAD =     2158560.0000
      RIVER LEAKAGE =     3810492.0000     RIVER LEAKAGE =     3810492.0000
           RECHARGE =    10570220.0000          RECHARGE =    10570220.0000
      LAKE  SEEPAGE =     1832902.6250     LAKE  SEEPAGE =     1832902.6250

           TOTAL IN =    18372174.0000          TOTAL IN =    18372174.0000

         OUT:                               OUT:
         ----                               ----
            STORAGE =           0.0000           STORAGE =           0.0000
      CONSTANT HEAD =     3579944.2500     CONSTANT HEAD =     3579944.2500
      RIVER LEAKAGE =    14616721.0000     RIVER LEAKAGE =    14616721.0000
           RECHARGE =           0.0000          RECHARGE =           0.0000
      LAKE  SEEPAGE =      368534.3438     LAKE  SEEPAGE =      368534.3438

           TOTAL OUT =    18565200.0000          TOTAL OUT =    18565200.0000

            IN - OUT =     -193026.0000           IN - OUT =     -193026.0000

 PERCENT DISCREPANCY =          -1.05     PERCENT DISCREPANCY =          -1.05
```

Figure 4.1: Volumetric budget for steady-state regional model after calibration.

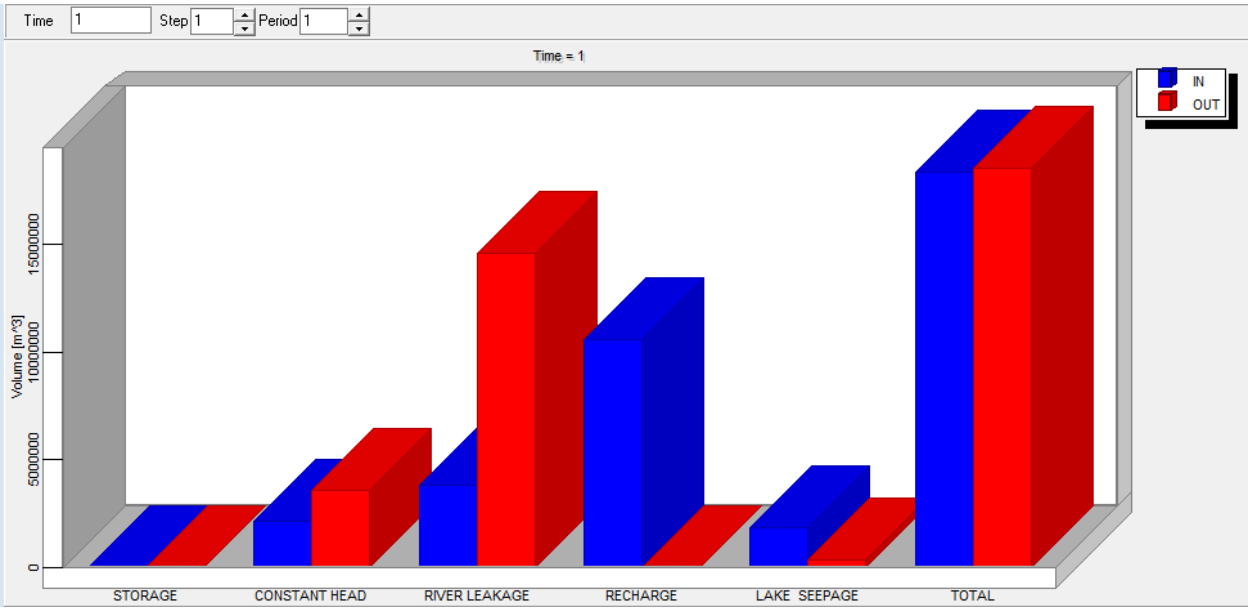

Figure 4.2: Mass balance chart of steady-state regional model after manual calibration.

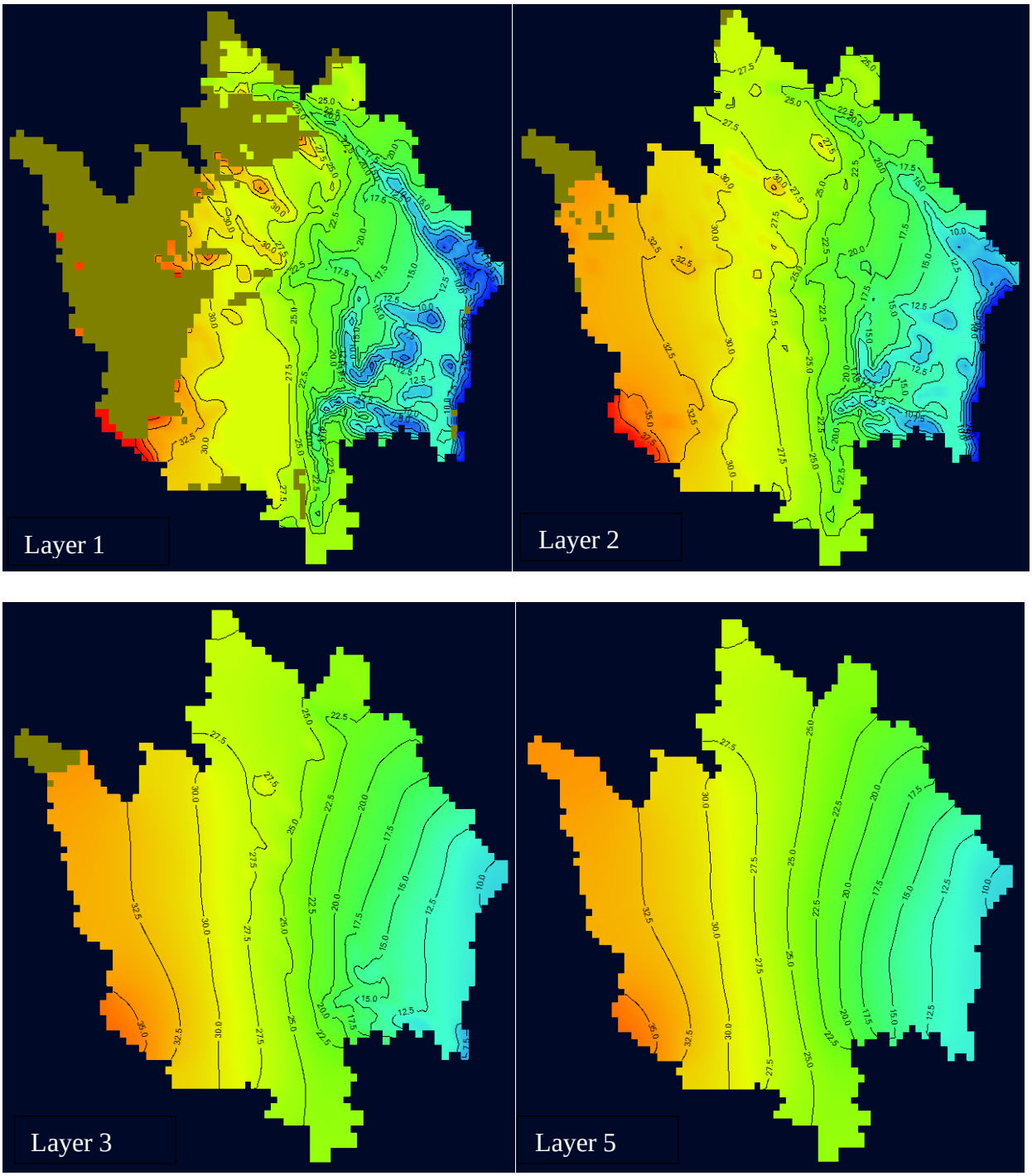

Figure 4.3: Hydraulic heads of the steady-state regional model after manual calibration.

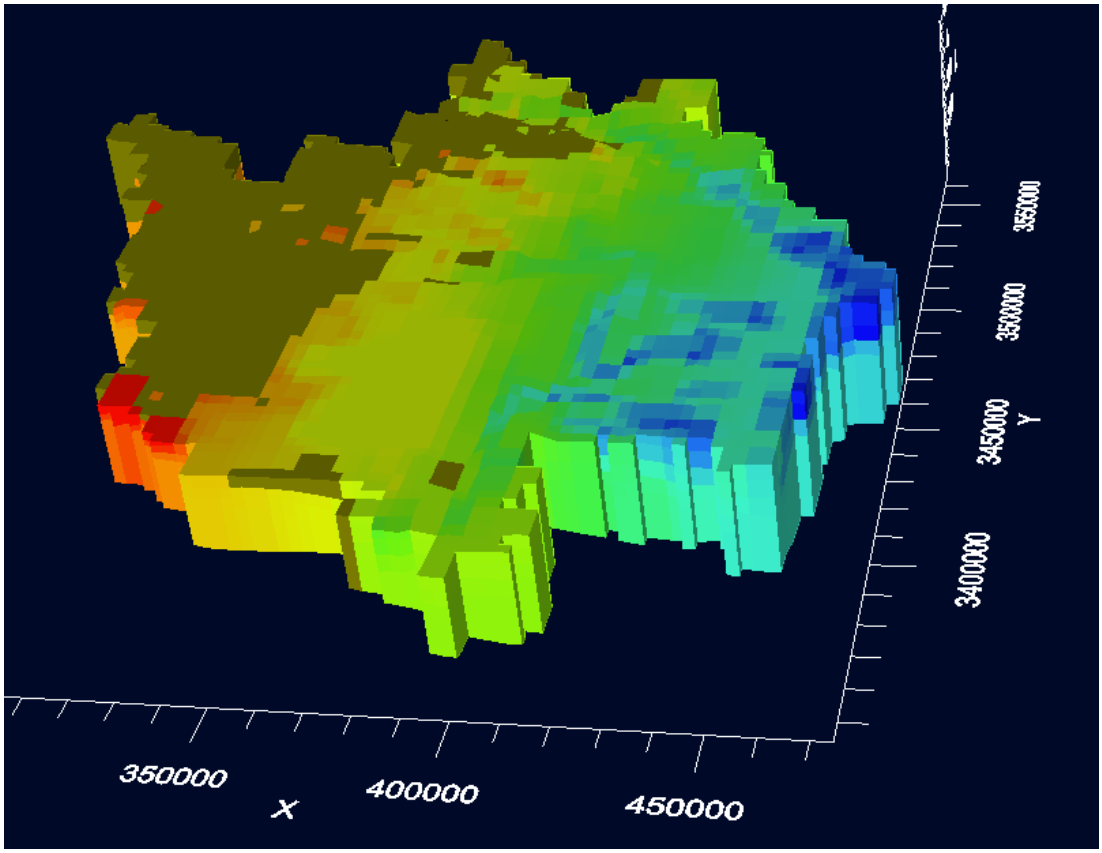

Figure 4.4: 3D view of the hydraulic heads within regional steady-state model after manual calibration.

Table 4.1: Comparison of observed hydraulic heads and modeled results for regional model.

Data Source	Well ID	Aquifer	Model Cell		Head (m) Above NAVD88		Percent Error	Difference (m)
			Row	Column	Observed	Modeled		
Chemours	CC1	SA	45	50	17.20	18.55	7.9%	1.35
	IBM-W8	SA	47	50	26.44	19.49	26.3%	6.95
	Z	SA	44	50	25.89	19.37	25.2%	6.52
USGS	27E004	UFA	53	36	13.91	27.93	100.8%	14.02
	27G003	FA	42	39	13.73	25.86	88.4%	12.13
	33G050	UFA	44	64	10.75	12.23	13.8%	1.48
	34G033	UFA	44	70	10.82	10.74	0.8%	0.08
	34H514	UFA	40	68	4.06	11.26	177.2%	7.20
SJWMD	02201152	UFA	63	36	14.59	28.37	94.4%	13.78
	27234753	SF	58	69	0.48	0.39	18.3%	0.09
	19324384	SF	58	51	24.69	21.03	14.8%	3.66
	19322924	UFA	58	51	12.12	18.87	55.7%	6.75
	10101064	SF	69	51	23.56	25.33	7.5%	1.77
	10101425	UFA	69	51	12.00	24.74	106.2%	12.74
	02920279	UFA	55	50	11.99	19.53	62.9%	7.54
	02920270	SF	55	50	24.81	17.54	29.3%	7.27
	02201151	SF	63	36	38.40	28.38	26.1%	10.02
	09770971	UFA	73	49	14.83	24.91	68.0%	10.08

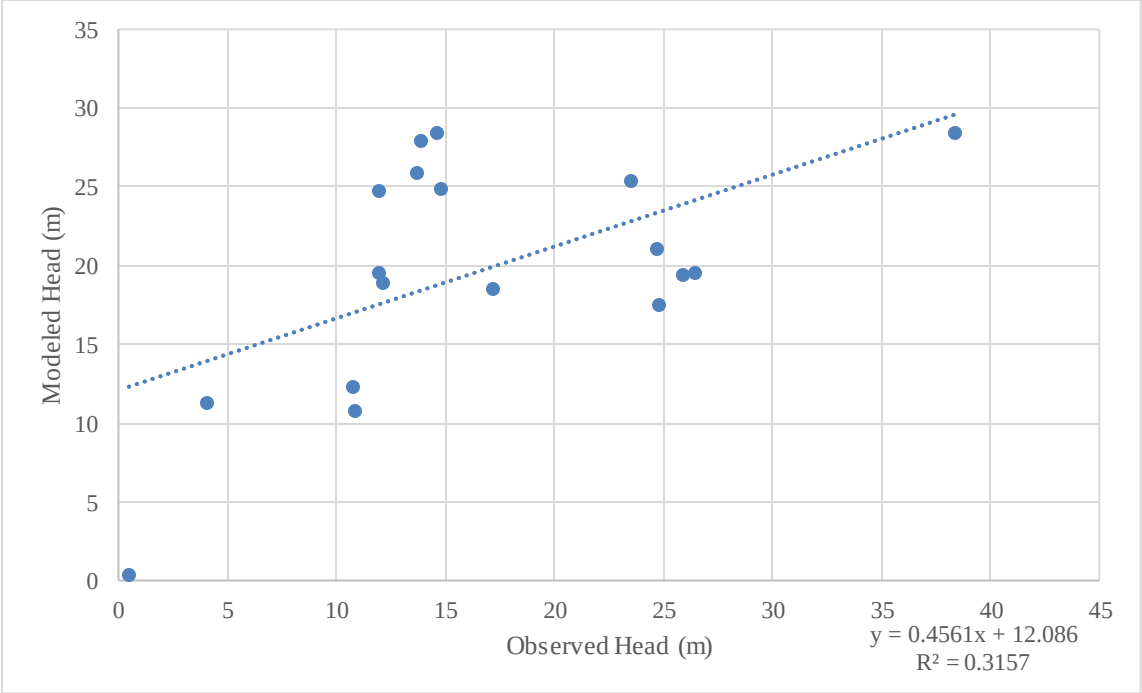

Figure 4.5: Observed vs modeled heads for steady-state regional model.

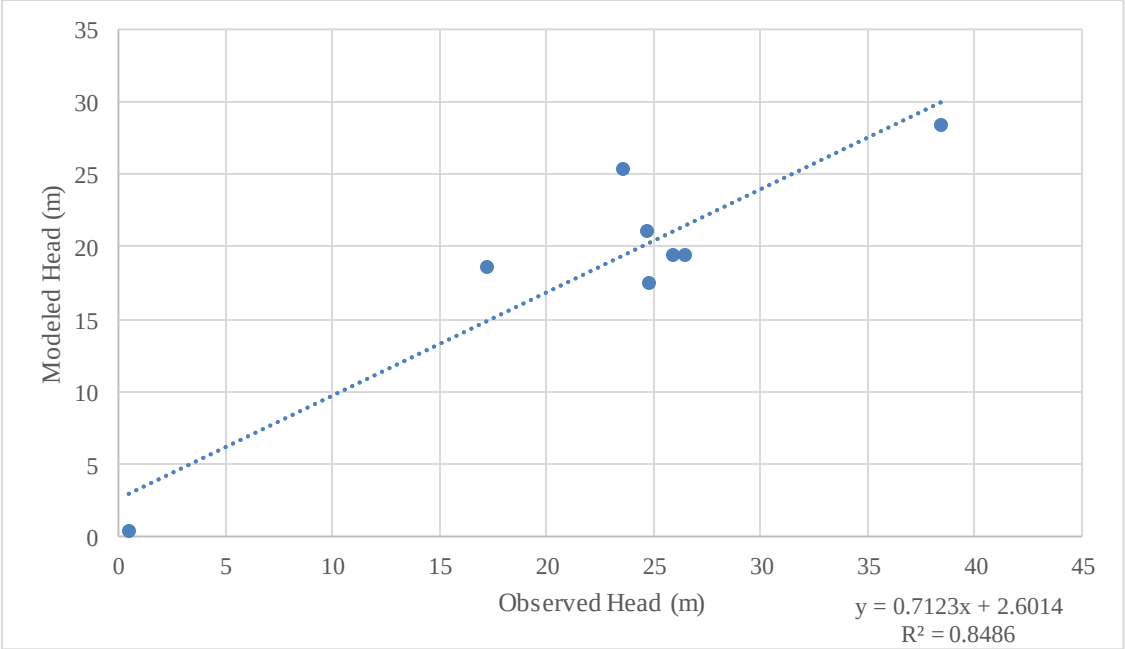

Figure 4.6: Observed vs modeled heads for surficial aquifer of steady-state regional model.

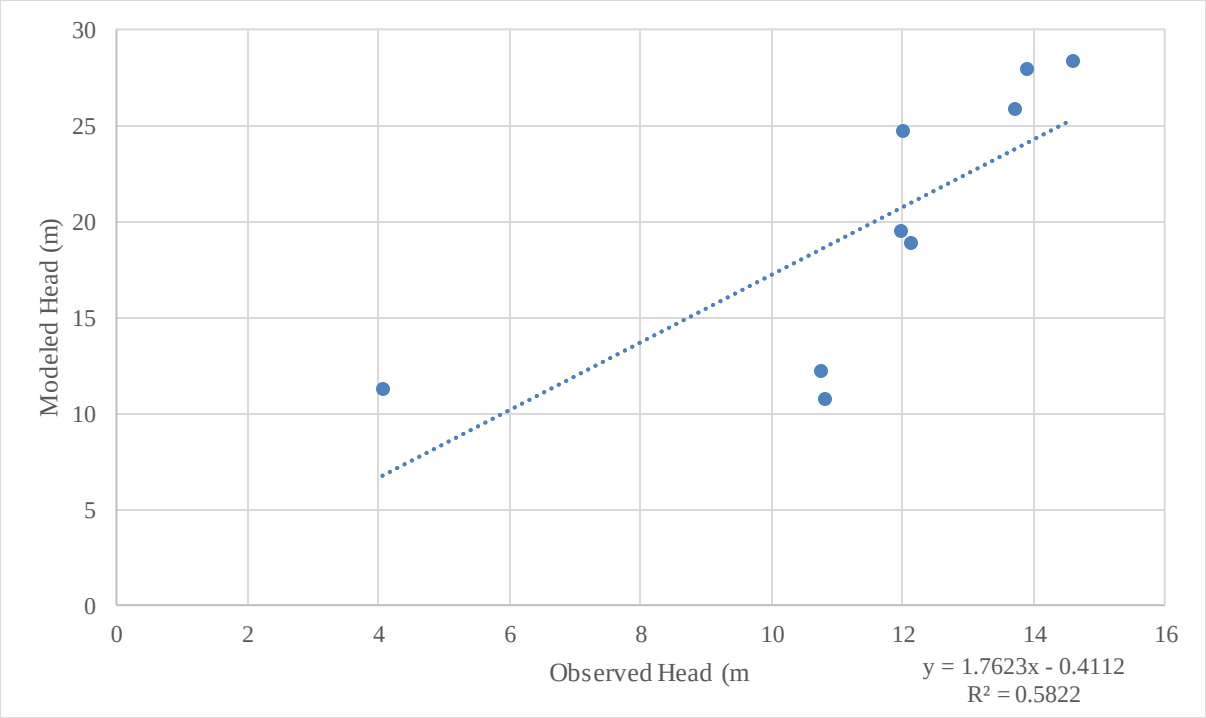

Figure 4.7: Observed vs modeled heads for Floridan aquifer of steady-state regional model.

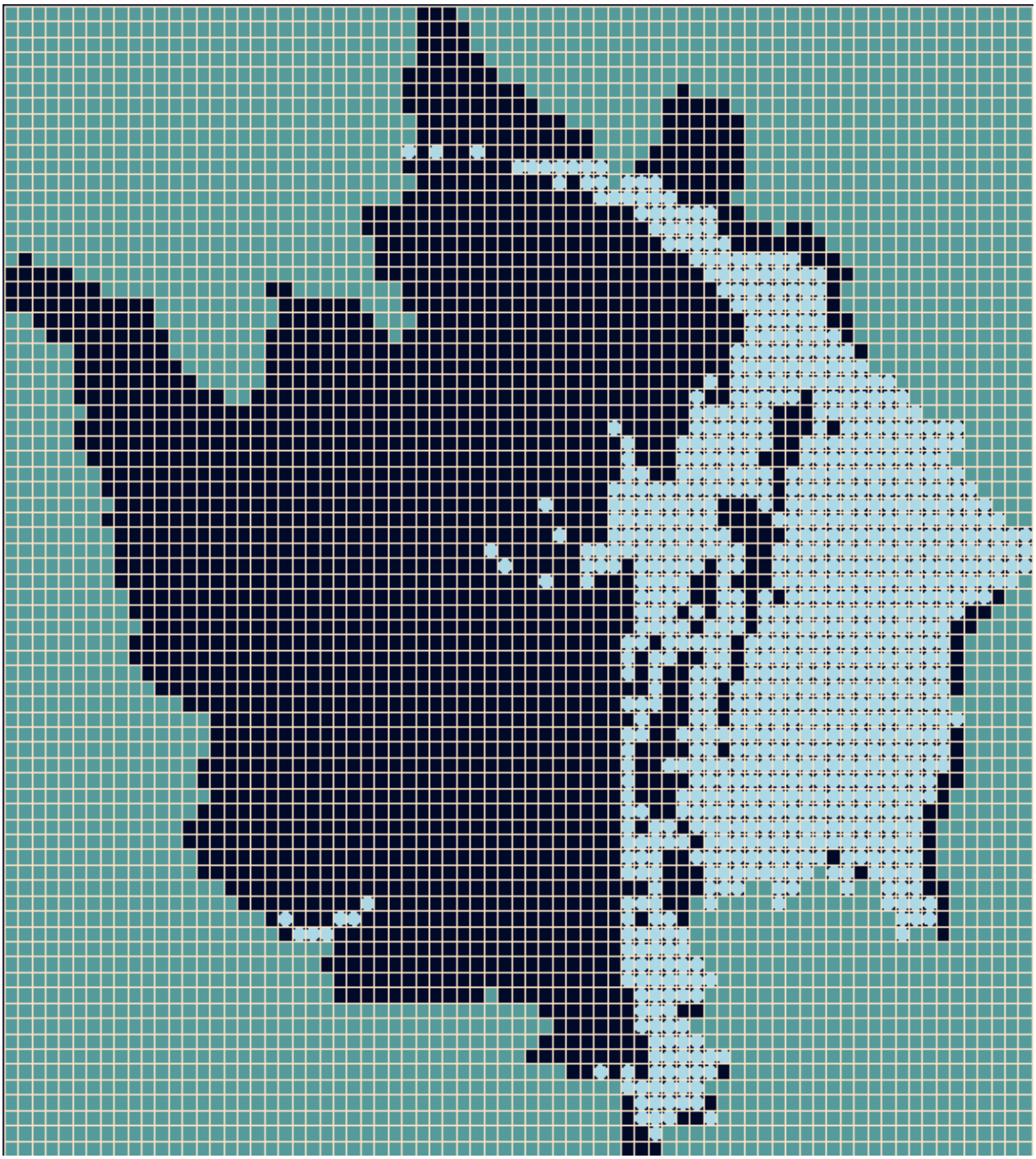

Figure 4.8: Flooded cells in layer 1 of the steady-state regional model after manual calibration.

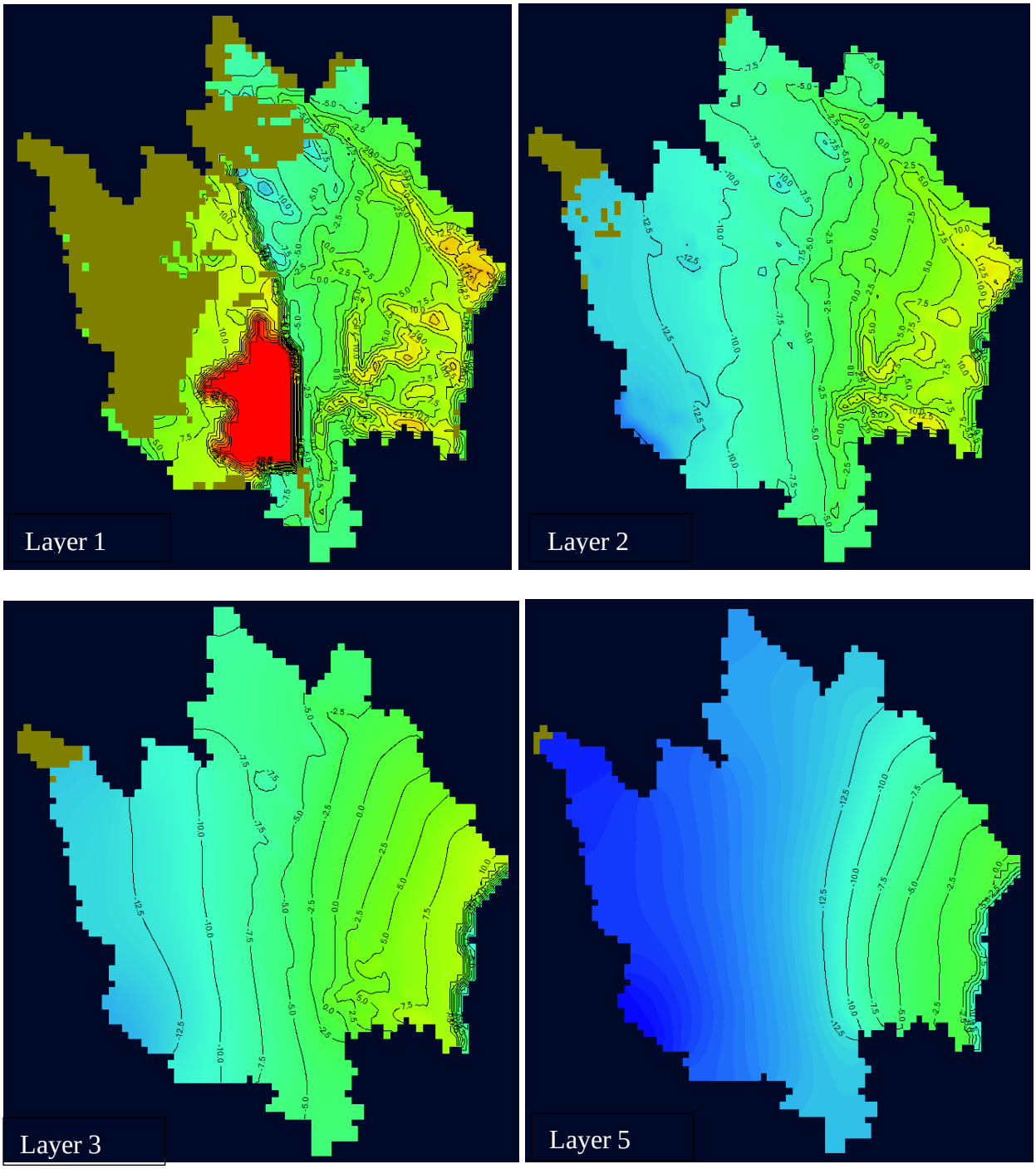

Figure 4.9: Drawdown in the regional steady-state model after calibration.

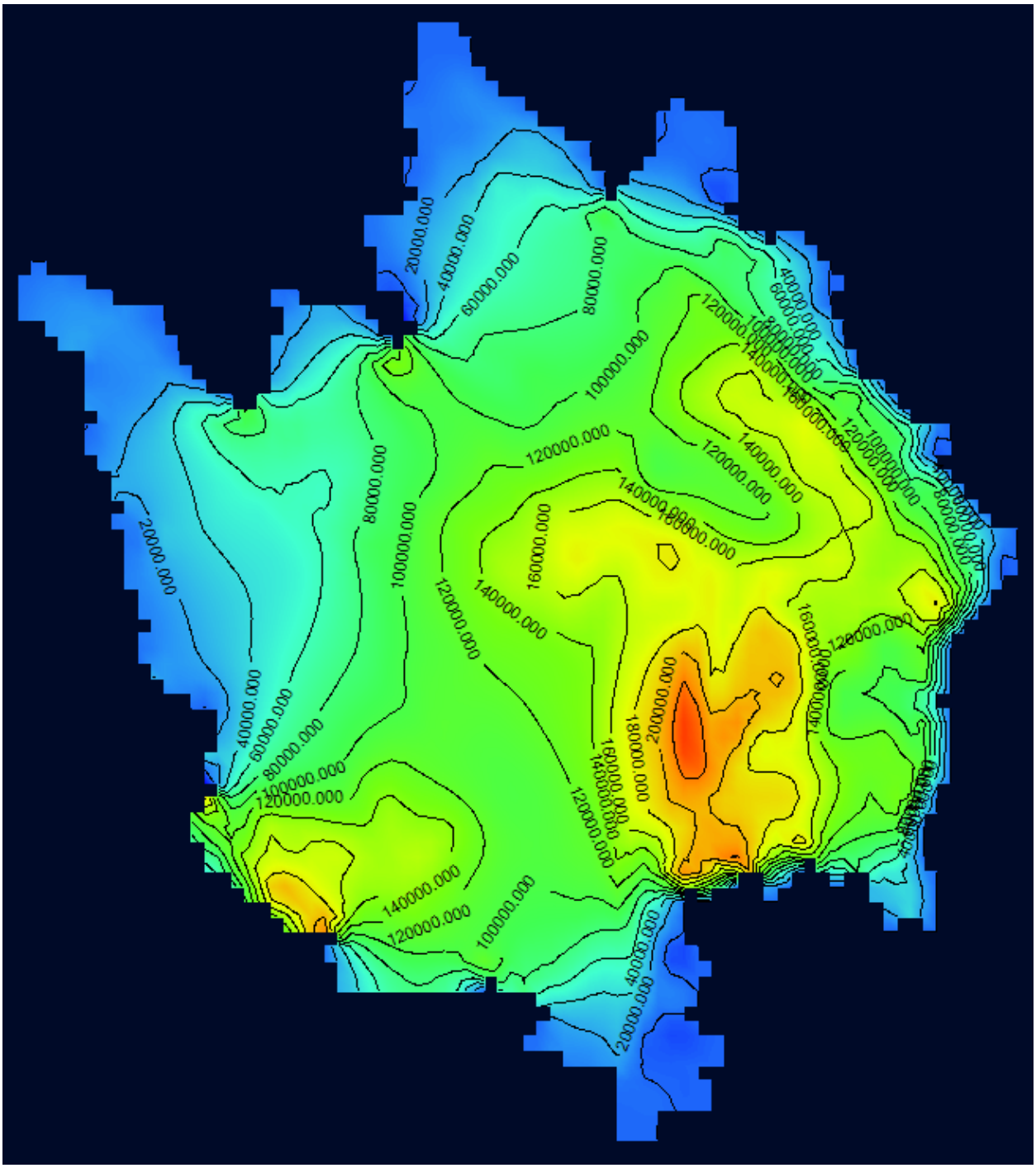

Figure 4.10: Water budget in layer 5 of the regional steady-state model after manual calibration.

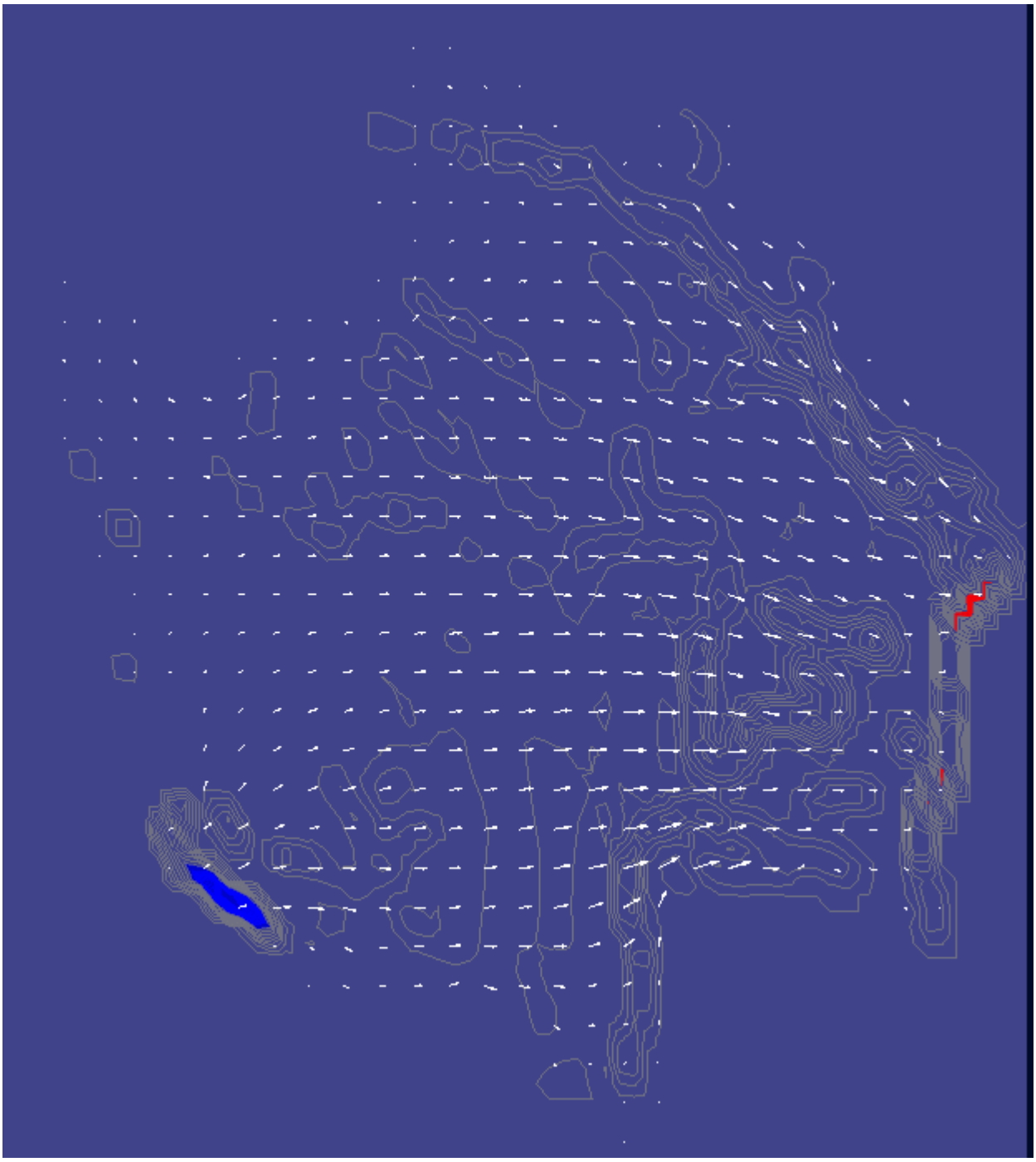

Figure 4.11: Velocity in layer 4 of the regional steady-state model after manual calibration.

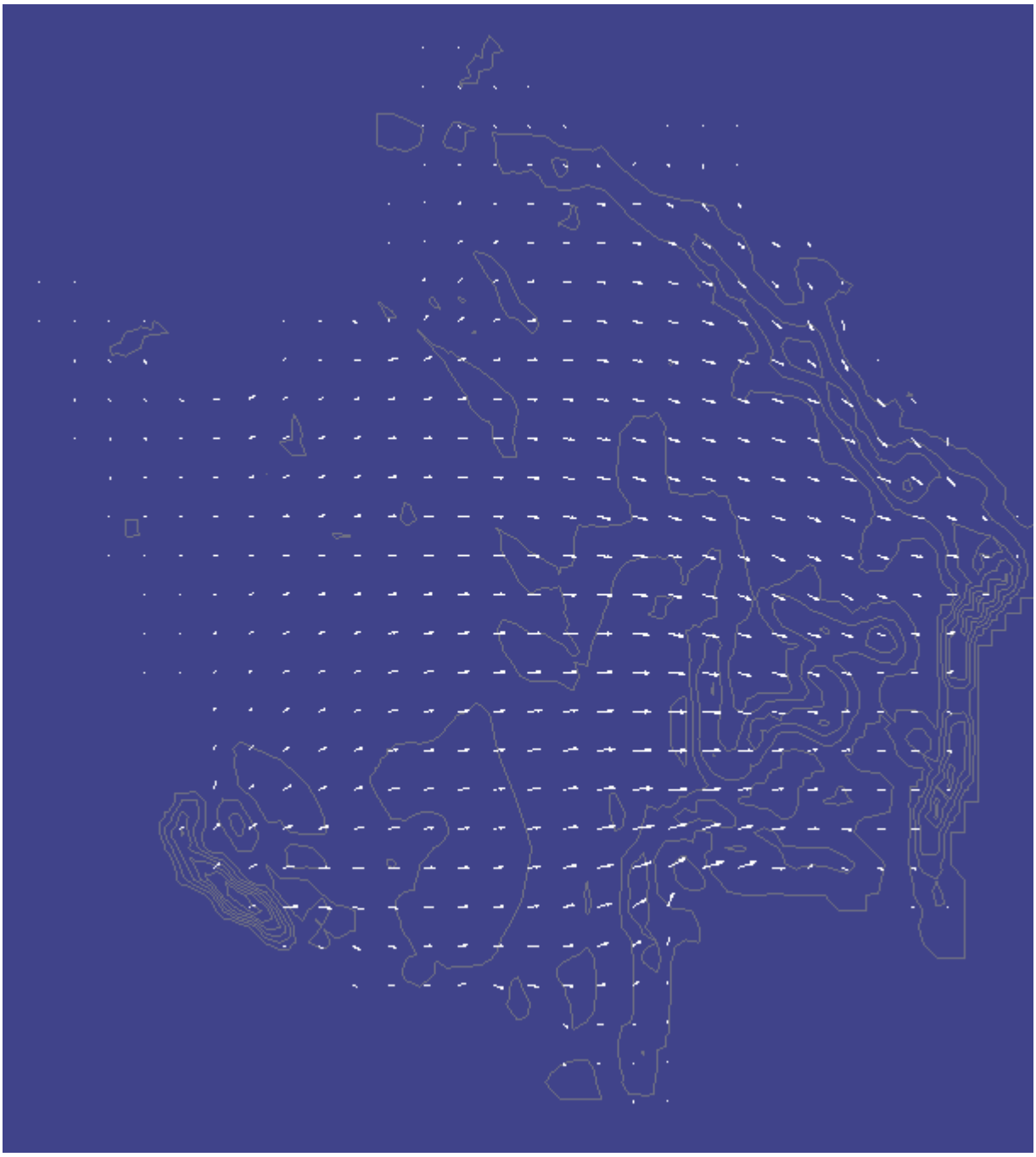

Figure 4.12:Velocity in layer 5 of the regional steady-state model after manual calibration.

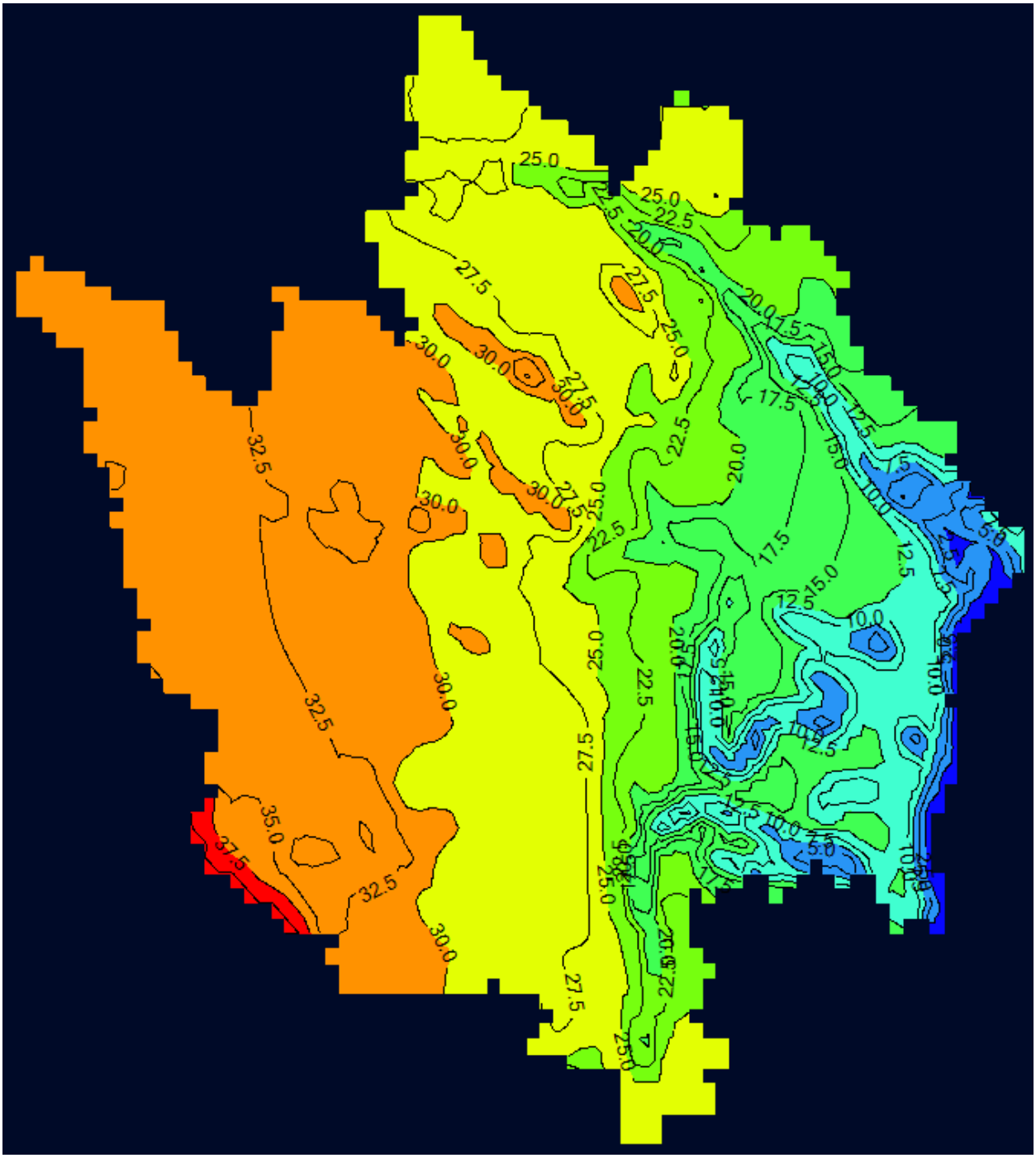

Figure 4.13: Water table elevation in regional steady-state model after manual calibration.

4.1.2 Mission Mine Pumping Well

After adding the Mission Mine pumping well conditions for October 1, 2020 as a well boundary conditions to the regional model, a new model run was conducted. **Figure 4.14** shows the resulting volumetric budget breakdown with the well condition included. The hydraulic head results from this run as compared to the observational heads and initial head results are shown in **Table 4.2**. The addition of the Mission Mine pumping well produced no significant difference on the results of the model that could be visible from the 2D results rendered by the model.

This run did not meet model convergence. However, the model did converge after the western constant head boundary condition was lowered to 40.5 meters. The results of a new run with this change produced hydraulic heads that were within a meter of the initial run. **Table 4.3** shows the resulting hydraulic heads after adjusting the constant head boundary.

VOLUMETRIC BUDGET FOR ENTIRE MODEL AT END OF TIME STEP 1, STRESS PERIOD 1

CUMULATIVE VOLUMES	L**3	RATES FOR THIS TIME STEP	L**3/T
IN:		IN:	
STORAGE =	0.0000	STORAGE =	0.0000
CONSTANT HEAD =	2218927.2500	CONSTANT HEAD =	2218927.2500
WELLS =	0.0000	WELLS =	0.0000
RIVER LEAKAGE =	3848961.7500	RIVER LEAKAGE =	3848961.7500
RECHARGE =	10570220.0000	RECHARGE =	10570220.0000
LAKE SEEPAGE =	1842001.7500	LAKE SEEPAGE =	1842001.7500
TOTAL IN =	18480110.0000	TOTAL IN =	18480110.0000
OUT:		OUT:	
STORAGE =	0.0000	STORAGE =	0.0000
CONSTANT HEAD =	3590090.5000	CONSTANT HEAD =	3590090.5000
WELLS =	624.7100	WELLS =	624.7100
RIVER LEAKAGE =	14705257.0000	RIVER LEAKAGE =	14705257.0000
RECHARGE =	0.0000	RECHARGE =	0.0000
LAKE SEEPAGE =	377618.0000	LAKE SEEPAGE =	377618.0000
TOTAL OUT =	18673590.0000	TOTAL OUT =	18673590.0000
IN - OUT =	-193480.0000	IN - OUT =	-193480.0000
PERCENT DISCREPANCY =	-1.04	PERCENT DISCREPANCY =	-1.04

Figure 4.14: Volumetric budget for regional model with the Mission Mine pumping well condition.

Table 4.2: Hydraulic heads in steady-state regional model with Mission Mine pumping well.

Data Source	Well ID	Aquifer	Model Cell		Head (m) Above NAVD88		
			Row	Column	Observed	Modeled Without Well	Modeled With Well
Chemours	CC1	SA	45	50	17.20	18.55	18.60
	IBM-W8	SA	47	50	26.44	19.49	19.55
	Z	SA	44	50	25.89	19.37	19.35
USGS	27E004	UFA	53	36	13.91	27.93	28.07
	27G003	FA	42	39	13.73	25.86	25.98
	33G050	UFA	44	64	10.75	12.23	12.27
	34G033	UFA	44	70	10.82	10.74	10.77
	34H514	UFA	40	68	4.06	11.26	11.29
SJWMD	02201152	UFA	63	36	14.59	28.37	28.51
	27234753	SA	58	69	0.48	0.39	0.39
	19324384	SA	58	51	24.69	21.03	21.11
	19322924	UFA	58	51	12.12	18.87	19.83
	10101064	SA	69	51	23.56	25.33	25.42
	10101425	UFA	69	51	12.00	24.74	24.83
	02920279	UFA	55	50	11.99	19.53	19.61
	02920270	SA	55	50	24.81	17.54	17.55
	02201151	SA	63	36	38.40	28.38	28.52
	09770971	UFA	73	49	14.83	24.91	25.00

4.1.3 Amelia Mine Pumping Well

Table 4.4 compares the results of the various hydraulic heads produced by the models with and without the inclusion of one or both Chemours pumping wells. With the addition of the second pumping well at the Amelia Mine site, the model again does not meet convergence on a single run. For the run of the regional model with the inclusion of both pumping wells, the constant head was gradually lowered until model convergence occurred with a constant head of 38 m. Model convergence with this adjustment occurred at iteration 210.

```
 VOLUMETRIC BUDGET FOR ENTIRE MODEL AT END OF TIME STEP    1, STRESS PERIOD   1
 ------------------------------------------------------------------------------

    CUMULATIVE VOLUMES      L**3       RATES FOR THIS TIME STEP      L**3/T
    ------------------                 ------------------------

          IN:                                IN:
          ---                                ---
            STORAGE =          0.0000             STORAGE =          0.0000
      CONSTANT HEAD =    1972939.2500       CONSTANT HEAD =    1972939.2500
              WELLS =          0.0000             WELLS =          0.0000
      RIVER LEAKAGE =    4019427.0000       RIVER LEAKAGE =    4019427.0000
           RECHARGE =    9519634.0000            RECHARGE =    9519634.0000
      LAKE  SEEPAGE =    1802180.6250       LAKE  SEEPAGE =    1802180.6250

           TOTAL IN =   17314180.0000            TOTAL IN =   17314180.0000

         OUT:                               OUT:
         ----                               ----
            STORAGE =          0.0000             STORAGE =          0.0000
      CONSTANT HEAD =    3449087.0000       CONSTANT HEAD =    3449087.0000
              WELLS =       2196.4099             WELLS =       2196.4099
      RIVER LEAKAGE =   13717729.0000       RIVER LEAKAGE =   13717729.0000
           RECHARGE =          0.0000            RECHARGE =          0.0000
      LAKE  SEEPAGE =     337796.9688       LAKE  SEEPAGE =     337796.9688

           TOTAL OUT =   17506808.0000            TOTAL OUT =   17506808.0000

            IN - OUT =    -192628.0000             IN - OUT =    -192628.0000

 PERCENT DISCREPANCY =         -1.11      PERCENT DISCREPANCY =         -1.11
```

Figure 4.15: Volumetric budget for regional model with the Mission Mine and Amelia pumping well conditions.

Table 4.3: Hydraulic heads in steady-state regional model with Amelia and Mission Mine pumping well.

Data Source	Well ID	Aquifer	Model Cell		Head (m) Above NAVD88			
			Row	Column	Observed	Modeled Without Wells	Modeled With MM Well	Modeled With Both Wells
Chemours	CC1	SA	45	50	17.20	18.55	18.60	17.83
	IBM-W8	SA	47	50	26.44	19.49	19.55	18.70
	Z	SA	44	50	25.89	19.37	19.35	18.59
USGS	27E004	UFA	53	36	13.91	27.93	28.07	26.79
	27G003	FA	42	39	13.73	25.86	25.98	24.83
	33G050	UFA	44	64	10.75	12.23	12.27	11.79
	34G033	UFA	44	70	10.82	10.74	10.77	10.35
	34H514	UFA	40	68	4.06	11.26	11.29	10.85
SJWMD	02201152	UFA	63	36	14.59	28.37	28.51	27.23
	27234753	SF	58	69	0.48	0.39	0.39	0.35
	19324384	SF	58	51	24.69	21.03	21.11	20.19
	19322924	UFA	58	51	12.12	18.87	19.83	19.03
	10101064	SF	69	51	23.56	25.33	25.42	24.41
	10101425	UFA	69	51	12.00	24.74	24.83	23.88
	02920279	UFA	55	50	11.99	19.53	19.61	18.81
	02920270	SF	55	50	24.81	17.54	17.55	17.38
	02201151	SF	63	36	38.40	28.38	28.52	27.27
	09770971	UFA	73	49	14.83	24.91	25.00	24.04

4.2 Local Steady-State Model

Table 4.4: Hydraulic heads in steady-state local model after PEST calibration.

Data Source	Well ID	Model Cell		Head (m) Above NAVD88		Error	Percent Error	Difference (m)
		Row	Column	Observed	Modeled			
Chemours	CC1	35	31	17.196	15.631	0.091	9.10%	1.565
	CCC2	35	30	21.299	18.13	0.149	14.88%	3.169
	IBM-W4	39	28	25.831	25.232	0.023	2.32%	0.599
	IBM-W8	40	28	26.437	25.6	0.032	3.17%	0.837
	WW1	36	30	22.283	18.32	0.178	17.79%	3.963
	Z	32	31	25.888	-2.9843	1.115	111.53%	28.873

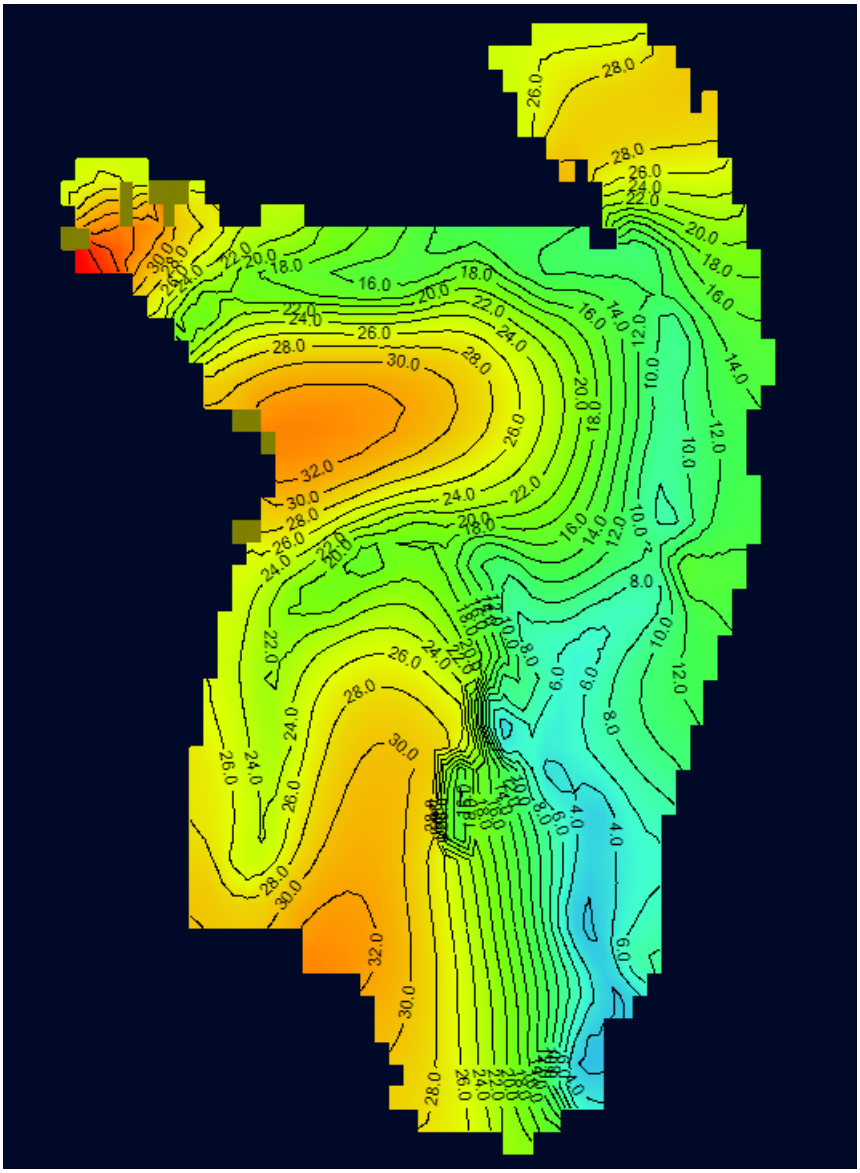

Figure 4.16: Hydraulic heads in steady-state local model after PEST calibration.

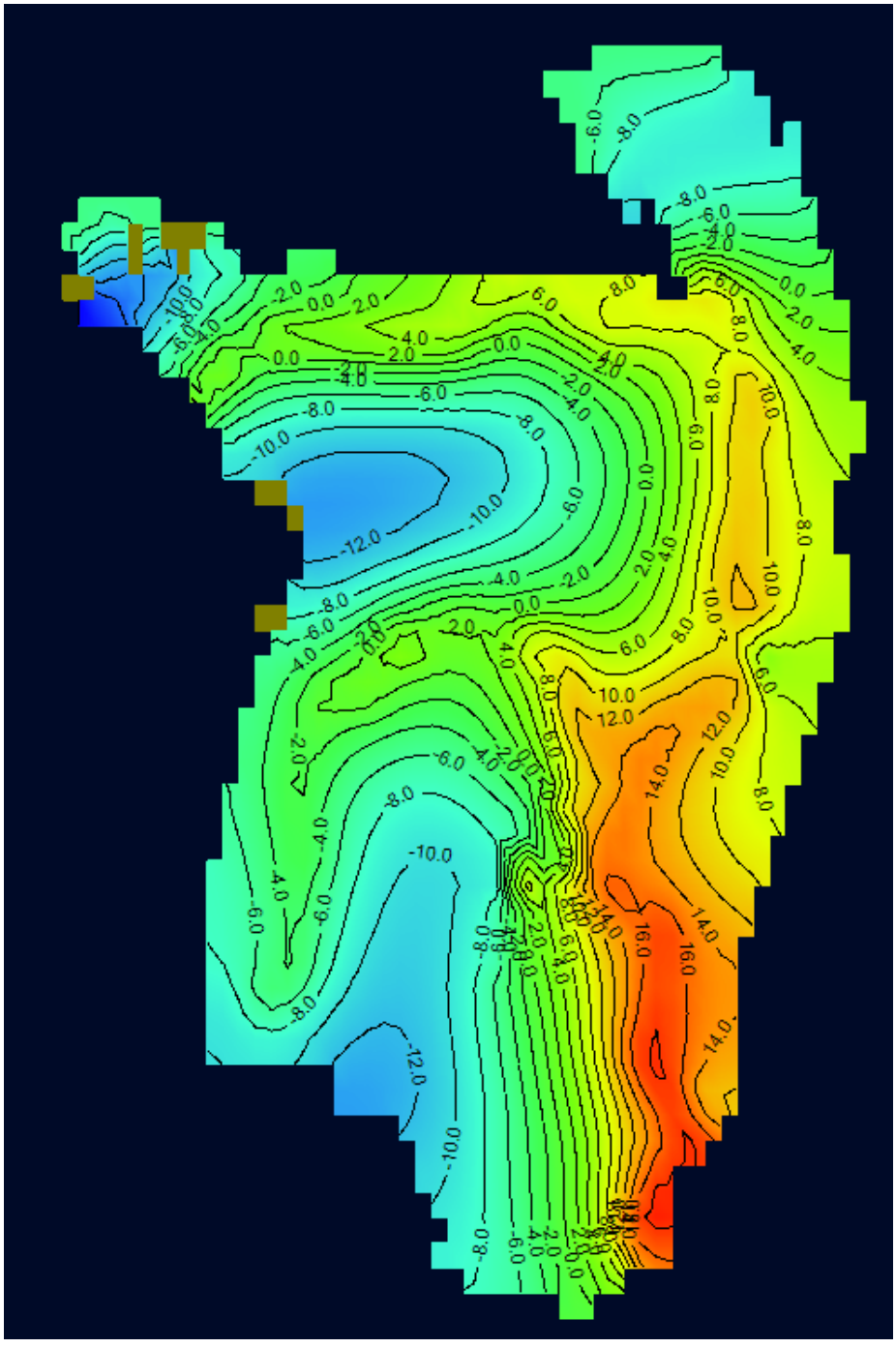

Figure 4.17: Drawdown in local steady-state model after PEST calibration.

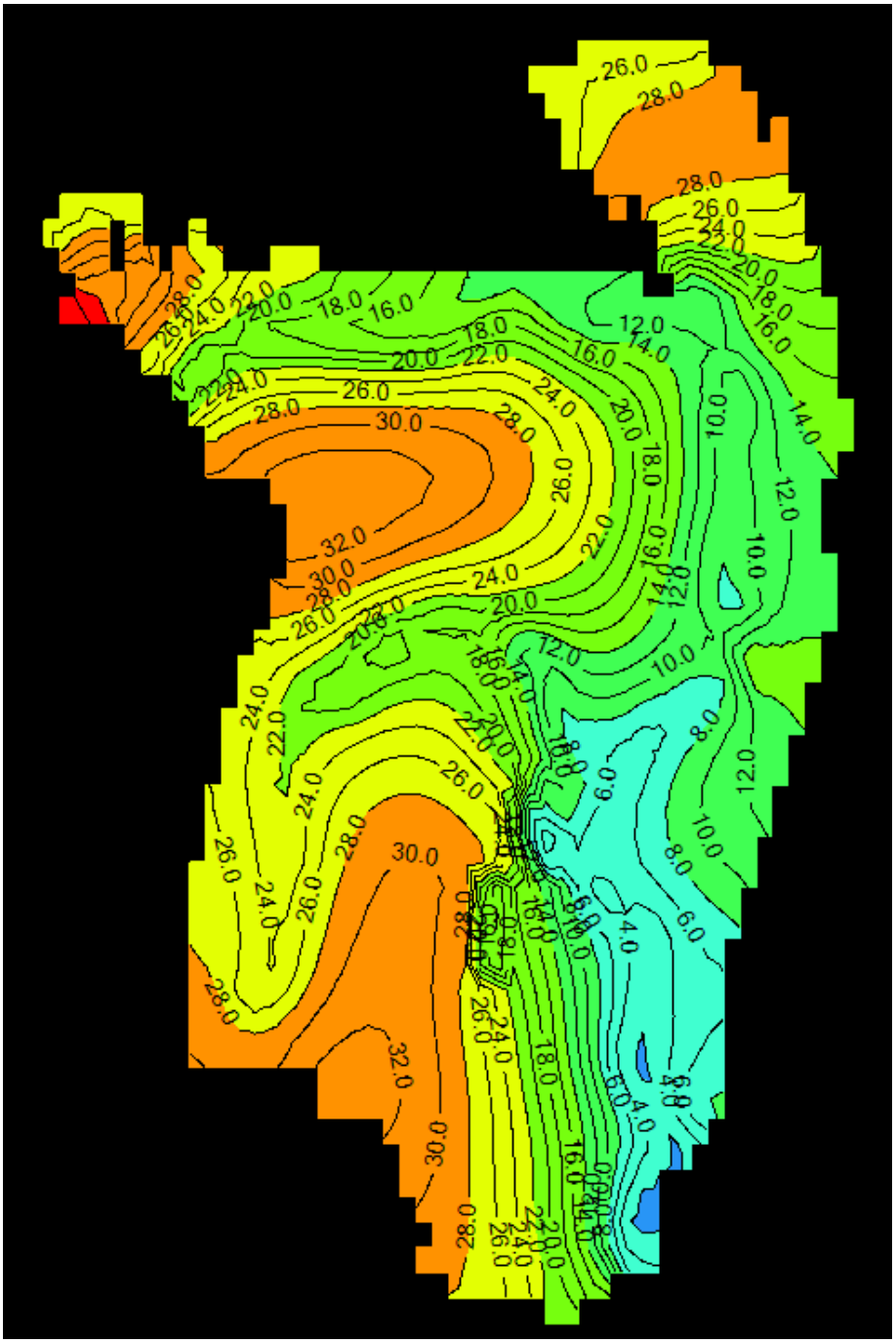

Figure 4.18: Water table elevation in steady-state local model after PEST calibration.

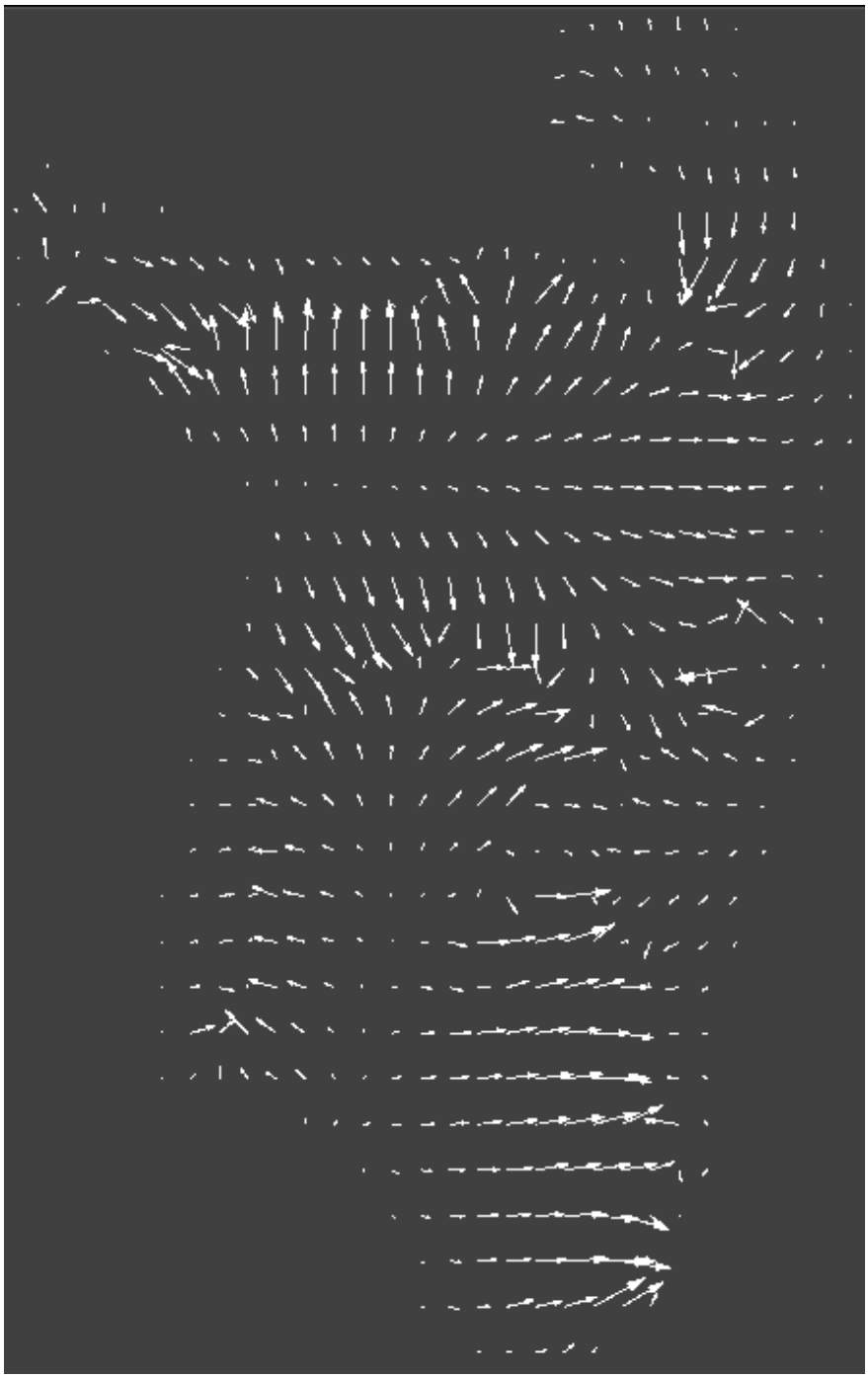

Figure 4.19: Groundwater flow velocities in local steady-state model after PEST calibration.

4.3 Transient Local Model

The initial run of the transient local model yielded hydraulic head results that were relatively similar to the observational data from the Mission Mine monitoring wells. Due to the similarity in results, no additional calibration was done to the transient local model at this time. Future calibration may be necessary if more observation points are obtained later.

```
 VOLUMETRIC BUDGET FOR ENTIRE MODEL AT END OF TIME STEP    1, STRESS PERIOD   1
 ------------------------------------------------------------------------------

    CUMULATIVE VOLUMES      L**3       RATES FOR THIS TIME STEP      L**3/T
    ------------------                 ------------------------

          IN:                                IN:
          ---                                ---
            STORAGE =     4173245.0000         STORAGE =     4173245.0000
       CONSTANT HEAD =           0.0000    CONSTANT HEAD =           0.0000
       RIVER LEAKAGE =           0.0000    RIVER LEAKAGE =           0.0000
            RECHARGE =           0.0000         RECHARGE =           0.0000
       LAKE   SEEPAGE =      272034.4688    LAKE   SEEPAGE =      272034.4688

           TOTAL IN =     4445279.5000          TOTAL IN =     4445279.5000

          OUT:                               OUT:
          ----                               ----
            STORAGE =      283627.3750         STORAGE =      283627.3750
       CONSTANT HEAD =           0.0000    CONSTANT HEAD =           0.0000
       RIVER LEAKAGE =     4152385.2500    RIVER LEAKAGE =     4152385.2500
            RECHARGE =           0.0000         RECHARGE =           0.0000
       LAKE   SEEPAGE =       27004.7207    LAKE   SEEPAGE =       27004.7207

          TOTAL OUT =     4463017.0000          TOTAL OUT =     4463017.0000

           IN - OUT =      -17737.5000          IN - OUT =      -17737.5000

 PERCENT DISCREPANCY =           -0.40    PERCENT DISCREPANCY =           -0.40
```

Figure 4.20: Volumetric budget for local transient model for day 1.

VOLUMETRIC BUDGET FOR ENTIRE MODEL AT END OF TIME STEP 1, STRESS PERIOD 364

CUMULATIVE VOLUMES	L**3	RATES FOR THIS TIME STEP	L**3/T
IN:		IN:	
STORAGE =	368921824.0000	STORAGE =	683184.8125
CONSTANT HEAD =	0.0000	CONSTANT HEAD =	0.0000
RIVER LEAKAGE =	22128484.0000	RIVER LEAKAGE =	19213.8086
RECHARGE =	221836864.0000	RECHARGE =	0.0000
LAKE SEEPAGE =	17458078.0000	LAKE SEEPAGE =	13687.1113
TOTAL IN =	630345216.0000	TOTAL IN =	716085.7500
OUT:		OUT:	
STORAGE =	227561952.0000	STORAGE =	254009.5312
CONSTANT HEAD =	0.0000	CONSTANT HEAD =	0.0000
RIVER LEAKAGE =	400841600.0000	RIVER LEAKAGE =	455690.9062
RECHARGE =	0.0000	RECHARGE =	0.0000
LAKE SEEPAGE =	2601163.0000	LAKE SEEPAGE =	4302.4600
TOTAL OUT =	631004736.0000	TOTAL OUT =	714002.8750
IN - OUT =	-659520.0000	IN - OUT =	2082.8750
PERCENT DISCREPANCY =	-0.10	PERCENT DISCREPANCY =	0.29

Figure 4.21: Volumetric budget for local transient model for day 364.

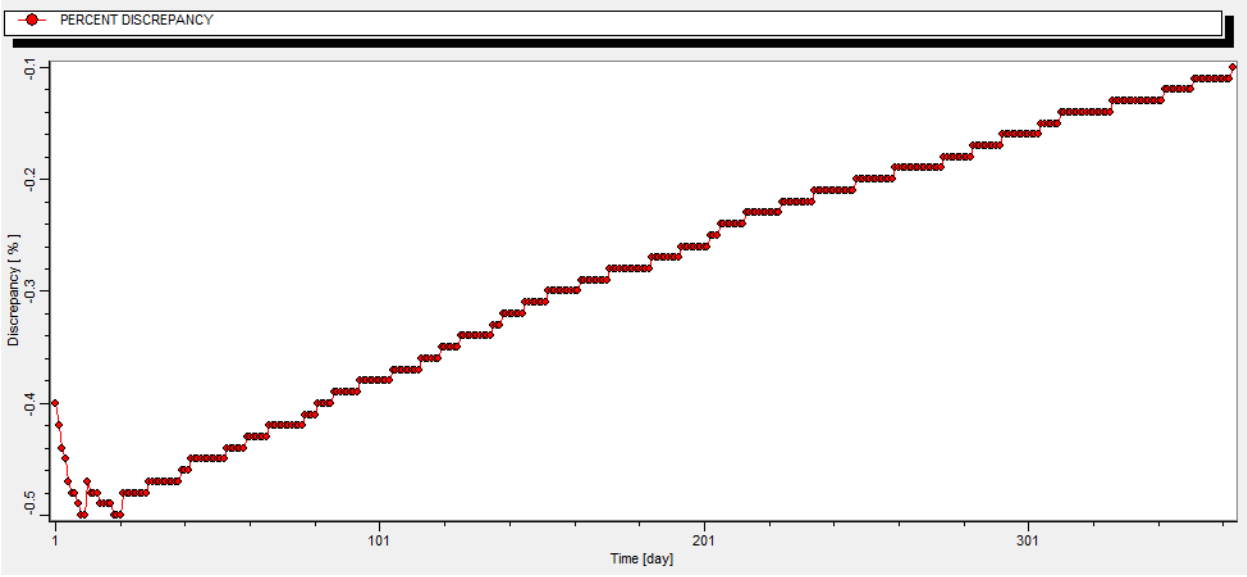

Figure 4.22: Percent discrepancy in inputs versus outputs in transient local model.

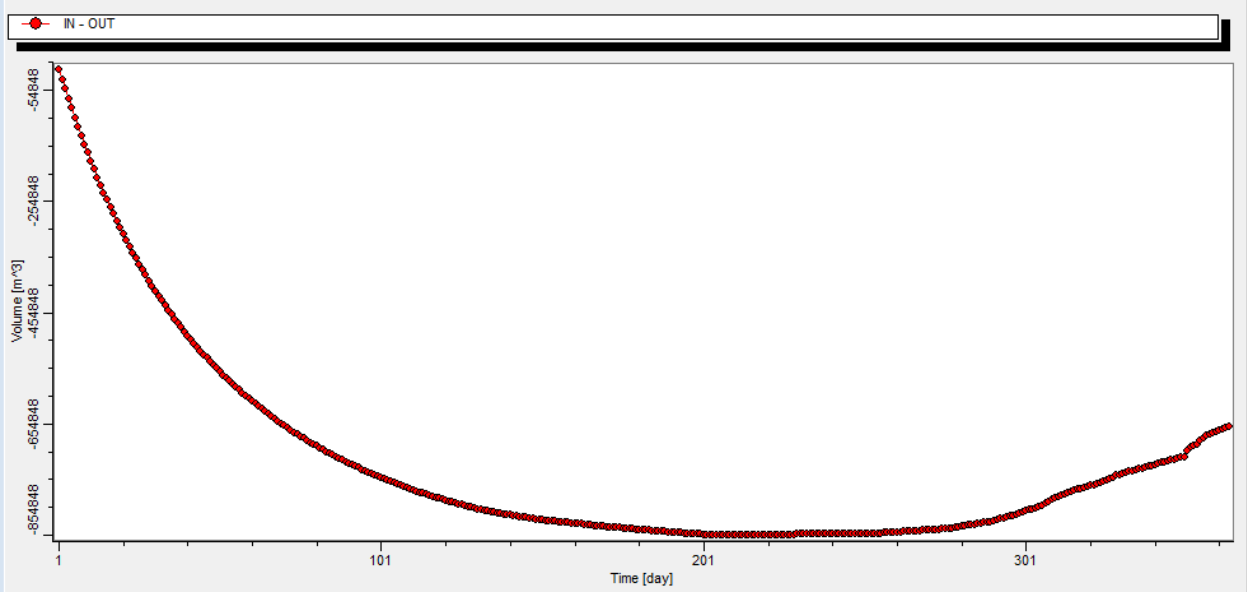

Figure 4.23: Difference in model input and outputs during transient local model run.

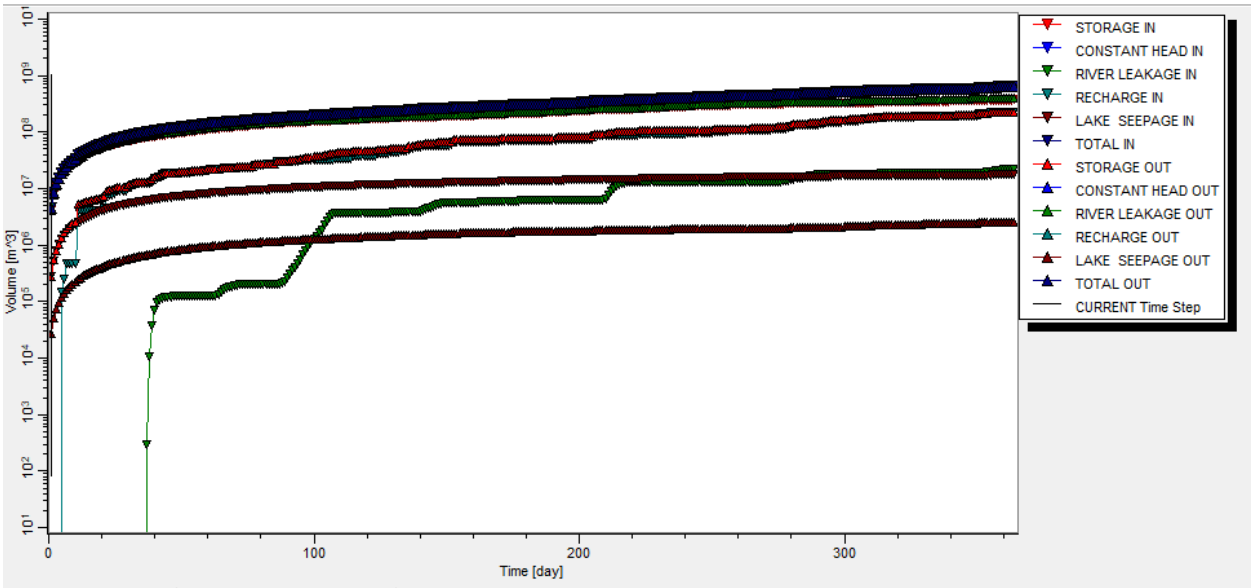

Figure 4.24: Mass balance through transient local model run.

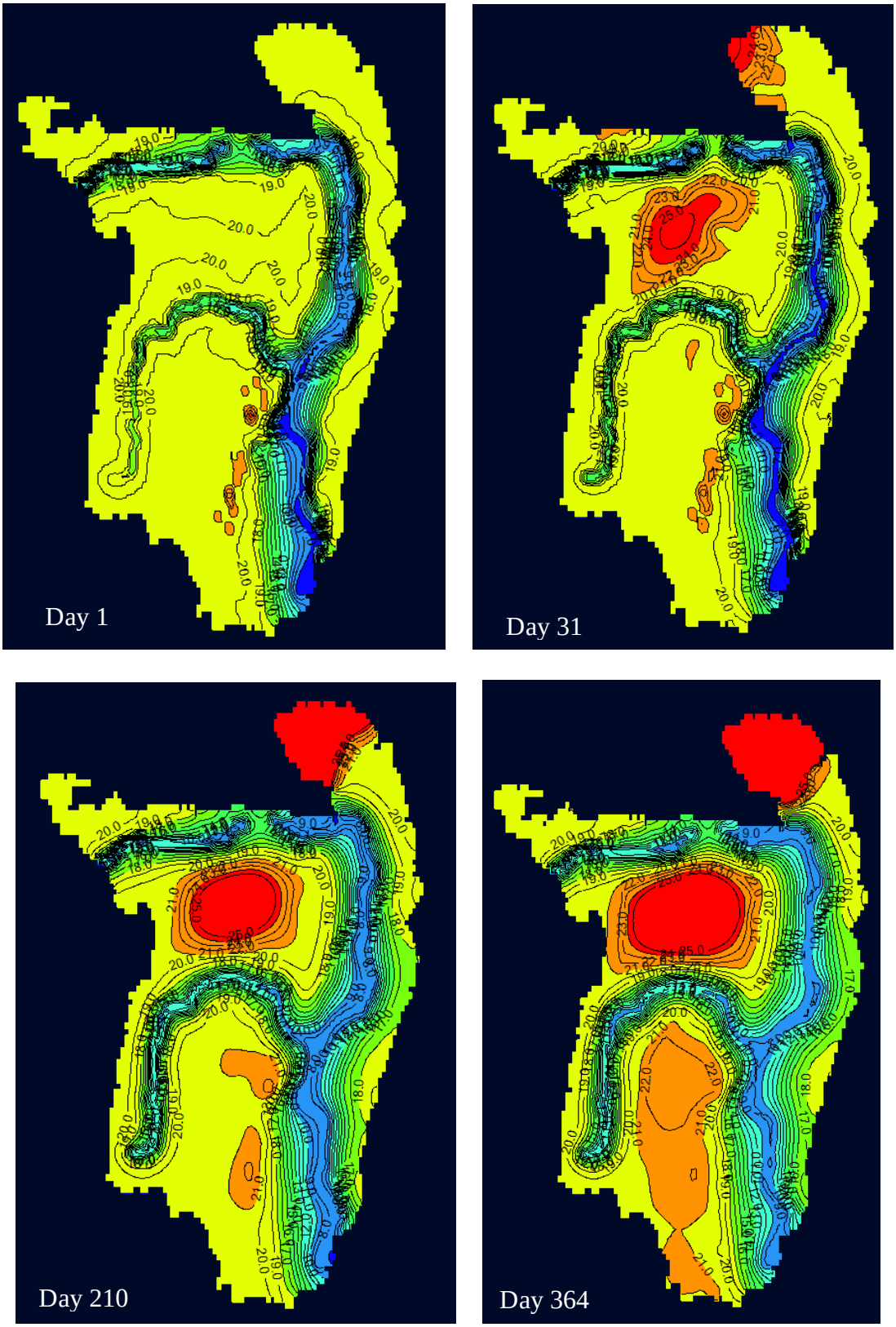

Figure 4.25: Water table elevations from run of transient local model.

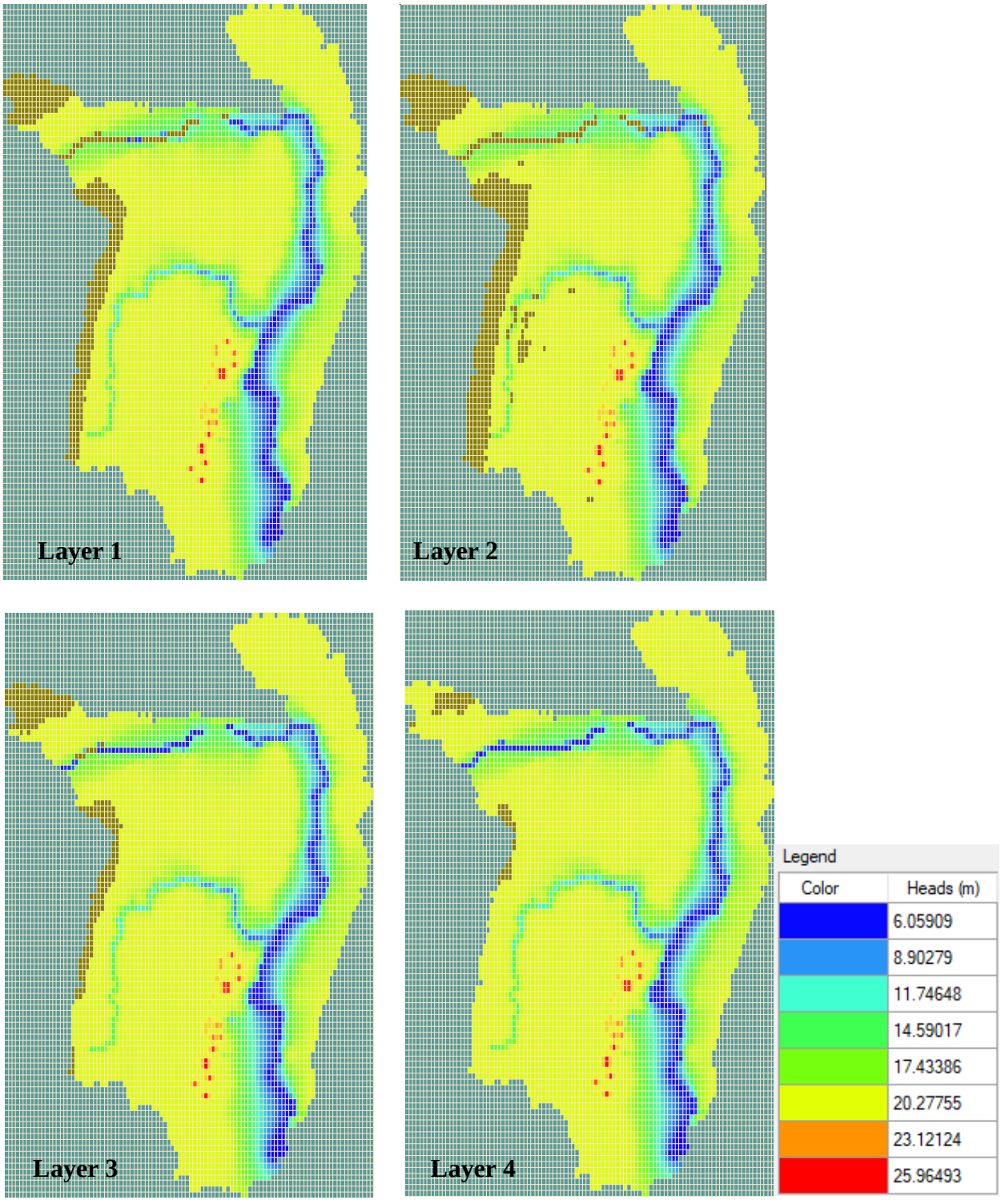

Figure 4.26: Simulated hydraulic heads on day 1 of the transient local model.

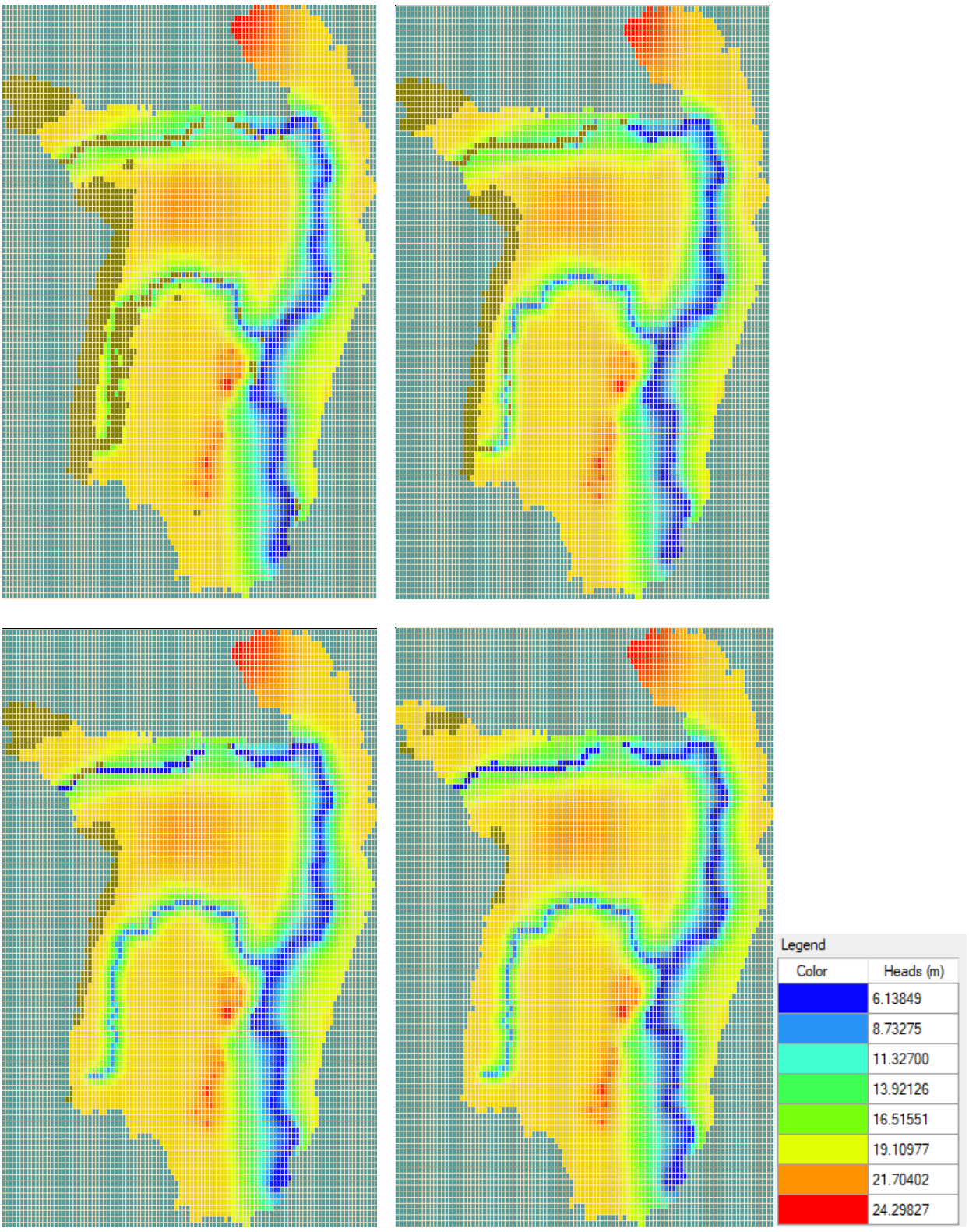

Figure 4.27: Simulated hydraulic heads on day 90 of the transient local model.

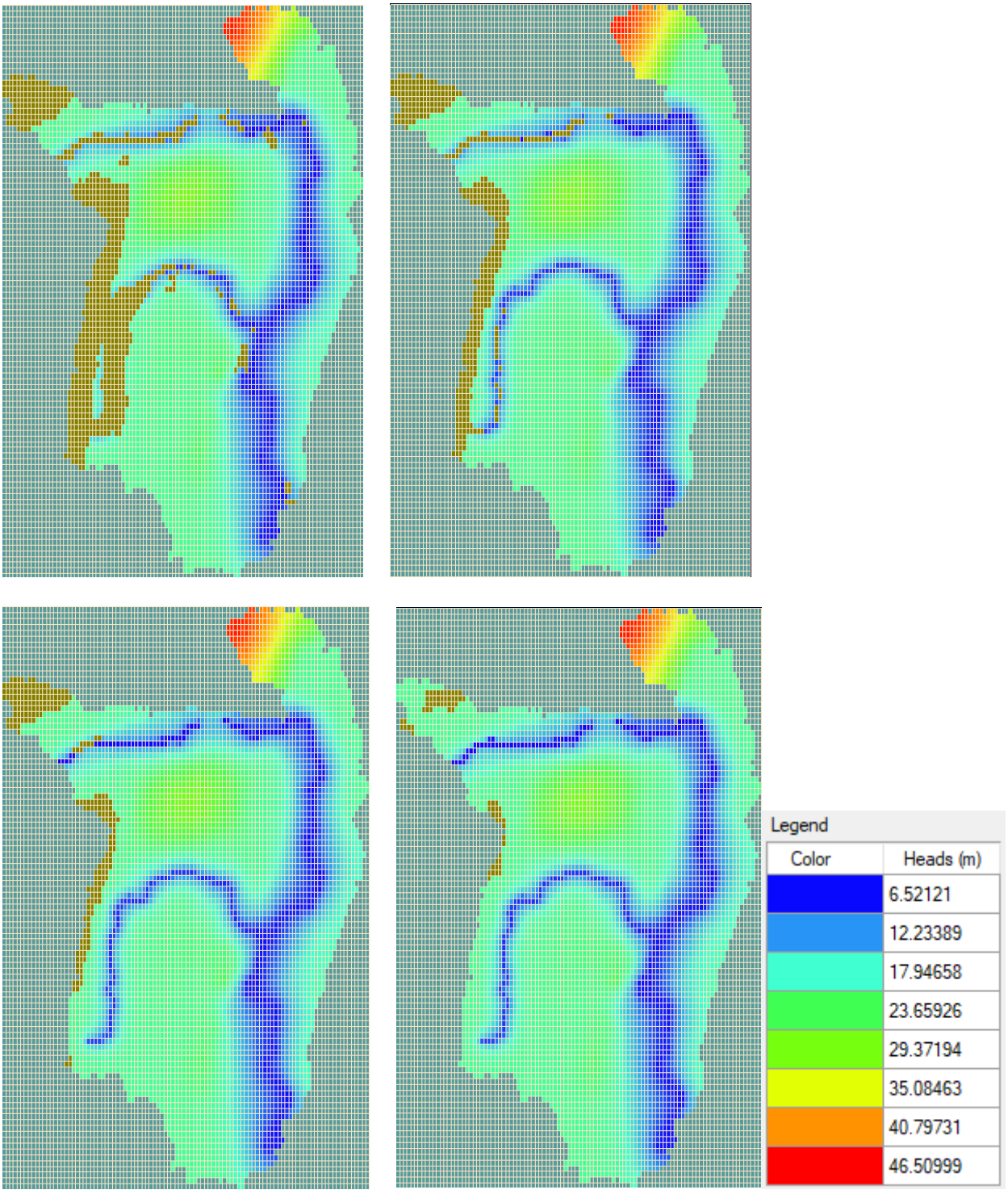

Figure 4.28: Simulated hydraulic heads on day 210 of the transient local model.

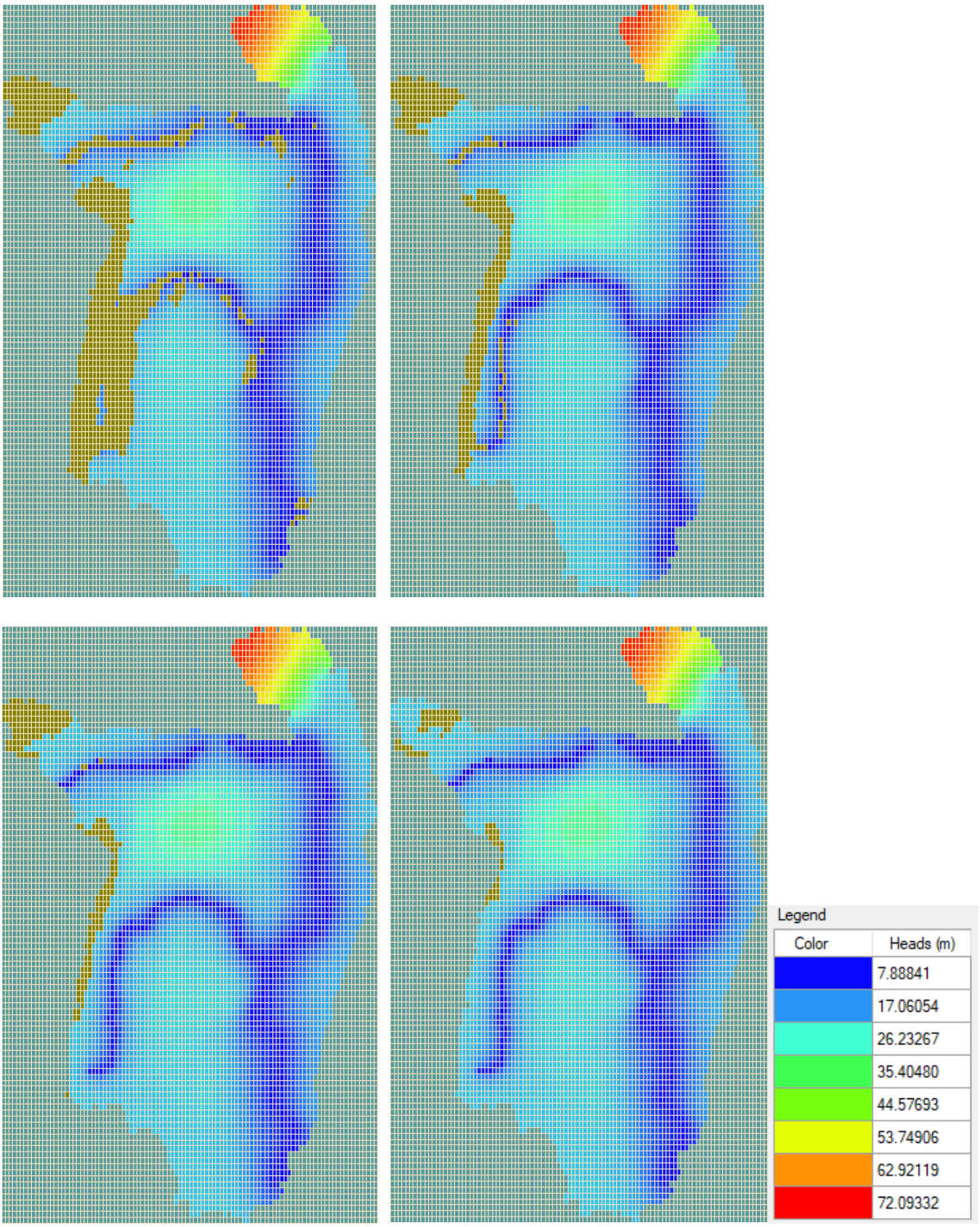

Figure 4.29: Simulated hydraulic heads on day 364 of the transient local model.

Table 4.5: Hydraulic heads in transient local model compared to observational data for day 31.

Data Source	Well ID	Aquifer	Model Cell		Head (m) Above NAVD88		Percent Error	Difference (m)
			Row	Column	Observed	Modeled		
Chemours	CC1	SA	70	61	17.1119448	16.25144	5.03%	0.8605048
	CCC2	SA	70	60	21.2440084	18.56396	12.62%	2.6800484
	IBM-W4	SA	77	56	25.8087256	22.15523	14.16%	3.6534956
	IBM-W8	SA	79	56	26.3394656	21.46699	18.50%	4.8724756
	Z	SA	64	62	25.8445748	21.9302	15.15%	3.9143748

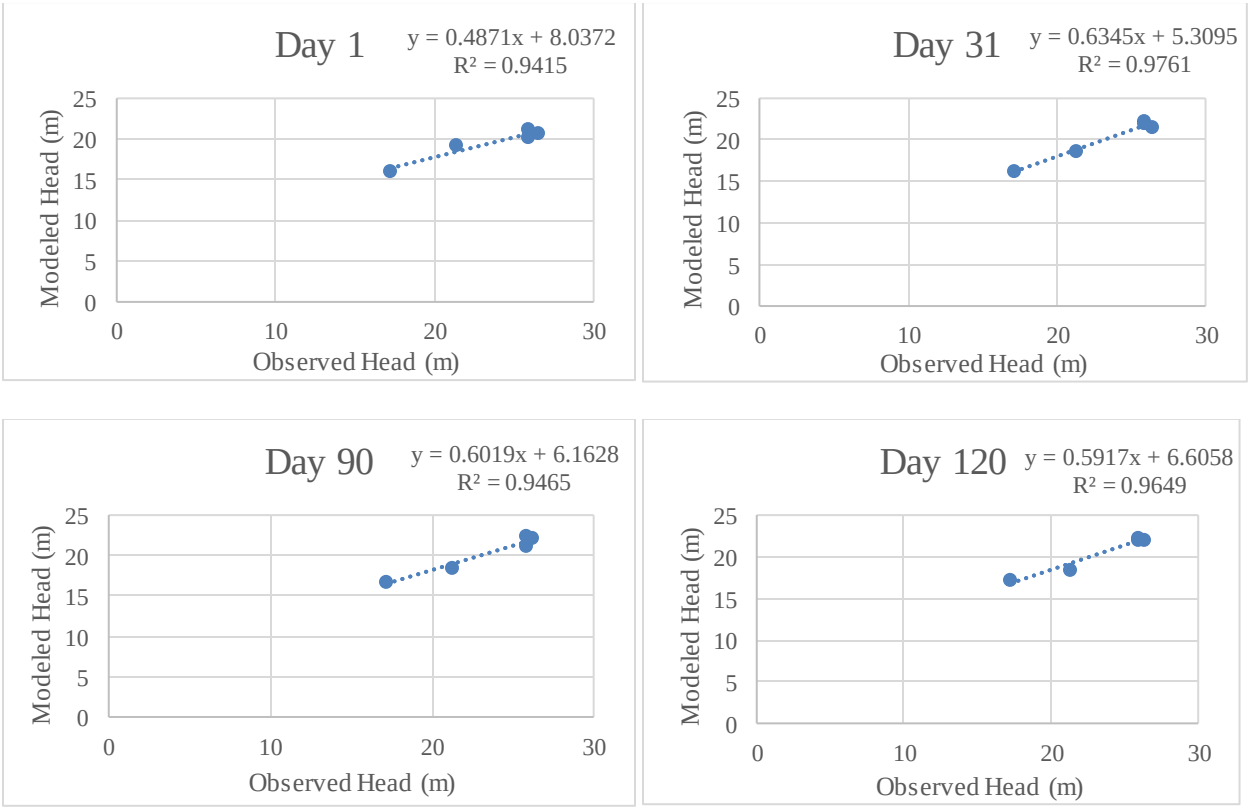

Figure 4.30: Comparisons between modeled and simulated hydraulic heads (m) for the transient local model at days 1, 31, 90, and 120.

CHAPTER 5

DISCUSSION

5.1 Results Analysis

5.1.1 Regional Model

The volumetric budget for the regional model shows that the Okefenokee Swamp has the least importance in terms of cumulative volume of the boundary conditions and is a net input for the simulation. On the other hand, the river boundary conditions had the greatest contribution in terms of cumulative volume on the simulation.

As expected, groundwater levels throughout the model gradually decrease towards the coastline mimicking the ground topography. Additionally, water table elevations in the eastern side of the model tended to be lower beneath major rivers. Based on the available observational data, the simulated hydraulic heads are a reasonable estimate for the general understanding of groundwater levels throughout the study area. The resulting hydraulic heads for the regional model were more accurate for the surficial aquifer than the Upper Floridan aquifer. Hydraulic heads in the SA around Mission Mine site generally ranged around 20 m. This range was within the observed range from the previous study (Landers, 2022). Simulated heads for Layer 5 (representing the UFA) were on average higher than observational data predicted. The observational data also suggests that groundwater elevations are more consistent and change far more gradually in the UFA compared to the SA. Simulated heads for the UFA increased more dramatically westward than was expected. Simulations of drawdown followed the same general trend of decreasing from west to east but was particularly high around the ONWR.

Simulated water budget calculations did not follow the same trend as groundwater elevations. The estimated water budget volume was highest around the area where Mission Mine is located, which may suggest that this region has a substantial influence on the surrounding hydrology. This consideration would likely be more substantiated if a transient version of the regional model was developed, and this region still had a high influence on the model water budget.

Groundwater flow velocities in all layers gradually increase eastward with the highest velocities occurring around the edge of the extent of the BAS. This may be an effect of the difference in hydraulic conductivity between the confining unit and the BA in Layer 3.

The addition of the Mission Mine did not have a substantial effect on the groundwater levels around the mine sites, but groundwater elevations with the inclusion of both wells were on average 0.68 m lower than was simulated without the wells. This difference may be an effect of adjusting the constant head, but this difference did not occur after only adding the Mission Mine well and still making this adjustment. On the other hand, the amount of groundwater withdrawal rate for at the Amelia Mine site is over double the daily rate used for Mission Mine. The combined effect of both pumping wells may have been substantial enough to be the main cause for the drop in groundwater elevations.

5.1.2 Steady-State Local Model

Simulated groundwater elevations for the steady-state local model showed a similar trend as the regional model and tended to follow the ground surface elevation changes. Simulated drawdown showed a reciprocal trend where drawdown was greatest in cells with rivers. The effects of river boundary conditions on hydraulic heads and drawdown were more noticeable in the local model than in the regional model. The higher resolution of the local model around

Mission Mine also allowed for more fluctuations in hydraulic head over a shorter distance, so the local model was better able to replicate the observed groundwater level changes around the mine site.

Groundwater generally flowed towards the river boundary conditions in this model and velocities increased following the same trend. Simulated groundwater flowed outwards from the Mission Mine site and towards these river boundary cells. Because this model did not include the UFA, which is the source of groundwater withdrawals for the mine, these groundwater flows do not represent groundwater flows that are directly affected by the mine pumping wells.

5.1.3 Transient Local Model

The initial run of the transient local model showed minimal changes in hydraulic heads through the year run time. This may suggest that hydraulic heads in this region are not substantially affected by seasonal changes which were represented in the recharge and river boundary conditions. Throughout the simulation, groundwater elevations were lower in cells that contained river conditions, which was similarly represented in the steady-state version of this model. Unlike the steady-state model, a location of high hydraulic heads developed in the northern part of the model. Additionally, the hydraulic heads throughout the model were more homogenous and changed more gradually over the area than the heads in the steady-state simulation. Drawdown again had a reciprocal trend where higher drawdown occurred in cells with lower hydraulic heads. Groundwater flow direction and velocities overall showed no substantial difference between the steady-state and transient versions of the local model.

5.2 Modeling Assumptions/Concerns

5.2.1 Numerical Grid Size

A trade-off exists between adding a higher resolution by decreasing grid cell size and increasing the computational requirements of a groundwater model. VMF has a feature for "refining" a numerical grid by dividing the cells within a series of rows or columns by a set factor. This process increases the resolution of regions of interest in the model and was used in the development of the numerical grid of the transient local model. While this does still increase the computational needs of the model, refining a model in only some areas is less computationally expensive than increasing the grid spacing throughout the entire model.

The grid spacing used for the regional model was large enough that several of the monitoring wells at both Chemours mining sites fell within the same cell. This reduces the number of wells that could be used for model calibration. The observational data from the monitoring wells at the Mission Mine site showed that the water levels in the surficial aquifer can range within a few meters difference throughout the site. With the current grid spacing of the regional model, this difference is not well represented, so the accuracy of the model in replicating the observational data was somewhat diminished. The accuracy of the model at replicating these differences through the mine site may be improved if the numerical grid is refined or the grid spacing decreased in the future.

5.2.2 Okefenokee Swamp Water Levels

Calibration of the regional model involved assuming that the connectivity between the Okefenokee Swamp and the aquifers beneath it is higher than previous literatures have suggested. Similarly, the bed conductivity used was about four magnitudes lower than the

literature estimates for peat soils. This may suggest that the modeled amount of leakance from the swamp is higher than is currently assumed. However, the high swamp water levels may be a result of assuming the whole area of the ONWR has a single stage height for simplicity. This assumption may have resulted in a substantially higher water volume being considered for the lake leakage than should be reasonably expected. A more accurate representation would require the ONWR to be broken down into multiple regions and assigned independent stage values based on monitoring data. This may resolve the need to increase the conductivity of the confining units since the total volume of leakance would be lower.

Another potential cause for the high-water levels around the Okefenokee Swamp during the initial model run could be that the evapotranspiration was underestimated. Although this was not examined during model calibration, this may be an area where further investigation is needed.

5.3 Future Work

5.3.1 Data Limitations

The expanded model domain used for this model improves the availability of groundwater gages used for model calibration which was a concern for the previous model (Landers, 2022). However, the distribution of these gages is more concentrated along the southern edge and coastline of the model. The inclusion of groundwater monitoring wells along the western edge of the model would allow for a more accurate estimate for the constant head boundary condition in that region.

Improving the accuracy of the model at predicting and replicating observational data will likely require adding heterogeneity to the model properties. Regional soil data throughout the

study area would allow for the development of multiple property zones with ranges of horizontal and vertical conductivities within each model layer. Increasing the heterogeneity of the layer properties would allow for more local-based calibration of areas of the model but would increase the data and computational needs of the model.

5.3.2 Transient Regional Model

Because of the slow nature of groundwater flows, using a steady-state model is likely not sufficient to analyze the effects of the pumping wells on groundwater heads and velocities. Additionally, one day's worth of groundwater withdrawal is not fully representative of the mining operations and their influence on the region's hydrology. A transient version of the regional model would be preferrable to better analyze the potential effects of these pumping wells on groundwater flows in the study area, A transient model would allow for the inclusion of storage effects which may improve the calibration process. However, a transient version of the regional model would require further observational data and would need to consider time-based hydrological patterns.

Water-table elevations are affected by tidal fluctuations along the coast (Clarke et.al., 1990). Should a transient version of the regional model be developed, a daily time-step may not be able to replicate these tidal fluctuations. If reproducing these tidal fluctuations in groundwater levels is an important goal of a future study, the model domain may need to be centralized on the coastline and/or the observational data taken at shorter time intervals. Similarly, tidal fluctuations within the estuary boundary conditions should be considered.

Recharge is difficult to represent over a large area especially within a transient model. Assuming a constant precipitation and evaporation rate throughout the selected period may be

sufficient for certain model conditions. However, in developing a transient regional model, it may be useful for the recharge boundary condition to be broken up into regions based on available precipitation data. Based on NCDC data used for the recharge boundary condition in the transient local model, the 2021 water year was somewhat wetter than average year. Considering this, it may be preferable for a future transient model of this study area to select a different period where the precipitation levels are more representative of the average conditions. This would allow for the recharge conditions to be more in-line with the averages used for the other model boundary conditions where observational data may not be available.

5.3.3 Public Pumping Wells

The FAS and other regional aquifers within Georgia are a main source for drinking water for rural and coastal communities. The FAS provides tens of millions of groundwater daily for several public county pumping wells in Georgia that fall within the model domain (Cherry, 2015). In 2021, an analysis of long-term monitoring well data obtained from the USGS monitoring well data within Georgia showed a declining trend in water table elevation. Most of the watersheds that showed a substantial decrease in water table elevation were within the southern half of the state where there is the most active irrigation (Sutton et.al., 2021), which suggests that agricultural groundwater usage has a substantial impact on regional groundwater levels. The combined effects of these public wells throughout the state likely have an influence on the groundwater flows and water levels within the study area. The inclusion of these withdrawal rates may reduce the hydraulic heads of the UFA and improve the accuracy of the model in replicating the observational heads for this aquifer.

5.3.4 Particle Tracking

Particle tracking is a useful tool for studying groundwater contamination. It can also be used to examine points of leakage in aquifers or intervening confining units. For this study, MODPATH could be used to track groundwater flows into and out of the mining sites. Tracking the groundwater flows around the mining sites, particularly around Mission Mine, would provide a better understanding of the interactions between the mining operations and the regional hydrology. This same process could be applied to any pumping wells added to the model to account for other public and private sources of groundwater withdrawal. The use of particle tracking in combination with pumping wells could help to identify where groundwater levels may lower in response to future groundwater withdrawals. Additionally, the use of particle tracking in this model could provide further context to the degree of connectivity between the Okefenokee Swamp and the UFA.

5.4 Conclusions

Groundwater is a vastly important resource for the security of freshwater access across the country. The UFA is one of the most productive aquifers in the nation and is a main source of drinking water and water for irrigation within Georgia. Groundwater use for irrigation is the main use for groundwater within Georgia, and its use for irrigation increased by 159% between 1990 and 2000 (Painter, 2019). Long-term monitoring data of USGS wells shows that groundwater levels have declined over the past few decades (Sutton et.al., 2021), likely in part because of increasing groundwater withdrawals across the state.

This project focused on studying the surficial and groundwater hydrology of a study area center around two mineral mining sites and the ONWR. The regional model was constructed to

include the surficial, Upper Floridan, and Brunswick aquifers. The purpose of this study was to examine the hydrology of this region and the effects of the pumping wells at each mine site on the surrounding hydrology.

The results and calibration process of the regional groundwater model suggests that: 1) the groundwater contribution and/or evapotranspiration rates of the Okefenokee Swamp have likely been underestimated by previous studies and 2) pumping wells have a substantial impact of the groundwater levels in southeastern Georgia, particularly in the UFA. Initial simulated heads around the Okefenokee Swamp were multiple orders of magnitude higher than previous swamp records would suggest is reasonable. The leakage from the swamp to the UFA was increased substantially to resolve the pooling effect on Layer 1, suggesting that the contribution of swamp outflow that recharges the aquifers below it may be higher than previously assumed. Hydraulic heads around Mission Mine did not decrease by a substantial degree after the inclusion of the Mission Mine pumping well to the regional mode, but simulated heads did decrease by 0.68 m on average compared to the simulated results without wells. This difference suggests that withdrawals from the UFA are likely an important factor in groundwater levels in the region. The inclusion of other public and private pumping wells that withdraw from the UFA would likely lower the groundwater levels in the UFA so that the model would better replicate observed heads without the need to increase the conductivity of the UCU. Meanwhile, the results of the steady-state and local models confirm the literature estimate for the conductivity of the surficial aquifer. The transient local model was better able to replicate real-world conditions and a transient version of the regional model would probably show a similar improvement in the accuracy of the model to represent the observational data. Overall, these models are a valuable tool for public

and private partners to examine current and future groundwater conditions in southeastern Georgia and make informed decisions on groundwater resource management.

REFERENCES

Anderson, M. P., & Woessner, W. W. (1992). Applied groundwater modeling : simulation of flow and advective transport. Academic Press.

Bellino, J.C., (2011). Digital surfaces and hydrogeologic data for the Floridan aquifer system in Florida and in parts of Georgia, Alabama, and South Carolina: U.S. Geological Survey Data Series 584. http:// pubs.usgs.gov /ds/584/index.html

Brianna Speldrich, Philip Gerla, & Emma Tschann. (2021). Characterizing Groundwater Interaction with Lakes and Wetlands Using GIS Modeling and Natural Water Quality Measurements. Water, 13(983), 983. https://doi.org/10.3390/w13070983

Brook, G. A., & Hyatt R. A. (1985). A Hydrological Budget for the Okefenokee Swamp Watershed, 1981-82. Physical Geology 5(2):127-141. https://doi.org/10.1080/02723646.1985.10642267

Brook, G. A., & Sun, C.-H. (2013). Hydrological Simulation of Okefenokee Swamp Upland Watersheds Using a Distributed Model: The Example of the Black River Catchment. Southeastern Geographer, 27(2), 71–89. https://doi.org/10.1353/sgo.1987.0006

Brooks, M. H., & McConnell, J. B. (1983). Inland travel of tide-driven saline water in the Altamaha and Satilla rivers, Georgia, and the St. Marys River, Georgia-Florida. U.S. Geological Survey.

Cherry, G. S. (2015). Groundwater flow in the Brunswick/Glynn County area, Georgia, 2000-04. U.S. Department of the Interior, U.S. Geological Survey. *Strategic Investigations Report: 2015-5061*.

Clarke, J. S. (2003). The surficial and Brunswick aquifer systems; alternative ground-water resources for coastal Georgia. *Proceedings - Georgia Water Resources Conference*, 2003.

Clarke, J. S., Hacke, C. M., & Peck, M. F. (1990). Geology and ground-water resources of the coastal area of Georgia. Dept. of Natural Resources, Environmental Protection Division, Georgia Geologic Survey.

Cohen, A. D. (1973). Possible influences of subpeat topography and sediment type upon the development of the Okefenokee Swamp-Marsh Complex of Georgia. Southeastern Geology, 15(3), 141–151.

Degnan, J. R., Lindsey, B. D., Levitt, J. P., & Szabo, Z. (2020). The relation of geogenic contaminants to groundwater age, aquifer hydrologic position, water type, and redox conditions in Atlantic and Gulf Coastal Plain aquifers, eastern and south-central USA. *Science of the Total Environment*, *723*. https://doi.org/10.1016/j.scitotenv.2020.137835

Drummond, D. D. (2007). Water-supply potential of the coastal plain aquifers in Calvert, Charles, and St. Mary's Counties, Maryland, with emphasis on the upper Patapsco and lower Patapsco Aquifers. *Report of Investigations - Maryland Geological Survey*.

Gibbons, W. (2002). Natural History of the Okefenokee Swamp. In New Georgia Encyclopedia. Retrieved Dec 1, 2020, from https://www.georgiaencyclopedia.org/articles/geography-environment/natural-history-of-the-okefenokee-swamp/

Harbaugh, A. W. (2005). *MODFLOW-2005, the U.S. Geological Survey modular ground-water model : the ground-water flow process*. U.S. Dept. of the Interior, U.S. Geological Survey.

Hariharan, V., & Uma, M. (2017). A review of visual MODFLOW applications in groundwater modelling. *IOP Conference Series: Materials Science and Engineering*, *263*(3), 032025.

Hefner, J. M. (1994). Southeast wetlands : status and trends, mid-1970's to mid-1980's. U.S. Department of the Interior, Fish and Wildlife Service.

Hughes, C. E., Binning, P., & Willgoose, G. R. (1998). Characterisation of the hydrology of an estuarine wetland. *Journal of Hydrology*, 211(1–4), 34–49.

Hyatt, R. A. (1984). Hydrology and geochemistry of the Okefenokee Swamp basin.

Kitchens, S., & Rasmussen, T. C. (1995). Hydraulic Evidence for Vertical Flow from Okefenokee Swamp to the Underlying Floridan Aquifer in Southeast Georgia. Georgia Water Resources Conference, 156–157.

Klassen, J., & Allen, D. M. (2017). Assessing the risk of saltwater intrusion in coastal aquifers. *Journal of Hydrology*, *551*, 730–745. https://doi.org/10.1016/j.jhydrol.2017.02.044

Landers, Brain S. (2022). Modeling Regional Surface and Groundwater Hydrology Near the Okefenokee National Wildlife Refuge. The University of Georgia.

Loftin, C. S., Aicher, S. B., & Kitchens, W. M. (2000). Effects of the Suwannee River sill on the hydrology of the Okefenokee Swamp: application of research results in the environmental assessment process. *Proceedings - Rocky Mountain Research Station*, USDA Forest Service, No. RMRS-P-15(Vol. 3), 102–110.

Loftin, C. S., Kitchens, W. M., & Ansay, N. (2001). Development and application of a spatial hydrology model of Okefenokee Swamp, Georgia. *Journal of the American Water Resources Association*, 37(4), 935–956. https://doi.org/10.1111/j.1752-1688.2001.tb05524.x

Mao, X., Cui, L., & Wang, C. (2013). Exploring the hydrologic relationships in a swamp-dominated watershed—A network-environ-analysis based approach. Ecological Modelling, 252, 273–279. https://doi.org/10.1016/j.ecolmodel.2013.01.002

Maupin, M. A., & Barber, N. L. (2005). Estimated withdrawals from principal aquifers in the United States, 2000. U.S. Dept. of the Interior, U.S. Geological Survey.

Okefenokee National Wildlife Refuge. (n.d.). FWS.gov. https://www.fws.gov/refuge/okefenokee

Oliveira, Manuel M. & Martins, Tiago N. (2019). A methodology for the preliminary characterisation of the river boundary condition in finite difference groundwater flow numerical models. Acque Sotterranee, 8(3). https://doi.org/10.7343/as-2019-400

Painter, J. A. (2019). Estimated use of water in Georgia for 2015 and water-use trends, 1985-2015. *Open-File Report - U. S. Geological Survey*. https://doi.org/10.3133/ofr20191086

Pandit, A., Ali, N., & Heck, H. H. (2011, January 1). Spatial Calibration of Vertical Hydraulic Conductivity below an Estuary. *Journal of Hydrologic Engineering*, 16(10), 763–771.

Parrish, F. K., & Rykiel, , Edward J. (1979). Okefenokee Swamp Origin: Review and Reconsideration. *Journal of the Elisha Mitchell Scientific Society*, 95(1), 17–31.

Pasos, M. (n.d.). North American Land Cover, 2020 (Landsat, 30m). Retrieved from http://www.cec.org/north-american-environmental-atlas/land-cover-30m-2020/

Pernik, M. (1987). Sensitivity analysis of multilayer, finite-difference model of the Southeastern Coastal Plain regional aquifer system; Mississippi, Alabama, Georgia, and South Carolina. Water-Resources Investigations - U. S. Geological Survey.

Phillips, S. W. (1987). Hydrogeology, degradation of ground-water quality, and simulation of infiltration from the Delaware River into the Potomac aquifers, northern Delaware. Dept. of the Interior, U.S. Geological Survey.

Pinder, G. F. (2002). Groundwater modeling using geographical information systems. Wiley.

Plummer, L. N., Eggleston, J. R., Andreasen, D. C., Raffensperger, J. P., Hunt, A. G., & Casile, G. C. (2012). Old groundwater in parts of the Upper Patapsco Aquifer, Atlantic Coastal Plain, Maryland, USA; evidence from radiocarbon, chlorine-36 and helium-4. *Hydrogeology Journal*, *20*(7), 1269–1294. https://doi.org/10.1007/s10040-012-0871-1

Pollock, D. W. (2016). *User guide for MODPATH version 7-A : a particle tracking model for MODFLOW*. U.S. Department of the Interior, U.S. Geological Survey.

Reese, R. S., & Memberg, S. J. (2000). Hydrogeology and the distribution of salinity in the Floridan Aquifer system, Palm Beach County, Florida. U.S. Dept. of the Interior, U.S. Geological Survey, Water-Resources Investigations Report 98-4253. https://doi.org/10.3133/wri984253

Rizzuti, A. M., Cohen, A. D., & Stack, E. M. (2004). Using hydraulic conductivity and micropetrography to assess water flow through peat-containing wetlands. *International Journal of Coal Geology*, *60*(1), 1–16. https://doi.org/10.1016/j.coal.2004.03.003

Ryder, P. D. (1985). Hydrology of the Floridan aquifer system in west-central Florida. *U. S. Geological Survey Professional Paper 1403-F*. https://doi.org/10.3133/pp1403F

Schlesinger, W. H. (1978). Community Structure, Dynamics and Nutrient Cycling in the Okefenokee Cypress Swamp-Forest. Ecological Monographs, 48(1), 43–65. https://doi.org/10.2307/2937359

SJWMD (n.d.) Hydrologic Data. http://webapub.sjrwmd.com/agws10/hdsnew/map.html

Small, C., & Nicholls, R. J. (2003). A Global Analysis of Human Settlement in Coastal Zones. *Journal of Coastal Research*, *19*(3), 584–599.

Smedley, J. E. (1968). Summary report on the geology and mineral resources of the Okefenokee National Wildlife Refuge, Georgia. *U. S. Geological Survey Bulletin*, N1–N10.

Sutton, C., Kumar, S., Lee, M.-K., & Davis, E. (2021). Human imprint of water withdrawals in the wet environment: A case study of declining groundwater in Georgia, USA. *Journal of Hydrology: Regional Studies*, 35. https://doi.org/10.1016/j.ejrh.2021.100813

United States, Congress, Joiner, Charles N., & Alan M. Cressler (1994). Ground-Water Conditions in Georgia, 1993, vol. 94-118, U.S. Geological Survey, 1994. *Open File Report*.

Wang, H., & Anderson, M. P. (1982). Introduction to groundwater modeling: finite difference and finite element methods. W.H. Freeman.

Waterloo Hydrogeologic. (2022). Integrated Conceptual & Numerical Groundwater Modeling Software User's Manual Visual MODFLOW Flex 8.0.

Waterloo Hydrogeologic. (n.d.) Visual MODFLOW Flex 8.0. https://www.waterloohydrogeologic.com/whats-new-visual-modflow-flex-80

Webb, M. D., & Howard, K. W. F. (2011). Modeling the transient response of saline intrusion to rising sea-levels. *Ground Water*, *49*(4), 560–569. https://doi.org/10.1111/j.1745-6584.2010.00758.x

Wicks, C. M., & Herman, J. S. (1994). The effect of a confining unit on the geochemical evolution of ground water in the Upper Floridan aquifer system. *Journal of Hydrology (Amsterdam)*, 153(1/4), 139-155.

Williams, L.J., & Dixon, J.F., 2015, Digital surfaces and thicknesses of selected hydrogeologic units of the Floridan aquifer system in Florida and parts of Georgia, Alabama, and South Carolina: U.S. Geological Survey Data Series 926, 24 p., http://dx.doi.org/10.3133/ds926.

Williams, L.J., & Kuniansky, E.L., 2016, Revised hydrogeologic framework of the Floridan aquifer system in Florida and parts of Georgia, Alabama, and South Carolina (ver 1.1, March 2016): U.S. Geological Survey Professional Paper 1807, 140 p., 23 pls, http://dx.doi.org/10.3133/pp1807.

Wojnar, Alicja J., et al. "Assessment of Geophysical Surveys as a Tool to Estimate Riverbed Hydraulic Conductivity." *Journal of Hydrology*, vol. 482, 2013, pp. 40–56., https://doi.org/10.1016/j.jhydrol.2012.12.018.

Yin, Z. Y., & Brook, G. A. (1992). Evapotranspiration in the Okefenokee swamp watershed: a comparison of temperature-based and water balance methods. *Journal of Hydrology (Amsterdam)*, 131(1–4), 293–312. https://doi.org/10.1016/0022-1694(92)90223-I

Zhang, W., & Montgomery, D. R. (1994). Digital elevation model grid size, landscape representation, and hydrologic simulations. *Water Resources Research*, 30(4), 1019–1028. https://doi.org/10.1029/93WR03553